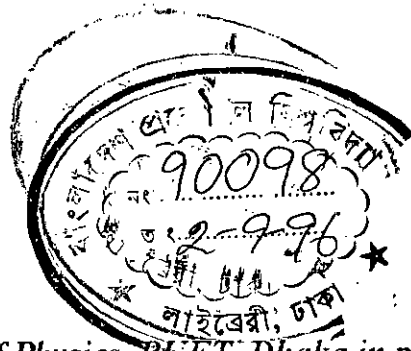


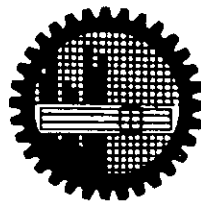
**STUDY OF MAGNETOSTRICTION AND MAGNETO MECHANICAL
COUPLING FACTORS OF SOME MAGNETOSTRICTIVE MATERIALS**

By

A. K. M. ZULFIQURE RAHMAN



*A thesis Presented to the Department of Physics, BUET, Dhaka in partial
fulfillment of the requirements for the degree of M.Phil.*



Bangladesh University of Engineering and Technology

Dhaka - 1000, Bangladesh

April 1996



CERTIFICATE

This is to certify that this work was done by me and it has not been submitted elsewhere for the award of any degree or diploma..



Countersigned

Ali Asgar

Prof. Ali Asgar

Signature of the candidate

A.K.M. Zulfiqur Rahman

A.K.M. Zulfiqur Rahman

**BANGLADESH UNIVERSITY OF ENGINEERING AND TECHNOLOGY,
DHAKA**

DEPARTMENT OF PHYSICS

Certification of Thesis work

A Thesis on

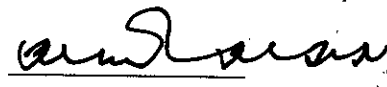
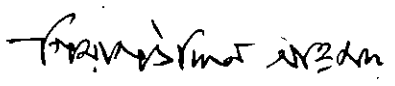
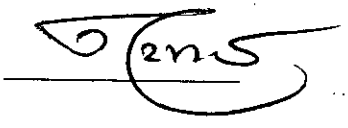
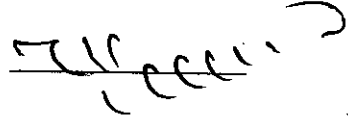
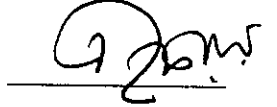
**STUDY OF MAGNETOSTRICTION AND MAGNETOMECHANICAL COUPLING
FACTORS OF SOME MAGNETOSTRICTIVE MATERIALS**

BY

A K.M Zulfigure Rahman

has been accepted as satisfactory in partial fulfilment for the degree of Master of Philosophy in Physics and certify that the student demonstrated a satisfactory knowledge of the field covered by this thesis in an oral examination held on 23rd April, 1996.

Board of Examiners

- | | | | |
|----|--|-----------------------|---|
| 1. | Dr. M. Ali Asgar
Professor of Physics.
BUET Dhaka. | Supervisor & Chairman |  |
| 2. | Dr. Gias Uddin Ahmed
Head & Professor of Physics
BUET Dhaka. | Member |  |
| 3. | Dr. Tafazzal Hossain
Professor of Physics
BUET Dhaka. | Member |  |
| 4. | Dr. Mominul Huq
Associate Professor of Physics
BUET Dhaka. | Member |  |
| 5. | Dr. A. K. Roy
Professor of Physics
Dhaka University. | Member External |  |

ACKNOWLEDGEMENT

First and foremost I would like to express my sincere gratitude to my reverend teacher Dr. M. Ali Asgar, Professor, Department of Physics, BUET, Dhaka for introducing me to the subject of magnetism and for his patient guidance, and fruitful suggestion throughout the course of this thesis work. His help and encouragement at moments of difficulty have made it possible to present this work.

My grateful thanks are also due to professor Gias uddin Ahmad, Head, Department of Physics, BUET, and Professor Tafazzal Hossain of the same department for their encouragements and keen interest in this work. I also wish to acknowledge my indebtedness to Dr. Mominul Huq and Dr. Nazma Zaman, Associate Professor of Physics Department, BUET, for their assistance and cooperation.

I wish to express my appreciation with thanks to Dr. Md. Feroz Alam Khan, Assistant Professor, Department of Physics, BUET, for his cooperation and technical assistance.

I acknowledge my gratitude to Dr. Md. Abu Hashan Bhuiyan, Dr. Jibon Podder, Mr. Md. Mostak Hossain, Mr. Md. Shaif-ul-Alam and all other teachers of the Department of Physics, BUET, for their assistance and encouragement. My appreciation is also extended to Mr. A.S.M. Sirajul Islam for his friendly cooperation.

I wish to express my sincere thank to Mr. M.A. Mazid C.S.O. Head, Magnetic Material Division, Atomic Energy Commission, Dhaka for his kind permission for using the V.S.M. during the experiment and able technical assistance for measuring the magnetization in their laboratory. I am also grateful to Dr. A.K.M. Abdul Hakim,

Principal Engineer, AEC for his valuable suggestion and substantial assistance during the experimental work.

I wish to express my thank to the technical persons of central instrument workshop and mechanical workshop of BUET for their help in the construction of sample holder. I also express my thanks to Mr. Md. Yusuf Harun, of IFCDR, BUET who has taken great pains in tracing the diagrams, Figures and graphs. It is my pleasure to express my thanks to fellow workers of the Dhaka Material Science group.

I want to express my indebtedness to my wife Mummun and to my daughters, Maliha, Fariha for their co-operation.

I gratefully acknowledge my indebtedness to Bangladesh University of Engineering and Technology for awarding a research grant.

ABSTRACT

The present work describes the experimental investigation of the magnetic properties of $\text{Fe}_{100-x}\text{Al}_x$, (where $x = 2, 8, 10, 12$ & 14), $\text{Tb}_{.27}\text{Dy}_{.73}\text{Fe}_2$ and also of Ni as a standard materials. Magnetostriction as a function of the magnetic field and saturation magnetostriction λ_s for different composition of iron aluminium, iron terbium dysprosium alloy and of nickel as a standard materials are measured. These measurement are confined at room temperature and under at varying field from 0 to 4.5 K Gauss.

The saturation field for magnetostriction in nickel is observed to be 1550 oersted. The value of magnetic field needed for the saturation magnetostriction in Ni determines the operating field for using Nickel as a magnetostrictive transducer. Fe-Al and $\text{Tb}_{.27}\text{Dy}_{.73}\text{Fe}_2$ alloys are highly magnetostrictive materials. The magnetostriction value for Fe-Al alloys increases with increasing amount of aluminium and become maximum at 12 atomic percent of Al as due to increased spin-orbit interaction. The decrease of magnetostriction above 12 atomic percent of Al is explained as due to decreasing value of magnetic moment.

The field dependance of magnetization for Fe-Al alloys of different composition are measured and the saturation magnetization of alloys decreases with the increasing concentration of Al and the field needed to saturate the magnetization also increases with the increase of Aluminium and the relation is found to be linear.

The first anisotropy constant K_1 for the iron aluminium alloys system as derived from field versus magnetization curves is similar to the old data derived from magnetization curves.

curves. In general, the addition of aluminium to iron changes the magnetization values. Previous work has shown that up to approximately 20 atomic percent aluminium the magnetic saturation moment of iron aluminium alloy decreases with increasing aluminium content at a rate comparable with what would be expected from simple dilution. Above this concentration the moment falls sharply with increasing aluminium content. The present work is motivated by a desire to investigate more fully the effect of order on the saturation magnetization and to find out the magnetization of alloys with aluminium content greater than that reported before who obtained the critical concentration for these specimen by extrapolation.

CONTENTS

Chapte-1	Introduction	1
Chapter-2	Magnetization and magnetostriction in ferro-magnetic alloy	
2.1	Magnetization	
2.1.1	Introduction to magnetization	7
2.1.2	Magnetization of Iron-alluminium alloy system	8
2.1.3	Intrinsic magnetization of alloys	10
2.1.4	Theory of magnetization	16
2.1.5	Magnetization of poly-crystalline specimen	18
2.1.6	The approach to saturation magnetization	19
2.2	Magnetostriction	
2.2.1	Introduction to magnetostriction	21
2.2.2	Theory of magneto-elastic energy	25
2.2.3	Physical origin of magnetostriction	26
2.2.4	Mechanism of magnetostriction	29
2.2.5	Magnetostriction of poly-crystal	31
2.2.6	Direction of linear magnetostriction	32
2.2.7	Magnetostriction Arising from domain rotation	34
Chapter-3	Measurement of magnetization of Fe-Al alloy system	
3.1.	Different methods for the measurement of magnetization	36
3.1.1	Extraction method	36
3.1.2	Force method	37
3.1.3	Faraday method	39
3.1.4	Gouy method	40
3.1.5	Sucksmith method	41
3.1.6	Vibrating sample magnetometer	41
3.1.7	VS M coil arrangement and field distribution	43

3.1.8	Working procedure of Vibrating sample magnetometer	48
3.1.9	Electronic circuit of V.S.M. and its operation principle	49
3.1.10	Description of mechanical parts	52
3.1.11	Sample and reference coil	55
3.1.12	Sensitivity of vibrating sample magnetometer	56
3.1.13	Advantage and Disadvantage	56
3.2.	Effective magnetic field	57
3.3	Measurement of magnetization	57
3.4	Results and discussion	68
Chapter-4	Measurement of magnetostriction of $Fe_{100-x}Al_x$, $Tb_{.27}Dy_{.73}Fe_2$ and Nickel	
4.1	Technique of measurement of magnetostriction	73
4.2	Wheatstone bridge principle	74
4.3	Strain gauge bonding	75
4.4	strain gauge technique	76
4.5	Orientation of the gauge position relative to the magnetic field	76
4.6	Bridge circuit sensitivity and calibration	77
4.7	Gauge circuit	79
4.8	D.C. amplifier	79
4.9	Sensitivity and calibration of the d.c. bridge	80
4.10	The choice of dummy material	81
4.11	The specimen holder	82
4.12	The specimen mounting	83
4.13	The calibration of electro-magnet	84
4.14	Magneto-mechanical coupling	87
4.15	Construction of solenoid	88
4.16	Measurement of magnetostriction	89
4.17	Results and discussion	115
4.17.1	Nickel	115
4.17.2	$Fe_{100-x}Al_x$ alloy	117
4.17.3	$Tb_{.27}Dy_{.73}Fe_2$ Alloy	119
4.18	Conclusion	121
4.19	Reference	122

Chapter-1



Introduction:

The aim of the present research is to investigate highly magnetostrictive Iron based $Fe_{100-x}Al_x$ $Tb_{.27}Dy_{.73}Fe_2$ alloys and also of Nickel as a standard material. Magnetostriction, which can be defined as lattice distortion of a magnetic crystal due to its magnetization is an important phenomena both for its theoretical interest and for technological applications. Modern civilization is largely dependent on electric power for its mobility, communication and various control devices. These in turn, depend on the phenomenon of ferromagnetism, which is found chiefly in iron, nickel, cobalt and the rare earth elements.

Theoretical interest involves the evaluation of magnetostriction which arises due to magneto-elastic interaction and contribute to the understanding of magnetization processes. Although magnetostriction of various magnetic materials have been studied with great theoretical and technological interest, the complexities of the problem and the trend in the development of new magnetic materials have kept this research field very dynamic and alive. As a result, various new problems are coming up which are related to the understanding and application of new magnetic materials.

The highly magnetostrictive materials are of special interest. Moreover, magnetostriction is one of the most important factors in determining the coercivity and hysteresis loop of ferromagnetic materials. In some anisotropic magnetic materials coercive force is thought to be dependent on magnetostriction, because in these cases the internal stresses determine the nucleation mechanism of domain formation.

Although many magnetic materials have been extensively studied for their saturation magnetostriction, little attention has been paid to their magnetostrictive behaviour below saturation. The reason for which magnetostriction measurement below saturation did not draw the attention of researchers is that, below saturation the domain distributions of magnetic specimens can not be uniquely determined. The results therefore, are not always reproducible. However for practical purposes magnetostriction measurement below saturation are important, because magnetic materials quite often are operated below saturation point. Moreover, since magnetostriction is related to domain rotation only and 180 degree domain wall movements do not contribute to magnetostriction, results in this region provide information about the nature of the domain and domain wall movements. In an ordinary ferromagnetic materials the domains are arranged in a complicated three dimensional pattern, an equilibrium state determined by the action and interaction of many different forces. It is confusing to study the nature and mode of action of these forces in the complicated cases and we shall therefore, as far as possible, try to deal with simple case where as few variables as possible have to be considered. Such cases can only be chosen if we have some knowledge of types of forces that have to be taken into account and we shall therefore give a brief general survey of the factors determining domain arrangements, before considering the separate forces in more detail. It is convenient to discuss the equilibrium conditions in terms of the forces acting on the system and to find the equilibrium state by finding the conditions to make the energy a minimum. The atomic magnetic moments in a ferromagnetic substance interact strongly with one another and tend to align themselves parallel to each other. The interaction is such as to correspond to an applied field of the order of magnitude 10^9 A/m and it results in a nearly perfect alignment of the spins in spite of the thermal agitation at room temperature. The presence of a strong internal magnetic field was first described by P. Weiss and termed it as a molecular field and developed a

theory of the temperature dependence of the saturation magnetization. Therefore, the application of magnetic field over Fe-Al alloy tends to align the atomic moments towards parallelism and thus produce an overall magnetization which has been described in detail in chapter- 2.

There are various method for the measurement of magnetization. In our experiment we have used V.S.M., an advanced type of apparatus developed by S.Foner, for measuring the magnetization of Fe-Al alloys with composition $Fe_{100-x}Al_x$ (where $x=2,8,10,12$ and 14) at room temperature of 300° K.Detail description and theoretical interpretation of VSM is given in chapter -3.

The idea of magnetostriction and its effect is important for the generation and creation of many devices and systems. In reality there are many magnetic materials and alloys for which no theoretical understanding is possible based on fundamental theory. In these situation we have to depend on phenomenological theory based on experimental results. The complexity of magnetostrictive phenomena below saturation prevents us from making accurate prediction based on first principle. In our case we have tried to simplify the phenomenological theory which is partly based on experimental facts and partly on some general features of the basic theory of magneto-elastic interaction.

The magnetostriction measurement is done using the strain gauge technique. The strain gauge technique is based on the principle of change of resistance produced by the strain in the gauge as transmitted by the materials on which gauge is bonded. A convenient method of determining change in length is to measure the change in resistance of a wire of the strain gauge that is firmly cemented to the test specimen and expands and contracts with it. This change is measure by measuring the change of resistance using the Wheatstone bridge in out of balance condition which produced a sharp deflection in the

nanovolt meter. There is a linear relationship between the deflection of the nanovolt meter and fractional change in resistance. This method was first developed by Goldman^{1.1} and since then, has become increasingly popular for its simplicity, compactness and precision. Asgar^{1.2} introduced this technique for the measurement of magnetostriction and magneto elastic constants of magnetic materials. Sikder^{1.3} using this method has also measured magnetostriction of Amorphous materials.

Magnetostriction is usually analyzed in terms of a general formalism which is empirical or semi-empirical and is controlled by symmetry considerations of the crystal. Callen and Callen^{1.4} showed magneto elastic energy E_{me} which arises from the strain dependence of the anisotropy energy and for small strains takes the form $E_{me} \approx \epsilon(\alpha)$. Bozorth and Walker^{1.5} showed an important characteristics of saturation magnetostriction along (111) direction which becomes zero at the composition for which the permeability is maximum. Beninger and Pavlovic^{1.6} defined magnetostriction in terms of five constants, but there was some discrepancy with the results obtained by Lee^{1.7}. Latter Asgar^{1.8} introduced a technique of analysis for the evaluation of five magnetostriction constants avoiding the error that arises due to the non alignment of the direction of magnetization and the direction of the applied magnetic field. The finite values of anisotropy constants which are responsible for these error was thus removed by the above mentioned work.

The present work is aimed at experimental determination and analysis of magnetostriction and magnetization of Iron-Aluminium alloy system. The magnetostriction of Iron-Terbium-Dysprosium sample and of Nickle sample have been measured and result is given in chapter 4.17.

Both the magnetization and magnetostriction of Iron-Aluminium for different compositions are measured as a funtion of magnetic field. The percentage of Aluminium

in iron are 2,8,10,12 and 14 percent respectively. These alloys were provided by Professor Asgar who prepared them in Southampton, England. Magnetization as a function of field for different compositions of Iron-Aluminium alloys have been measured using vibrating sample magnetometer. This has been explained in the light of existing theories of 3d transition metals and alloys. Kittel^{1.12} successfully co-related the conventional magneto-elastic constants and the symmetry constants. Clark and Belson^{1.13} made it clear that reliable values of the saturation magnetization can not be obtained on polly-crystalline samples even if the field strength applied are in excess of 100 killo oersted. The same results were obtained by Abbundi, Clark and Koon^{1.14}. The magnetostriction of highly magnetostrictive rareearth compound of composition $Tb_{0.27}Dy_{0.73}Fe_2$ sample is measured at room temperature. Terfenol-D of composition $Tb_{0.27}Dy_{0.73}Fe_2$ alloy is obtained from AB Sweeden in the form of 6 mm diameter rod which was directionaly solidified. The sample was cut, grinded and polished into a disk of diameter $4.855 \pm .005$ mm with a mass 0.552 gm. Magnetostriction of pure Nickle sample is also measured as a standard substance for calibration and comparison of the results of Iron-Aluminium alloy system and Iron-Terbium-Dysprosium alloy.

Magnetostriction is a mechanism that can be used to convert electro-magnetic energy to mechanical energy by designing and developing electro-mechanical transducer. This transducer can be used for producing high energy mechanical vibration of the sonic waves that can be used in under water signalling and for identificatin of objects. Since the amount of sound energy produced by this method is enormous due to the high value of elastic constants and magnetostriction of Iron base alloys under going deformation. This method of producing sound energy can have application in under water fishing and under ground signalling for minig. The study of the magneto-mechanical coupling factors of highly magnetostrictive alloys also provide information related to the design

and development of magnetostrictive oscillators, filters, magnetic tape head, magnetic amplifier, delay lines in electronic and acoustic memory circuit device, transformer core materials and in eliminating transformer noises caused by magnetostrictive vibration of the core and minimization of the core loss. The present work for the development of Iron base alloys and their application are expected to be useful in meeting the ever increasing demand of the present time.

Chapter-2

MAGNETIZATION AND MAGNETOSTRICTION IN FERRO-MAGNETIC ALLOYS

2.1 Magnetization

2.1.1 Introduction to Magnetization

Magnetic property of a solid originates from the electronic structure of its atoms and their orientations. Partially filled atomic shells give rise to uncompensated spins which are responsible for spin magnetic moments. Orbital angular momentum also contribute to magnetic moment of the atom. The magnetism that arise due to the outer most electrons, called Pauli para magnetism and is temperature independent. Magnetism of interest arises due to unfilled inner shells of the atom. Examples are the $3d$ electrons in transition metals and $4f$ electrons in rareearth metals. In para-magnetic materials, the magnetic moment associated with each atom or molecule, arising from the orbital motion or spin of the electrons, is treated as non interacting. The application of a magnetic field tends to align the atomic moments towards parallelism with the field so as to produce an overall magnetization in the specimen. At a finite temperature the effect of thermal agitation is towards reducing the alignment. Theoretically perfect alignment is achievable only at absolute zero temperature, when the thermal energy is zero or when the external magnetic field is infinitely large. This para-magnetic substances exhibit a positive susceptibility and the permeability is greater than 1. When there exists an interaction between the magnetic atoms in a solid occur some degree of alignment of magnetic moments even in the absence of any external magnetic field. This type of materials are called ordered magnetic materials. Ferro-

magnetism, Ferri-magnetism and anti Ferri-magnetism belong to this class of magnetic materials. For ordered magnetic materials, the ordered arrangement of the magnetic cores of the elementary magnets is achieved with little external field. Therefore, it is evident that a very high internal field spontaneously comes in to play. In the case of ferro-magnetic substances the atomic moments are ordered on the crystal lattice with all the moments aligned parallel to each other at absolute zero of temperature. The effect of increasing temperature is to reduce the ordering until at the curie temperature T_c where the order is completely destroyed and the system is para-magnetic. When the system is ordered and the magnetic moments are anti parallel to each other the net moment is zero and the substance is called anti ferro-magnetic. Ferri-magnetism is a modification of this mechanism which results when the anti parallel moments in the sub lattices are unequal, so that there is a net overall magnetization.

2.1.2. Magnetization of Iron Aluminium Alloy System:

The modern theory of magnetization processes have been summarized in several books, Bozorth^{2.1}, Bates^{2.2}, Kneller^{2.3}, Chikazumi^{2.3} and Morish^{2.5} attempt to improve its rigor by replacing "domain theory" by "micro-magnetics". This has been also summarized by Shtrikman^{2.6}, Treves and Brown^{2.7}. In this form of the theory, still in its infancy, the body has usually been assumed rigid in order to simplify the problem. A general outline of the processes of magnetization for $Fe_{100-x}Al_x$ alloy system can be built up as follows. The magnetocrystalline and magnetostrictive forces together will define two or more easy directions-directions of lowest energy of magnetization at every point in materials. In a strain free single crystal these directions may be the same throughout a large volume, while in our material $Fe_{100-x}Al_x$ (where $x = 2, 8, 10, 12$ and 14) are polycrystalline and have irregular internal

stresses. They may vary rapidly from place to place. The simplest cases are those in which either the magnetocrystalline or the magnetostrictive effect is of overwhelming importance and the others can be neglected in finding the easy directions of magnetization. In the absence of an external field, the domains will be arranged so that every domain is magnetized in one of the local easy directions, with the additional requirement that the general and local demagnetizing field shall be as small as possible. The magnetization can increase only through actual rotation of the domain magnetization away from easy directions and closer to the field direction. This process of rotation against the action of forces of anisotropy usually requires much larger fields than those needed for the translational movement of domain walls. Magnetocrystalline anisotropy plays an important part in the behaviour of nearly all ferromagnetic materials. Weiss showed that magnetic properties could depend strongly on crystal orientation. Akulov^{2.8} extended the idea of a direction dependent energy of magnetization to give a formal theory. He suggested that the effect of magnetocrystalline forces could be represented by a magnetocrystalline energy term in the expression for the free energy of the crystal. This magnetocrystalline energy would of course, depend on the direction of the domain magnetization relative to the crystal lattice and Akulov^{2.9} expressed it by a series of ascending power of $\alpha_1, \alpha_2, \alpha_3$, the direction cosines of the magnetization relative to the principle axes of the crystal. The symmetry conditions cause many terms in the series to drop out since the final energy expression must be independent of a change in sign of any of the α 's or interchange of any two of them. However, in our investigation, we have used a simplified expression for the distortion accompanying a given state of magnetization. The co-efficient appearing in this treatment for polycrystalline alloys has less fundamental significance than those of Becker's fuller treatment.

2.1.3. Intrinsic Magnetization of Alloys

Almost all magnetic alloys contain at least one of the three ferro-magnetic metals Iron, Cobalt or Nickel which exhibit ferro-magnetism at room temperature. By alloying these metals with other elements, we can prepare magnetic substance which have various magnetic properties. The properties of magnetic materials depend on chemical composition, fabrication and heat treatment. These properties are mainly determined by the magnetic anisotropy, magnetostriction and secondary structure of the substances. The intrinsic magnetization of an alloy is determined by its electronic structure.

On the basis of an elementary knowledge of atomic structure two possible origins are proposed for the atomic magnetic moment. One of these is the orbital motion of the electron around the nucleus and the other is a spin motion of the electron about its own axis. Ferro-magnetism has its origin in the spin and orbital magnetic moments in an unfilled electron shell. Each of the three ferro-magnetic element *Fe, Co, Ni* has an unfilled *3d* shell. Variation of atomic magnetic moment in these materials with the number of electrons in the $(3d+4s)$ shell is shown in figure-2.1. This curve is usually referred to as the Slater^{2.10}-Pauling^{2.11} curve. The average atomic magnetic moments of various alloys depend only on the number of electrons per atom. This is reasonable when the alloying atoms are only one or two atomic numbers apart as in the series *Ni-Cu* and *Fe-Ni* alloy.

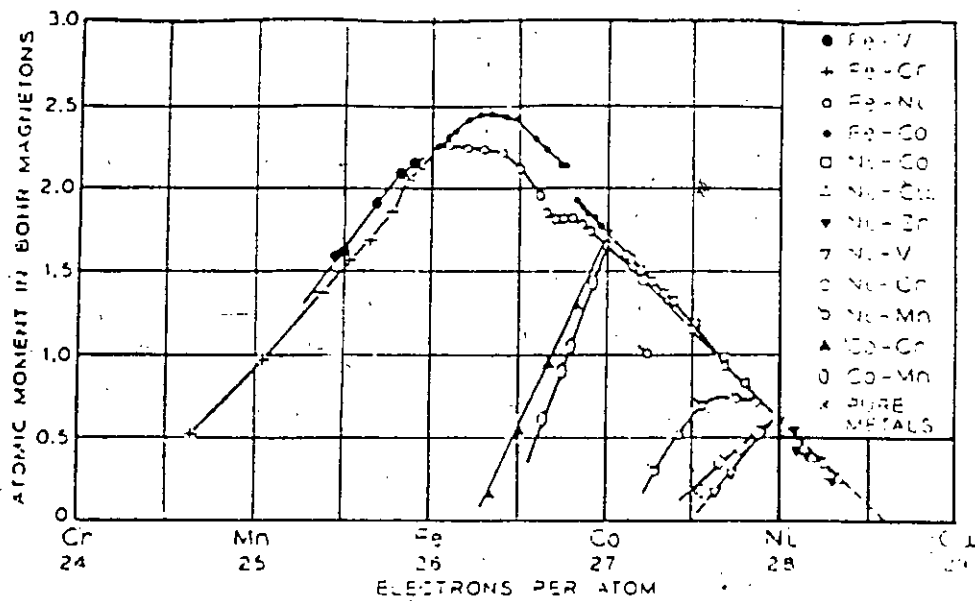


Fig. 2.1 : Slater-Pauling Curve

Most of the alloys are represented by points falling on a curve consisting of the two straight lines. One of these line rises from 0 Bohr magnetons at *Cr* at the rate of about $1\mu_B$ per electron, while the other falls from $2.5\mu_B$ at about 30 at% *Co-Fe* at the rate of about $-1\mu_B$ per electron. We have seen that ferro-magnetism, in *3d* transition metals appear for average electron concentration ranging from 24 to 28.6. Since the argon shell ($1s^1 2s^2 2p^6 3s^2 3p^6$) is filled by 18 electrons, the number of *3d* and *4s* electrons in these ferro-magnetic alloys ranges from 6 to 10.6. If we assumed that the number of conduction electron is about 1.0 at *Cr* and 0.6 at *Ni*, the number of *3d* electrons is then 5 to 10 in the range where ferro-magnetism is realized.

For a particular pair of atoms, situated at a certain distance apart, as in the case of a hydrogen molecule, there are certain electrostatic attractive forces between the electrons and protons and repulsive forces between the two electrons and between the two protons. These can be calculated by Coulomb's law. But there is still another force, entirely non-classical, which depends on the relative orientation of the spins of the two electrons. This is the exchange force. If the spins are anti-parallel, the sum of all the forces is attractive and a stable molecule is formed. The total energy of the atoms is then less for a particular distance of separation than it is for smaller or larger distances. If the spins are parallel, the two atoms repel one another. The exchange force is a consequence of the Pauli's exclusion principle applied to the two atoms as a whole. This principle states that two electrons can have the same energy only if they have opposite spins. If their spins are parallel, the two electrons will tend to stay far apart. The ordinary (Coulomb) electrostatic energy is therefore modified by the spin orientations. This means that the exchange force is fundamentally electrostatic in origin. The term exchange arises in the following way. When the two atoms are adjacent, we can consider electron-1 moving about proton-1 and electron-2 moving about proton-2. But the electrons are indistinguishable, and we must also consider the possibility that the two electrons exchange places. So that electron-1 moves about proton-2 and electron-2 moves about proton-1. This consideration introduces an additional term, the exchange energy, into the expression for the total energy of the two atoms. This interchange of electrons takes place at a very high frequency about 10^{18} times per second in the hydrogen molecule.

In order to explain the appearance of ferro-magnetism it is essential to identify the physical origin of the molecular field proposed by Weiss^{2.12} which give rise to the parallel alignment of spins. The accepted interpretation of the nature of the molecular

field as presented by Heisenberg^{2,13} in 1928 is quantum mechanical in origin. The potential energy between two atoms having spins s_i and s_j is given by

$$w_{ij} = -2Js_i s_j \quad 2.1$$

where J is the exchange integral. If J is positive the energy is least when s_i is parallel to s_j . When s_i is parallel to s_j , the exchange integral J is positive and the energy will be minimum and when s_i is anti parallel to s_j , the exchange integral J is negative.

The spin configuration can be explained on the basis of localized model and itinerant or collective electron model. According to localized model, the electrons responsible for ferro-magnetism are regarded as localized at the respective atomic sites. Most ferro-magnetic oxide, compound and rare earth metals can be explained in terms of localized model. For itinerant or collective electron model, electrons responsible for ferro-magnetism are thought of as wandering through the crystal lattice

According to the localized moment theory, the electrons responsible for ferro-magnetism are attached to the atoms and can not move about in the crystal. These electrons contribute a certain magnetic moments to each atom and that moment is localized at each atom. This view is implicit in the molecular field theory, either in the original form given by Weiss or in the quantum mechanical form obtained by substituting the Brillouin function for the Langevin. This theory in general explain the variation of the saturation magnetization σ_s with temperature and the Curie-Weiss law, at least approximately above T_C .

But it can not explain the fact that the observed moment per atom M are non integral for metals. Since the moment is entirely due to spin, the magnetic moment per atom due to localized electrons, should be an integer. Other defects of the theory are that M and the molecular field constant are different above and below the Curie temperature.

The collective electron theory emphasize the fact that the electrons responsible for ferro-magnetism are consider to belong to the crystal as a whole. Here the electron can move from one atom to another rather than being localized at the position of atoms. This theory accounts quite naturally for the non integral values of the moment per atom. It also explains fairly well the relative magnitudes of M in iron, cobalt and nickel and the value of the average magnetic moment per atom in certain alloys. These are important accomplishment of the theory. However, the band theory, at least in its simple form, can not account for these alloys which depart from the Slater-Pauling curve.

The general conclusion is that the molecular field theory, with its attendant assumption of localized moments, is not simply valid for metals. Instead the band theory is regarded basically correct, and the problem then becomes understanding the precise form of the various bands, how they are occupied by electrons and how the exchange forces operate etc.

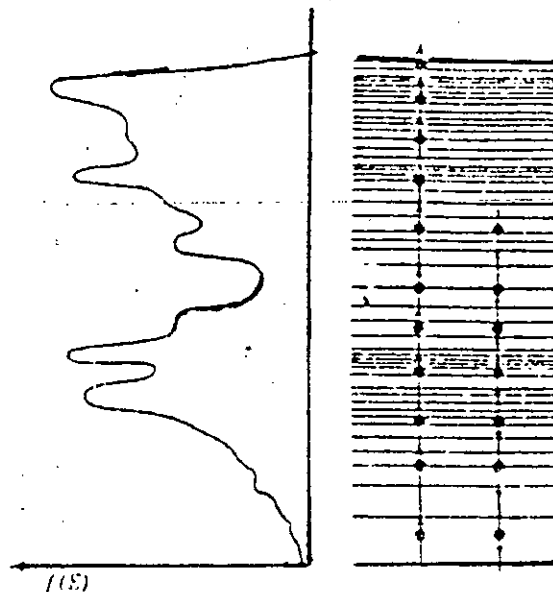


Fig. 2.2 : State-density curve of 3d band of Nickel and the arrangement of spins in the band

The band theory of ferro-magnetism was first proposed by Stoner^{2.14} and later by Slater^{2.15}. On the basis of the knowledge of the density of states in the $3d$ shell of copper as calculated by Krutter^{2.16}. Slater assumed that the density of states in nickel may be also very high at the top of the $3d$ band as it is for copper. Figure-2.2 shows the density of state in the $3d$ shell of nickel as a function of energy as calculated recently by Koster^{2.17}. Figure-2.2 shows schematically the corresponding energy level, each of which can be occupied by two electrons, one of plus spin and one of minus spin (Pauli principle) is also shown in Figure-2.2. In order to have a net magnetic moment, therefore, it is necessary that some minus spin electron be excited to higher energy levels and reverse the sign of their spins from minus to plus. Such an excitation should not require too much energy in the case of $3d$ shell because of the high density state.

If therefore, a positive exchange interaction is acting between $3d$ electrons the number of plus spins should increase until they fill up half of the $3d$ shell, having vacant levels in the other half. Then the net magnetic moment will be proportional to the number of vacant levels in the $3d$ shell. In that case, if we add one electron to the atom, this addition should result in a decrease of 1 Bohr magneton per electron because the electrons into a vacant minus spin level. In this way we can understand the -45° inclination of the right half of the Slater-Pauling curve. The $+45^\circ$ slope of the left half of the Slater-Pauling curve has been less adroitly treated by the band theory. One possible explanation is that, if the high density or states portion at the top of the $3d$ band is able to contain 2.5 electrons, the plus spin band remains full until the minus spin band loses 2.5 electrons. Further loss of electrons would deplete the plus spin band because otherwise the Fermi surface of the minus spin band might drop to too low level. The loss of plus spin electrons then results in a decrease of atomic magnetic moment.

Zener^{2.18} tried to explain this point in terms of anti ferro-magnetic alignment of two kinds of atomic moments, $+5\mu_B$ and $-1\mu_B$ for iron, on the two substances of the body-centered cubic lattice.

2.1.4. Theory of Magnetization

The interaction between the spins in a magnetic field H_w is proportional to the net magnetization.

$$H_w = N_w I \quad 2.2$$

It is to be emphasized that the interaction between the spins can not be due to a magnetic field. The magnetostatic field arising from the magnetic dipole action is not sufficient to bring about any alignment. In fact, it require a field of the order of 10^7 oersted for Iron. The model of the Weiss molecular field is purely phenomenological but is of great assistance in the development of the necessary theory.

The Weiss theory is a development of the Langevin model. The interacting field H_w is taken as proportional to the intensity of magnetization I . So that in place of the energy term in μH in the equation we have

$$\mu H_{eff} = \mu(H + N_w I) \quad 2.3$$

Where H_{eff} is the effective field acting on the atomic moment and N_w is the Weiss co-efficient. At high temperature the expression for the susceptibility becomes

$$X = \frac{\sigma}{H} = \frac{C}{T - \theta_c} \quad 2.4$$

where

$$C = \frac{\sigma_0^2}{3K_A}, \quad \text{and} \quad \theta_c = \frac{NP\sigma_0^2}{3mK} = N_w PC \quad 2.5$$

and $\sigma_0 = n\mu$ is the saturation magnetization per gm. below the curie temperature θ_c , the system is ferro-magnetic with the magnetization given by the Brillouin function $B(\alpha)$ i.e $\sigma/\sigma_0 = B(\alpha)$ with α in zero applied field is given by

$$\alpha = \mu \frac{H_0}{kT} = \mu n \rho \frac{\sigma}{kT} \quad 2.6$$

The derivation of the saturation magnetization at a temperature T requires the simultaneous solution of equation (2.4) and (2.5). The evaluation of the saturation magnetization from the measurement of magnetic moment of a specimen requires extrapolation as σ varies with the field. Results for a given temperature T are usually expressed as σ_{0T} extrapolated to $H=0$ or σ_{∞} extrapolated to $H=\infty$, the former is more usual but the choice depends on the results. The value of σ at 0°K is written σ_{00} or $\sigma_{0\alpha}$. The saturation magnetization may also be expressed in Bohr magnetons μ_B per atom. This should be written n_{00} or n_{0T} but n_B is in common usage for both. The saturation magnetization per gm atom $\sigma_{0\alpha} = 5586n_B$, the atomic moment n_B may also be derived from the results of neutron diffraction. The values of n_B at 0°K corresponds to the atomic moment $jg\mu_B$ given by the modified weiss treatment. The magnetic moment derived from the saturation magnetization is $n_B = jg\mu_B$ compared with the effective moment

$$P = g\mu_B \sqrt{j(j+1)} \quad 2.7$$

can be derived from susceptibility measurements.

2.1.5. Magnetization of Polycrystalline specimen

For a specimen with its grains oriented quite at random, Gans^{2.19} obtained expressions for the magnetization in the form of a series of powers of H , giving the curve shown in Figure-2.3.

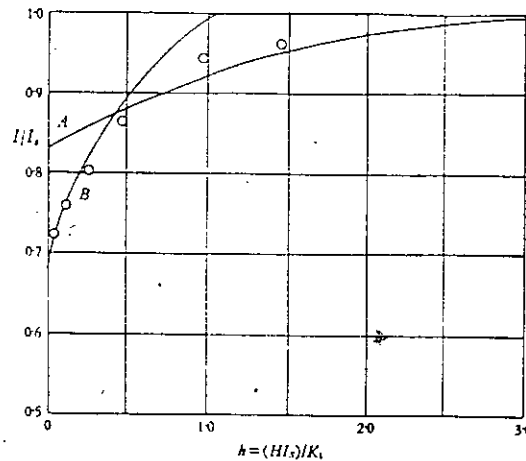


Fig. 2.3 : Magnetization of polycrystalline ferromagnetics materials as a function of reduced field

It is clear that Gans treatment is inadequate, except possibly in very high fields, for it assumes that each crystal grain is subject only to the external field and ignores the effects of the demagnetizing fields that will be set up by the discontinuities in magnetization at the boundaries between grains. It is nearer the truth to assume that the magnetization in each grain is very nearly the same and equal to the mean magnetization of the specimen. Any deviation from this mean value will produce divergences in the magnetization vector and give rise to demagnetizing fields that tend to restore the uniformity of magnetization. It is difficult to say with what precision this uniformity of magnetization will be maintained. Since the size of demagnetizing field produced by any given deviation of the magnetization will depend on the effective

demagnetizing coefficient for the particular crystal grain, a quantity determined by the shape of the grain and the properties of the surrounding grains.

2.1.6. The Approach to Saturation Magnetization

The general form of the law of approach to saturation was indicated by Weiss^{2.20} If the effect of a magnetic field is to turn the magnetization vectors towards itself, the turning being resisted by internal forces, then the law of approach to saturation, when the vectors of field and magnetization are nearly parallel, must be of the form

$$I = I_s(1 - b/H^2) \quad 2.8$$

This follows from the equation for the equilibrium direction of magnetization.

$$HI_s \sin\theta = C \quad 2.9$$

Where θ is the angle between the field H and the magnetization vector I_s and C is the couple due to internal forces resisting rotation of the magnetization. For sufficiently small angle, C can be assumed independent of θ and the magnetization in the field direction. $I_s \cos\theta$ can be written $I_s(1 - \frac{\theta^2}{2})$ giving the law of approach to saturation,

$$I = I_s[1 - C^2 / (2I_s^2 H^2)] = I_s(1 - b / H^2) \quad 2.10$$

Akulov^{2.21} was the first to calculate the values of b assuming that magnetocrystalline forces were the only important ones and his method was followed by Gans and Becker and Doring^{2.22}. They derived values of the coefficient b for a single crystal with any given orientation. By averaging overall possible orientation, obtained a mean value which should apply to polycrystalline specimens with their grains oriented at random. Experimental results have usually been expressed in the form

$$I = I_s(1 - a/H + b/H^2 - \dots) + \chi H \quad 2.11$$

The last term representing an increase in magnetization due to increase in the intrinsic magnetization of the material. The value of χ can be calculated on the basis of the simple Weiss-Heisenberg theory. Observed values are several times larger than this calculated value but Holstein and Primakoff^{2.23}. They have shown that the discrepancy can be removed by more detail quantum mechanical considerations. The most complete experiment near saturation are those of Weiss and Forrer^{2.24} and Czerlinski^{2.25} for iron and Polley^{2.26} for nickel.

An explanation of the a/H term was given by Brown^{2.27} in terms of several local stresses in the material but this explanation has been criticized by Neel^{2.28} who reinforces Weiss's demonstration that the law of approach must be of the form $I = I_s(1 - b/H^2)$ in sufficiently high fields by pointing out that a law $I = I_s(1 - a/H)$ would lead to an infinite energy at saturation. Neel attributes the discrepancies between experiment and the Akulov theory where he neglects interaction between grains of the polycrystal, the demagnetizing effects. He shows that it is only when $H \gg 4\pi I_s$, i.e. in fields greater than any so far used, that these interactions become negligible and the simple Akulov theory can be applied. In fields lower than this, but still so high that all magnetization lies very close to the field direction, exact expressions taking account of the interactions between the grains have been obtained by Neel and Holstein and Primakoff^{2.29} using Fourier series method of representing the structure of a polycrystal. They show that in the two extreme cases $H \ll 4\pi I_s$ and $H \gg 4\pi I_s$ the law of approach to saturation takes the form $I = I_s(1 - b/H^2)$, the constant b having the value which tends to be just half of this in the low field region. In the intermediate region the law is complicated but can in practice be reduced approximately to the form

$$I = I_s(1 - a/H) \quad 2.12$$

2.2. Magnetostriction

2.2.1. Introduction to Magnetostriction

Akulov^{2.30} introduced the concept of magnetostriction for the first time and developed a simple expression to describe the magnetostriction of a cubic crystal. Becker and Doring^{2.31} developed the original analysis about the magneto-elastic interaction. Mahajani^{2.32}, Hirone^{2.33} and Fallot^{2.34} flourished the subject by their outstanding contributions. Modern concept has been given by Stoner^{2.35}, Neel^{2.36}, Vanvleck^{2.37}, Brown^{2.38}, Kittel^{2.39} and many others. A comprehensive review of magnetostriction is given by Lee^{2.40}, Carr^{2.41}, Karamuri^{2.42}, Birss^{2.43} and Asgar^{2.44}.

Magnetostriction is the name given to the changes of size and shape which accompany the magnetization of a ferro-magnetic specimen. Such changes were first noticed by Joule^{2.45} in 1842 and have since been studied by many workers. Eventually Becker (1930) and Akulov (1931) became successful in providing the outline of the formal theory of magnetostriction and showed how it could be used to elucidate the more important experimental results. Becker and Doring (1939) used a formal expression which is written down for the dependence of the free energy of a crystal on the direction of magnetization on the mechanical distortion. This is analogous to, but more general than Akulov's expression for magneto-crystalline energy, since it refers to a distorted crystal. Kittel (1949) tried to find out the nature of free energy and magneto-crystalline energy of *Ni* and *Fe* metal. He calculated magnetostriction of these metals but the results were smaller by one order of magnitude than the observed values. This encouraged Masumoto and Otomo^{2.46} (1950) to investigate

magnetostriction of Iron-Aluminium alloys system. They made a compromise of large value of magnetostriction constants with small value of anisotropy constant.

The equilibrium state of magnetization and distortion in given conditions of field and stress can be found by minimizing the free energy. Various simplifying assumptions have to be made to obtain manageable formulae. Brown clarified the concept of electric or magnetic force in a polarized material. It therefore, did not treat magnetostriction specifically. Brown applied the theory to one special problem in magnetostriction in 1953. The problem was investigated further in 1960 by Gersdorf^{2.47} In all these papers the concept of strain, when it occurred, was handled by use of the small displacement approximation usual in physical theory. Lee^{2.48} tried to correlate these various assumption by measuring magnetostriction and magneto-mechanical effect of poly-crystalline Ni at different temperature. He also measured the thermal expansion of Ni. In the treatment of magnetostriction, despite the smallness of the strains actually encountered experimentally, the small displacement approximation leads to certain difficulties. A formal treatment of the analogous electric problem, based on the rigorous equations of finite strain theory, was published by Toupin^{2.49} in 1956. Toupin's treatment requires some modifications, beyond the mere replacement of electric by magnetic quantities for the case of a ferro-magnetic material with a spontaneous magnetization caused by exchange forces. The resulting modified theory was presented by Brown^{2.50} Meanwhile, Tiersten^{2.51} has published an equivalent theory. It is clear from these treatment that magnetostriction can be regarded as a consequence of strain dependence of magneto-crystalline energy and co-efficients introduced in the theory which can be determined by comparison with experiment define the dependence. Corner and Hutchinson^{2.52} (1958) investigated the variation of saturation magnetostriction of Ni with temperature variation in the (111) and (100) direction. Hall^{2.53} reported the saturation magnetostriction in (100) and (111)

crystallographic direction of Iron-Aluminium alloy. In the same year Birss^{2.54} computed the saturation magnetostriction of ferro-magnetic materials. The large value of λ_{100} encouraged Borodkina et al^{2.55} to investigate the possibility of improving λ_s via texture control. He prepared a sheet material by rolling to thickness reduction of 50-60% sandwiched and by intermediate annealing at about 900°C. X-ray examination showed that in the rolled condition the ideal sheet texture contained three prominent component (111) (112), (100) (011) and (112) (110). The first being the strongest, the saturation magnetostriction is fairly low between 10 and 20×10⁻⁶ with 45° direction having the highest value. After a two hour anneal at 900°C, the sheet recrystallized to a dual texture of <110> (001) and <100> (00) with the value of λ_s rising to 42×10⁻⁶ in the rolling direction. The texture is still far from perfect, however as λ_{100} is over 90×10⁻⁶ for alloy. If the rolled sheet is annealed at temperature greater than 900°C the texture become diffuse and λ_s is decreased. Latter on Bulycheva, Borodkina and Sandomirskaya^{2.56} carried out an extensive work on this process and showed that oriented materials can be made with $\lambda_s \approx 75 \times 10^{-6}$. Legvold, Alstad and Rhyne^{2.57}, Clark, Bozorth and Desavage^{2.58}, Rhyne and Legvold^{2.59} made a breakthrough in magnetostrictive materials that is found to occur with the measurement of the basal plane magnetostriction of Tb and Dy at low temperature. These basal plane strains are 100 to 10,000 times. Typical magnetostriction of these rareearth metals still remain today the largest known values, about 1%. In the same year Tatsumoto, Okumoto, Iwata and Kadana^{2.60} measured the value of magneto-crystalline anisotropy constants K_1 and K_2 of Nickel. Aubert^{2.61} studied the Nickel and observed the temperature dependence of the anisotropy constants. Asgar^{2.62} carried out extensive investigation of single crystal Ni sample for the measurement of magnetostriction and magneto-elastic coupling factors in which he has related the magnetostriction co-efficients with magneto-elastic coupling co-efficients and successfully separated the various temperature dependences. Elastic and magneto-

elastic constants of ReFe_2 compound were studied by Klimker, Rosen, Dariel and Atzmony^{2.63} by means of ultrasonic sound velocity measurements. These properties, together with rather impressive magnetostriction properties of binary and pseudo-binary $R\text{-Fe}_2$ compounds are shown by Clark^{2.64}

The standard treatment of magneto-elastic interaction is given by Becker and Doring^{2.65}, Lee and Asgar^{2.66}. They state that the free energy expression can be written down for a magnetizable body incapable of deformation and for an elastic body incapable of magnetization. To the sum of these is added an interaction term in the form of volume integrals of an interaction energy density of phenomenologically acceptable form. Every thing else follows from this by exact or approximate minimization procedures. Savage, Clark and Power^{2.67} worked with $\text{Tb}_x\text{Dy}_{1-x}\text{Fe}_2$ sample and calculate the magneto-mechanical coupling and ΔE effect. For $x=0.26$ their result for peak coupling is 0.6. Asgar^{2.68} calculated the magneto-elastic interaction and its relation to the development of magnetic materials. In his paper he detailed out the strain gauge technique for evaluation of magnetostriction constants. N.C. Koon, C.M. Williams and B.N. Das^{2.69} carried out an extensive experiment on giant magnetostrictive materials of a new class of rareearth intermetallic compounds. The $R\text{Fe}_2$ laves phase, which were found to exhibit room temperature magnetostrictive strain and the reported value approaches 2×10^{-3} which is an order of magnitude larger than any values previously known. Greenough, Jenner, Schulze and Wilkinson^{2.70} investigated the properties and application of magnetostrictive rareearth iron compounds. Folks, Milham and Street^{2.71} examined the rareearth iron compounds and their works was mainly to observe the magnetic viscosity at low temperature.

In the present work magnetostriction of polycrystalline Iron-Aluminium alloy and Iron Terbium Dysprosium have been measured systematically at room temperature.

2.2.2. Theory of Magneto-Elastic Energy

The magneto-elastic energy is proportional to $\epsilon f(\alpha)$. This term in order to process the correct transformation properties of the crystal, must be a direct product of strain components and direct cosine polynomials which transform according to the same symmetry representation given by Callen and Callen^{2.72}. Asgar^{2.73} explicitly explained and developed theoretical basis of magneto-elastic coupling which is stated below.

For non-S-state ions the orbital angular momentum has non zero value of L with $(2l+1)$ degeneracy in the lowest energy ground state. The orbital charge distribution for these ions is highly asymmetrical. When these paramagnetic ions are surrounded by a crystalline electric field within crystal, the orbital degeneracy is removed and the resultant wave functions form new linear combinations which reflect the local symmetry of the crystal. The charge distributions with lobes directed towards negatively charged anions will be relatively less favourable compared with charge distribution having lobes directed between anions. If the neighbouring anions are displaced due to straining of the crystal, the charge distribution lobes will also move to a new configuration to minimise the energy. The rotation of the charge distribution lobes alters the orbital angular momentum and hence the spin angular momentum because of spin-orbit coupling.

The magnetization associated with spin will thus be rotated. Spin-orbit coupling also contributes to the anisotropy by way of another mechanism called anisotropic exchange introduced by Vanvleck^{2.74}. If the wave functions are asymmetrical, the amount of overlap of two neighbouring ions will change when the parallel spins of the two ions are rotated by the spin orbit coupling. Since the exchange coupling is related

to the amount of overlap, the exchange energy will vary with the orientations of the orbital moments of the neighbouring atoms relative to one another and the axis joining them.

For-S-state ions orbital angular momentum is zero and the charge distribution is symmetrical. However the spherical distribution is somewhat distorted by the crystal field. The spin-orbit coupling thus contributes to the anisotropy energy and magnetostriction in this case as well, although of much smaller magnitude.

2.2.3. Physical Origin of Magnetostriction

Magnetostriction is due mainly to spin-orbit coupling. This coupling is also responsible for the creation of anisotropy energy. The relation between the magnetostriction and spin-orbit coupling can be developed from the Figure-2.4. The block dots represent atomic nuclei. The arrows show the net magnetic moments per atom and the oval lines enclose the electrons belonging to and distributed non spherically about each nucleus. The upper row of atom depicts the para magnetic state above T_c . If for the moment we assume that the spin orbit coupling is very strong then the effect of the spontaneous magnetization occurring below T_c would be to rotate the spins and the electron clouds in to some particular orientation determined by the crystal anisotropy left to right, the nuclei would be forced further apart and the spontaneous magnetostriction would be $\Delta L/L$. If we then apply a strong field vertically, the spins and the electron clouds would rotate through 90° and the domain of which this atom are a part would magnetostrictively strain by an amount $\Delta L/L$.

The spin orbit coupling thus contributes to the anisotropy energy and the magnetostriction is small in magnitude. Exchange energy can make contribution to

and the electron clouds would rotate through 90° and the domain of which this atom are a part would magnetostrictively strain by an amount $\Delta L/L$.

The spin orbit coupling thus contributes to the anisotropy energy and the magnetostriction is small in magnitude. Exchange energy can make contribution to magnetoelastic energy due to the strain dependence of the exchange integral J_{ij} . When the magnetic moments of neighbouring ions are rotated away from parallelism. The exchange energy while increasing the elastic energy gives rise to magnetostriction.

There are three mechanism of anisotropy:

1. Crystal field anisotropy
2. Exchange anisotropy
3. Exchange striction

Which is shown schematically in Figure-2.4a, 2.4b and 2.4c respectively



(a). CRYSTAL FIELD ANISOTROPY



(b). EXCHANGE ANISOTROPY



(c). EXCHANGE STRICTION

Fig. 2.4 Physical Origins of Magnetostriction.

2.2.4. Mechanism of Magnetostriction

Expression for Linear Magnetostriction:

Magnetostriction is developed due to interaction between the atomic magnetic moment, when the distance between the atomic magnetic moments is variable, Neel's developed a theory which represent the interaction energy

$$W(r, \cos \phi) = g(r) + l(r)(\cos^2 \phi - \frac{1}{3}) + q(r)(\cos^4 \phi - \frac{6}{7}\cos^2 \phi + \frac{3}{35}) \pm \dots \quad 2.14$$

Upon the generation of magnetic ordering the crystal lattice is spontaneously deformed because of the dependence of the interaction energy on bond length. The amount of deformation of bond length will depend on its direction with respect to the magnetization direction through the angle ϕ . The first term $g(r)$ is the exchange interaction term and is of relevance only when volume magnetostriction is considered as manifested in thermal expansion anomaly at the magnetic ordering temperature.

The second term represent the dipole-dipole interaction which depend on the direction of magnetization and can be the main origin of the usual magnetostriction. The following terms also contribute to the usual magnetostriction but normally their contribution are small compared to those of the second term. Neglecting this higher order terms, the equation-2.14 becomes

$$W(r, \phi) = l(r)(\cos^2 \phi - 1/3) \quad 2.15$$

Let $(\alpha_1, \alpha_2, \alpha_3)$ denote the direction cosine of domain magnetization and $(\gamma_1, \gamma_2, \gamma_3)$ those of bond diameter then the equation-2.15 becomes

$$W = l(r)[(\alpha_1\gamma_1 + \alpha_2\gamma_2 + \alpha_3\gamma_3)^2 - 1/3] \quad 2.16$$

Considering a deformed cubic lattice and relating the direction cosine γ_I to the strain tensor L_{ij} , we can get the expression for magneto-elastic energy. Since the magneto-elastic energy has a linear dependence on strain, the crystal will deform without limit unless it is counter balance by elastic energy which increases rapidly because of its quadratic dependence on strain. By differentiating the total energy $E_T = E_{mag.elastic} + E_{elastic}$ with respect to the strain components and setting the partial derivatives equal to zero for minimum energy condition, we can obtain the relation as

$$-e_{ii} = \frac{b_0}{(a_{11} + 2a_{12})} + \frac{b_1}{(a_{11} - a_{12})} (\alpha_i^2 - 1/3) + b_3 \frac{S}{(a_{11} + 2a_{12})} + \frac{b_4}{(a_{11} + 2a_{12})} (\alpha_i^2 + 2/3 S - 1/3) \quad 2.17$$

$$-e_{ij} = \frac{b_2}{c_{44}} \alpha_i \alpha_j + \frac{b_5}{c_{44}} \alpha_i \alpha_j (1 - \alpha_i^2 - \alpha_j^2) \quad 2.18$$

The fractional change in length of the crystal in any arbitrary direction is given by

$$\lambda_B = \sum_{i,j=1}^3 e_{ij} \beta_i \beta_j \quad 2.19$$

Substituting the values of e_{ij} from equation-2.16 to equation-2.17 we get

$$\lambda_B = b_0 + b_1 (\sum \alpha_i^2 \beta_i^2 - 1/3) + 2b_2 c_{ij} (\alpha_i \alpha_j \beta_i \beta_j) + b_3 S + b_4 (\sum \alpha_i^2 \beta_i^2 + 2/3 S - 1/3) + 2b_5 c_{ij} \alpha_i \alpha_j (1 - \alpha_i^2 - \alpha_j^2) \beta_i \beta_j \quad 2.20$$

Where c_{ij} indicates a summation over terms with a cyclic permutation of the indices. For hexagonal crystals the relation become modified due to different symmetry condition and have been treated in detail by Mason and Lewis^{2,75}. For cubic crystal

$$\frac{\Delta l}{l} = 1/2 \lambda_{100} (\alpha_1^2 \beta_1^2 + \alpha_2^2 \beta_2^2 + \alpha_3^2 \beta_3^2 - 1/3) + 3\lambda_{111} (\alpha_1 \alpha_2 \beta_1 \beta_2 + \alpha_2 \alpha_3 \beta_2 \beta_3 + \alpha_3 \alpha_1 \beta_3 \beta_1) \quad 2.20$$

Where λ_{100} and λ_{111} indicates strain along (100) and (111) direction respectively. Thus the magnetostriction of a cubic crystal may be expressed in terms of λ_{100} and λ_{111} . The elongation in (110) is not independent of λ_{100} and λ_{111} but is related to them by

$$\lambda_{110} = 1/4 \lambda_{100} + 3/4 \lambda_{111}$$

If $\lambda_{100} = \lambda_{111} = \lambda$ then equation-5 becomes

$$\frac{\Delta}{l} = \frac{3}{2}\lambda[(\alpha_1\beta_1 + \alpha_2\beta_2 + \alpha_3\beta_3)^2 - \frac{1}{3}] = \frac{3}{2}\lambda(\cos^2 \theta - \frac{1}{3}) \quad 2.22$$

For polycrystalline materials the longitudinal magnetostriction is calculated by averaging equation -2.20 for different crystal orientations by assuming $\alpha_i = \beta_i$ where $i= 1,2$ and 3 thus

$$\lambda = \frac{2}{3}\lambda_{100} + \frac{1}{3}\lambda_{111} \quad 2.23$$

2.2.5. Magnetostriction of Polycrystal

The saturation magnetostriction of polycrystalline specimen parallel to the magnetization is characterized by a single constant λ_p . Its value depends on the presence or absence of preferred domain or grain orientation. If the grain orientations are completely random, the saturation magnetostriction of the polycrystal should be given by some sort of average over the orientations. When a polycrystal is saturated by an applied field, each grain tries to strain magnetostrictively in the direction of the field by a different amount than its neighbours because of its different orientation. One of the two extreme assumptions may then be made

1. Stress is uniform throughout but strain varies from grain to grain.
2. Strain is uniform and stress varies from grain to grain.

The condition of the uniform strain is usually considered to be physically more realistic. For cubic crystal averaging equation-2.20 for overall orientation of the Ms vector with a set of fixed crystal axes. We first express $\alpha_1, \alpha_2, \alpha_3$ in terms of the angle θ and ϕ . The relations are

$$\alpha_1 = \sin \phi \cos \theta, \alpha_2 = \sin \phi \sin \theta \text{ and } \alpha_3 = \cos \phi \quad 2.24$$

on the surface of a sphere of unit radius centered on the origin, the element of area is $dA = \sin \phi d\phi d\theta$. Averaging over the upper hemisphere, we find the average value of λ_{si} to be

$$\lambda_{si} = \frac{1}{2} \int_{\theta=0}^{\pi} \int_{\phi=0}^{\frac{\pi}{2}} \lambda_{si} \sin \phi d\phi d\theta \quad 2.25$$

Substitution of equation-2.21 for λ_{si} and integration lead to

$$\lambda_{si} = \frac{2\lambda_{100} + 3\lambda_{111}}{5} \quad 2.26$$

2.2.6. Direction of linear Magnetostriction

Experiment have shown that the deformation depends upon the direction of magnetization. For a cubic material magnetized in the direction given by the direction cosines α_1, α_2 and α_3 with respect to the cube axes. This deformation is expressed in strain component ϵ_{ij} where $i, j = x, y, z$ become in the first approximation

$$\epsilon_{xx} = \frac{3}{2}\lambda_{100}(\alpha_1^2 - \frac{1}{3}), \epsilon_{yy} = \frac{3}{2}\lambda_{100}(\alpha_2^2 - \frac{1}{3}), \epsilon_{zz} = \frac{3}{2}\lambda_{100}(\alpha_3^2 - \frac{1}{3}) \quad 2.27$$

$$\epsilon_{xy} = \frac{3}{2}\lambda_{111}(\alpha_1\alpha_2), \epsilon_{yz} = \frac{3}{2}\lambda_{111}(\alpha_2\alpha_3), \epsilon_{zx} = \frac{3}{2}\lambda_{111}(\alpha_3\alpha_1)$$

The extra terms (-1/3) make the total change of volume null. Trace of the matrix is zero. The factors 3/2 ensure that the strain in the direction of magnetization with respect to the non magnetized state

$$(\alpha_1^2 = \alpha_2^2 = \alpha_3^2 = \frac{1}{3}) \quad 2.28$$

is λ_{100} and λ_{111} in the (100) and (111) directions respectively by the strain in a direction perpendicular to the field is $1/2\lambda_{100}$ and $1/2\lambda_{111}$ respectively. In an arbitrary direction we then have magnetostriction parallel to the magnetization is given as

$$\lambda(\alpha_1, \alpha_2, \alpha_3) = \lambda_{100} + 3(\lambda_{111} - \lambda_{100})(\alpha_1^2\alpha_2^2 + \alpha_2^2\alpha_3^2 + \alpha_3^2\alpha_1^2) + \dots \quad 2.29$$

In discussing the effect of a unidirectional stress it is convenient to divide materials in two classes which are

1. Positive magnetostriction
2. Negative magnetostriction

In materials of class-1 the magnetostriction is increased by tension and the materials expands when magnetized. In class-2, the magnetization is decreased by tension as a results materials contract when magnetized.

2.2.7. Magnetostriction Arising from Domain Rotation

Magnetostriction is associated with domain orientation. The change in dimension of a single domain can be rotated in a simple quantitative way to change in direction of magnetization in the domain as follows.

$$\lambda_1 = \frac{3}{2}\lambda_s(\cos^2 \theta - \frac{1}{3}) \quad 2.30$$

Here θ is the angle between the direction in which the change in length is measured. It is assumed now that magnetostriction is independent of the crystallographic direction of magnetization and that the change in volume is zero. The zero point of λ_1 is chosen so that the change in volume is zero. The zero point of λ_1 to the longitudinal change in length λ_s when $\theta=0$ at saturation. When the length is measured at right angle to the direction of magnetization (Transverse effect) $\theta=90$ and the change in length $\lambda=-\lambda_s/2$. For polycrystalline or amorphous materials the domain are initially oriented at random. The same relation is applicable if one uses the average of $\cos^2\theta$ overall the domains. When the materials is unmagnetized $\langle \cos^2\theta \rangle_{av} = 1/3$ and $\lambda=0$. Upon application of a strong field become zero and $\lambda = \lambda_s$. If the domain are not initially random, one can use the relation

$$\begin{aligned} \lambda &= \frac{3}{2}\lambda_s[\langle \cos^2 \theta \rangle_{av} - \frac{1}{3}] - \frac{3}{2}\lambda_s[\langle \cos^2 \theta \rangle_o - \frac{1}{3}] \\ &= \frac{3}{2}\lambda_s[\langle \cos^2 \theta \rangle_{av} - \langle \cos^2 \theta \rangle_o] \end{aligned} \quad 2.32$$

Where $\langle \cos^2\theta \rangle_o$ = Initial domain distribution

$\langle \cos^2\theta \rangle_{av}$ = Domain distribution at any time.

If the domain are oriented originally so that $\theta=0$ for half of them and $\theta=180$ for other half $\langle \cos^2\theta \rangle_o = \langle \cos^2\theta \rangle_{av} = 0$ the reference point in a strong field $\theta = 0$ and there

is no change in $\cos 2\theta$ and again $\lambda=0$. When used in this sense, λ depends decidedly on the initial domain distribution while λ_s can be determined in any specimen by measuring λ applying a saturation field applied first parallel and then at 90° to the direction of measurement of λ . The total change in length caused by the change in field in the polycrystalline materials is then

$\Delta l/l = 3/2 \lambda_s$ which is independent of initial domain distribution.

Chapter-3

MEASUREMENT OF MAGNETIZATION OF Fe-Al ALLOY SYSTEM:

3.1 Different Methods for the Measurement of Magnetization

The methods, so far used for measuring magnetization of para, dia and anti ferro-magnetic substances are grouped in to three major classes. These are as follows.

- (1) Extraction method
- (2) Vibrating sample method
- (3) Force method:
 - (a) Faraday method
 - (b) Sucksmith method
 - (c) Gouy method

3.1.1. Extraction Method:

This method involve the measurement of voltage or current which are induced in a directional coil by a flux change when the applied magnetic field, coil position or sample position is changed. Recently oscillatory coil or sample techniques have been used to observe the magnetization of a sample by an *a.c.* method. All of these techniques have employed an arrangement in which the detection coil is symmetrically distributed about the sample with the axis of the detection coil parallel to the applied magnetic field. One major disadvantage of such a method is that unless an air-core solenoid type magnet is used, the usual Laboratory magnet must be extensively modified. This method has

insufficient sensitivity when the susceptibility is small and it is normally limited to measurements at room temperature and below, because susceptibility decreases with increasing temperature for dia and antiferromagnetics materials.

3.1.2. Force Method:

There are various techniques for the measurement of magnetization by this methods. These include measurements using the Faraday effect, analysis of galvanomagnetic effects, ferromagnetic resonance measurements e.t.c. These methods are based on the measurement of the force acting on a body when it is placed in a non uniform magnetic field. An instrument designed for this purpose is usually called a magnetic balance.

Theory of Force Method:

If a body is placed in a uniform magnetic field, it will rotate untill its long axis is parallel to the field. The field then exerts equal and opposite forces in the two poles, so that there is no net force of translation. On the other hand, if the field is non uniform increasing from left to right, as shown in Fig. -3.1.

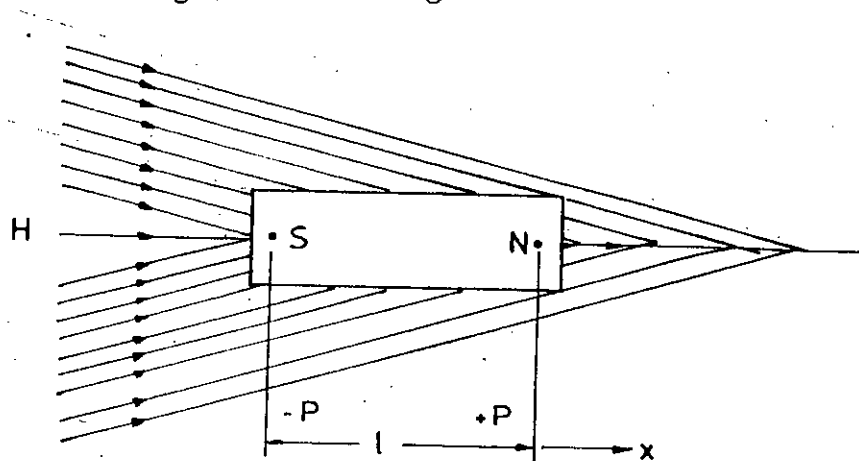


FIG. 3.1 A BODY IN A NON UNIFORM MAGNETIC FIELD (H)

a pole strength P will be produced. As the field is stronger at the north pole than at the south, there will be a net force to the right given by

$$F_x = -PH + P\left(H + \frac{dH}{dx}\right) = P\frac{dH}{dx} = m\frac{dH}{dx} = Mv\frac{dH}{dx} = \frac{M}{H}vH \quad 3.1$$

$$F_x = \chi v H \frac{dH}{dx} = \frac{\chi v}{2} \left(\frac{dH^2}{dx}\right)$$

Where m magnetic moment v volume of the body. Thus the body if free to do so, will move to the right i.e. in to the region of greater field strength. For dia-magnetic substances $\chi \Rightarrow$ -ve, its polarity in the field will be reversed and so it will move toward a region of lower field strength. That is why it is known as dia-magnetic substance which is repelled by the field. The phenomenon is shown in Figure-3.2.

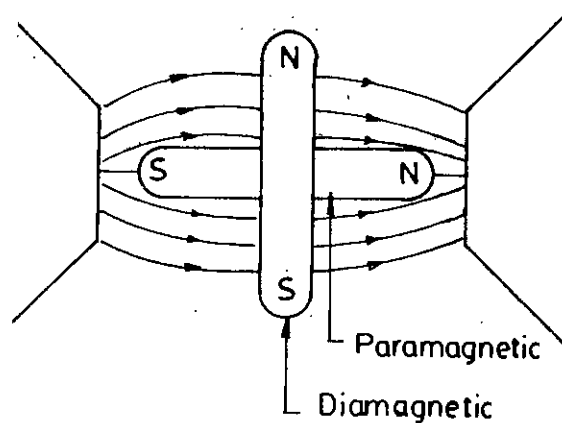


FIG. 3.2 POSITIONS OF DIAMAGNETIC AND PARAMAGNETIC SUBSTANCE IN MAGNETIC FIELD

If the field H is three dimensional, then

$$H^2 = H_x^2 + H_y^2 + H_z^2 \quad 3.2$$

and the force on the body along x-direction are

$$F_x = \frac{\chi v}{2} \left(\frac{\partial H_x^2}{\partial x} + \frac{\partial H_y^2}{\partial x} + \frac{\partial H_z^2}{\partial x} \right)$$

$$\text{or } F_x = \chi v \left(H_x \frac{\partial H_x}{\partial x} + H_y \frac{\partial H_y}{\partial x} + H_z \frac{\partial H_z}{\partial x} \right) \quad 3.3$$

It is often necessary to correct for the effect of the medium, usually air, in which the body is placed. As the susceptibility χ of the body may not be greater than the susceptibility χ_0 of the medium, the force on the body then becomes

It is often necessary to correct for the effect of the medium, usually air, in which the body is placed. As the susceptibility χ of the body may not be greater than the susceptibility χ_0 of the medium, the force on the body then becomes

$$F_x = (\chi - \chi_0)v(H_x \frac{\partial H_x}{\partial x} + H_y \frac{\partial H_y}{\partial x} + H_z \frac{\partial H_z}{\partial x}) \quad 3.4$$

because the motion of the body in the +x direction must be accompanied by motion of an equal volume of the medium in the -x direction.

3.1.3. Faraday Method:

In this method the specimen is small enough so that it can be located in the region where the field gradient is constant throughout the specimen volume. The experiment set up is shown in Figure-3.3.

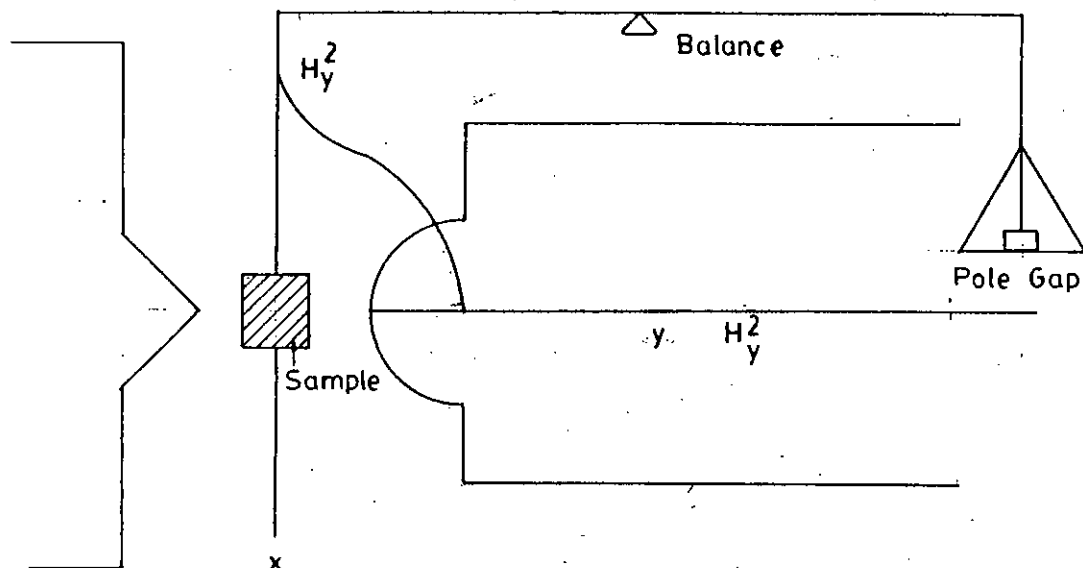


FIG. 3.3 EXPERIMENTAL ARRANGEMENT OF FARADAYS METHOD

The field predominantly in the Y -direction and in the region occupied by the specimen, H_x and H_z and their gradients with x are small. The variation of H_y^2 with x is shown by the curve superimposed in the diagram and it is seen that

$$\frac{dH_y^2}{dx} = (2H_y \frac{dH_y}{dx}) \quad 3.5$$

is approximately constant over the specimen length. Equation 3.4 then become

$$F_x = (\chi - \chi_0) v H_y \frac{dH_y}{dx} \text{ dynes} \quad 3.6$$

F_x is measured by suspending the specimen and H_y and dH_y/dx will be measured by the flux-meter.

3.1.4. Gouy Method:

Where the volume of the sample available is not limited, the method originated by Gouy is useful. In this case, if the powder sample is packed in a long thin tube so that one end can be in the region of maximum field between the poles of the magnet and the other end in a virtually field free region outside the poles.

It is of course difficult to observe the magnetization in a truly uniform magnetic field. Since the field gradient is essential for the production of the force. Moreover this method is not easily adaptable to routine measurements of magnetization versus applied field for crystal with magnetocrystalline anisotropy. Objection to the use of force methods for magnetic measurement of highly anisotropic materials have recently been raised by Wolf.

3.1.5. Sucksmith Method:

By Sucksmith ring balance one can measure susceptibility of the order of 10^{-6} . It consists of a ring balance. The ring is of phosphor bronze of 10 cm diameter made from 0.5"×0.01" strip. Two mirrors M_1 and M_2 are cemented on it. The ring is suspended from above and the specimen is hung from it between the magnetic poles. As the specimen experiences a force the ring gets distorted and light beam reflected from M_1 and M_2 is deflected. The deflection is directly proportional to the force. The specimen can be enclosed in a furnace for high temperature measurements or a cryostat for low temperature measurements. Calibration is carried out by the use of a sample of known susceptibility.

3.1.6. Vibrating Sample Magnetometer:

The vibrating sample magnetometer is a highly sensitive and versatile equipment for measuring magnetization of small sample very accurately. It was first invented by "Van oster hout" in 1956. In the same year another V.S.M was constructed by Simon Foner independently. Because of some new and extra facilities of Foner^{3.1-3} instrument, it is largely used in research laboratories and known as Foner type magnetometer and its diagram is shown in Figure-3.4.

The most convenient arrangement is to drive either the sample or the detection coil with a vertical rod, which passes between the pole faces of the magnet. The vibrating coil technique has been developed by D.O. Smith and this technique has been used by M.A. Mazid, M.A. Chowdury and S. Akther^{3.4} to build the present V.S.M. in A.E.C. which has been used to measure the magnetization of the Fe-Al alloy samples.

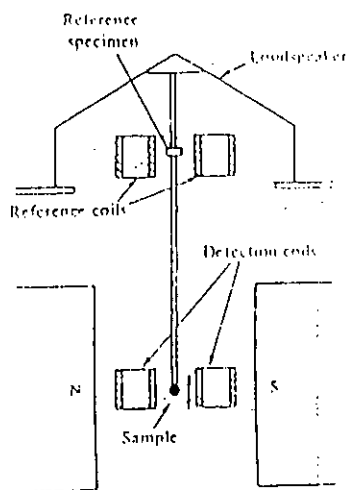


Fig. 3.4 : V.S.M. (Foner type)

The most convenient arrangement is to drive either the sample or the detection coil with a vertical rod, which passes between the pole faces of the magnet. The vibrating coil technique has been developed by D.O. Smith and this technique has been used by M.A.Mazid, M.A. Chowdury and S. Akther^{3,4} to build the present V.S.M. in A.E.C. which has been used to measure the magnetization of the Fe-Al alloy samples.

The V.S.M. is based on the flux change in a coil when the sample is vibrated near it. Sphere or disc shaped sample is glued to one end of the rod. The other end is connected to a loud speaker cone or to a mechanical vibrator. Current through the vibrator vibrates the rod and the sample with 80 cycles/sec and with an amplitude of about 0.1 mm in a direction at right angles to the magnetic field. The oscillating magnetic field of the sample induces an alternating e.m.f. in the detection coil. The vibrating rod also carries a reference specimen in the form of a small permanent magnet near its upper end. The oscillating field of this magnet induces another e.m.f. in the reference coils. The voltages from the two sets of coils are compared and the difference is proportional to the magnetic moment of the sample. The flux change induces an e.m.f. signal proportional to the magnetization of the sample in two pick-up coils placed symmetrically on either side

of the sample and connected in series to add up the e.m.f.'s. The axis of the coils are parallel to the direction of vibration of the sample. A reference signal is obtained by vibrating a permanent magnet of known magnetic moment inside a coil with the frequency and amplitude similar to the sample. Then the reference signal is brought in phase with the sample signal compared in a null-detector, i.e. lock-in amplifier. The magnetic moment produced by a current I through the primary coil is given by

$$\mu = \pi r^2 N_1 I \quad 3.7$$

where r is the radius of the primary coil and N_1 is the number of turns. The flux through one of the secondary coils of radius R and at a distance Z from the dipole is given by

$$\phi = \frac{\mu_0 \mu}{4\pi} \int_0^\pi \left[\frac{3x^2 \cos^2 \theta}{(z^2 + x^2)^{3/2}} - \frac{x}{(z^2 + x^2)^{3/2}} \right] 2\pi x dx = \frac{\mu_0 \mu}{2} \frac{R^2}{(Z^2 + R^2)^{3/2}} \quad 3.8$$

The induced e.m.f. in the secondary coils (N_2 turns) in add-up configuration is given by

$$E = - \left(\frac{\partial \phi}{\partial Z} \right)_{Z=Z_0} \frac{\partial Z}{\partial t} = - \left[\frac{\mu_0 \mu}{2} \left\{ \frac{\partial}{\partial Z} \left(\frac{R^2}{Z^2 + R^2} \right) \right\} \right]_{Z=Z_0} \frac{\partial Z}{\partial t} \quad 3.9$$

$$= \frac{3}{2} \frac{\mu_0 \mu R^2 Z_0 W \Delta Z_0 (2N_2) \cos \omega t}{(Z_0^2 + R^2)^{3/2}}$$

Where the instantaneous position of the primary coil is given by

$$Z = Z_0 + \Delta Z_0 \sin \omega t \quad 3.10$$

ΔZ_0 is the amplitude of vibration and ω is the angular frequency of vibration.

3.1.7. Vibrating sample Magnetometer coil arrangement and Field Distribution:

The advantage of sample vibration perpendicularly to the applied field can be fully utilized only if a suitable detection coil arrangements can be devised as part of the

vibrating dipole field. The scalar potential of fixed dipole M at the origin and pointed along the x - direction is given by the relation

$$\phi = \frac{M_x}{r^3} \quad 3.11$$

If M is vibrated in the z -direction with sufficiently small amplitude a , the time varying potential in the surrounding space will be $\phi_1 e^{i\omega t}$, Where

$$\phi_1 = -a \left(\frac{\partial \phi}{\partial z} \right) = \frac{a M_x z}{r^5} \quad 3.12$$

The flux pattern of the time varying part of the field is given by $\text{grad } \phi_1$. Its configuration in the xz plane is shown in Fig-3.5 with coils at 45° .

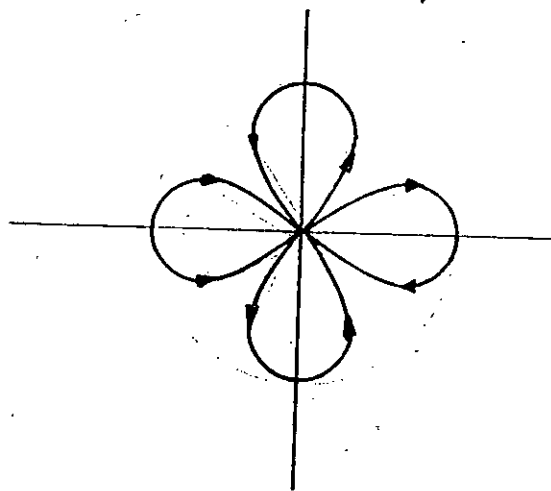


Figure 3.5: Time varying part of dipole field in x - z plane for vibration parallel to z and dipole moment parallel to x .

One of the most convenient detection coil arrangements is the use of double coils, shown in Fig. 3.6a. A special variations of relative output signal for two typical double coil assemblies are plotted in Figure-3.7 and 3.8. The coil configuration shown in Figure 3.6a has been employed extensively for almost all our magnetic measurements. This arrangement has proved both easy to assemble and most convenient in operation. Coils, shown in Figure-3.6c have the general characteristics features shown in Figure-3.7 and Figure-3.8. The arrangement of a single coil is useful when very high fields are required and is shown in Figure-3.6b. The out-put voltage in such a case can be maximized for position in the x or y direction, so that the out-put signal is then insensitive to small sample displacements in these directions.

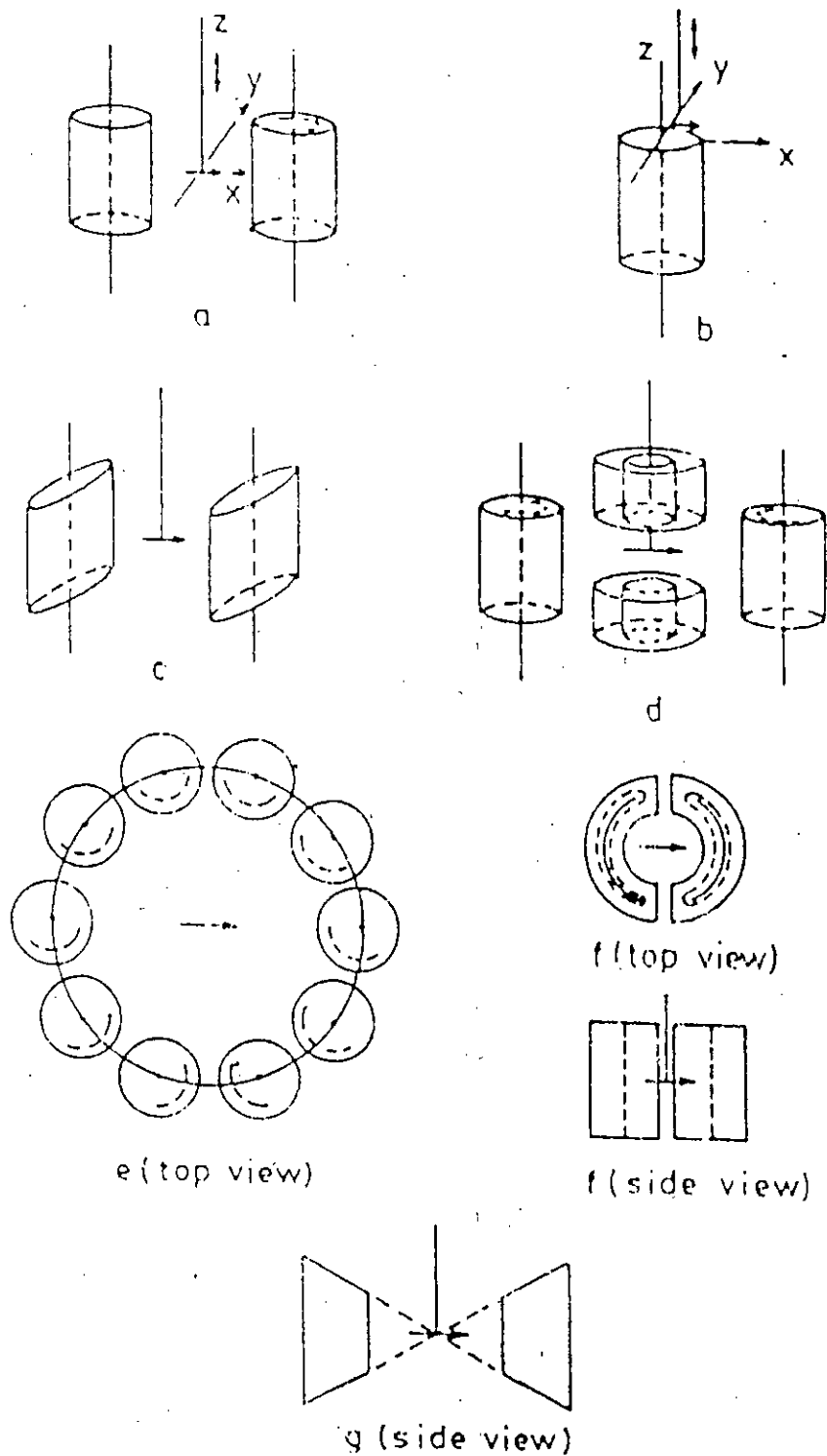


Fig 3.6 Examples of useful detection coil arrangements described in the text. The sample, indicated by the heavy arrow, is vibrated along the Z direction.

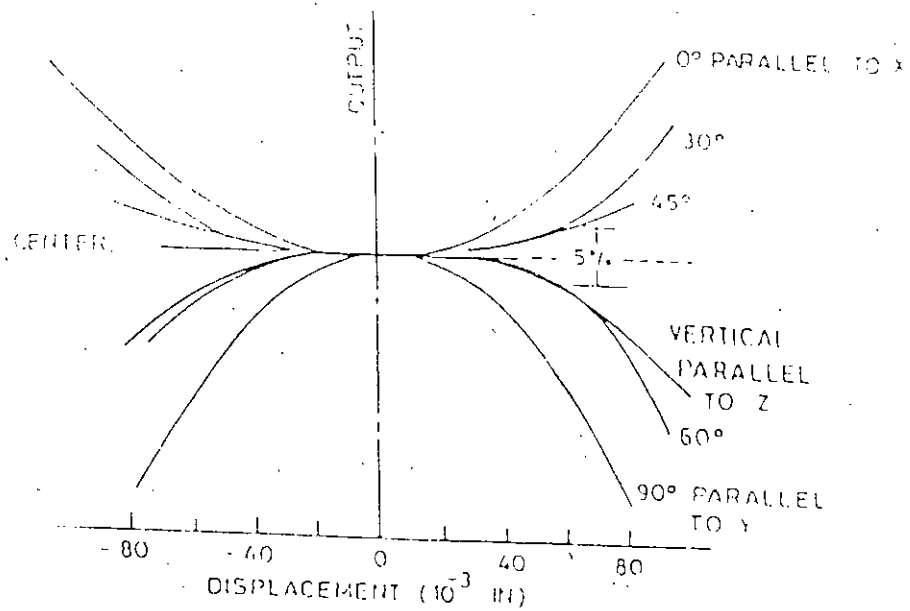


Fig 37 Relative output signal from a double-coil system vs. sample position. The contours of the "saddle point" are illustrated by measurements along various directions in the XY plane.

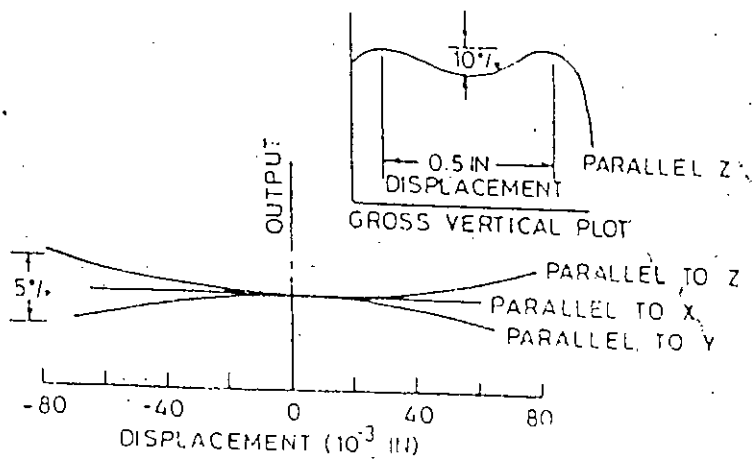


Fig 38 Relative output signal from a double-coil system vs. sample position. Bottom curves show relative output vs. displacement along the three orthogonal directions in neighborhood of "saddle point". Upper right insert shows relative output for large sample displacement along the Z direction.

Figure-3.6a shows the addition of a pair of coils coaxial with the z-axis. With such an arrangement the magnitude and direction of the magnetic moment vector in space can be determined. Figure-3.6c shows a multiple coil arrangement which attempt to intercept a maximum of the sample dipole coils. An efficient modification of Figure-3.6c is shown in Figure-3.6f. This coil geometry however is not easy to fabricate. Finally, the cross-section of a coil geometry which reflects most of the dipole field symmetry properties is shown in Figure-3.6g. It is directly derived from Figure-3.6f and leads to rather simple computation of out put voltage versus geometric parameters.

3.1.8. Working procedure of Vibrating sample Magnetometer:

This is a sensitive equipment and it should be handled carefully. The following procedure may be followed. The sample is fitted to a drive rod assembly and positioned at about the mid point of the sample coils by eye estimation. The switches of the electromagnet power supply unit, the signal generator, the audio amplifier and the shifter are then turned on. At least half an hour is spent for the warming up of all the component unit. The frequency of the sine wave from the signal generator is set at 80 Hz.

The gain of the audio amplifier is adjusted to make the out put signal driving the speaker to about 3 volts peak to peak. This signal make the rod assembly vibrate with sufficiently large amplitude. The sample signal alone is first seen on the d.c. meter of the lock-in-amplifier. The meter reading is maximised by changing the phase of the locking signal in the reference channel.

The locking signal in the reference channel is brought in exact quadrature with the sample signal to give a correct null reading on the meter. The two signals are then brought in the same phase. The signal produced in the reference coil system is then found to be a maximum reading on the meter to the right. Similarly the reference coil signal alone is next seen on the meter. This signal is first brought in quadrature with the locking signal with the help of external phase shifter in such a manner that it gives a deflection to the left on the meter, when it is again brought in phase with the sample signal. The lock-in-amplifier is then set in the differential mode.

3.1.9. Electronic circuit of V.S.M. And its operation principle:

The vibrating sample magnetometer consists of a mechanical vibrator, a sine wave generator, an audio amplifier, a ratio transformer, a phase-shifter, a lock-in-amplifier, a pick-up coil system, a reference coil system, x-y recorder and an electro-magnet. A schematic diagram of V.S.M. is given in Figure-3.9. The function of the associated electronic circuits are

1. To permit accurate calibration of the signal obtained from the detection coil.
2. To produce a convenient a.c. out put signal which is directly related to the in-put and which can be recorded.
3. To produce sufficient amplification for high sensitivity operation.

The signal generator *SG* feeds a sine wave of 80 Hz frequency to the audio amplifier *AA*. The audio amplifier drives the loud speaker *SP*. Loud speaker is specially prepared vibrator which vibrates a glass rod of assembly at the signal frequency 80 Hz. The out put of the signal generator is also connected to the reference channel in-put of the lock-in-amplifier *LA*. The drive rod assembly *R* tightly coupled to the vibrating paper

cone of the speaker which vibrates in a vertical direction along its length. The amplitude of vibration may be varied at will by changing the gain of the audio amplifier *AA*. A permanent ($BaO, 6Fe_2O_3$) magnet *P* of cylindrical shape is fitted to the drive rod at its lower end with the help of a sample holder *H*. Two cylindrical sample coils, *SC*, with their axis kept vertical, are placed on the opposite sides of the sample and along the line joining the centres of the pole tips (*N.S*) of the electro-magnet. They are connected in series opposition and net out put signal is connected to the phase shifter through a shielded cable. This pair of coils is referred to as the sample coil system. Another pair of co-axial coils *RC* also connected to each other in series opposition is placed symmetrically around the permanent magnet *P*. This coil pair is the reference coil system.

As the drive rod assembly is vibrated with a particular frequency and amplitude, the sample *S* induces a signal of the same frequency in the sample coil system. This signal is proportional to the dipole moment of the sample *S*. As the field in the pole gap is gradually increased by increasing the current through the electro-magnet *EM*, the sample becomes magnetized more and more and induces a larger signal in the sample coil system till it reaches saturation magnetization. This signal directly goes to one of the inputs of the Lock-in-amplifier. Similarly another signal of the same frequency is induced in the reference coil system due to vibration of the permanent magnet *P*. Since the moment of the magnet is fixed, this signal is also of fixed amplitude for a particular frequency and vibration amplitude.

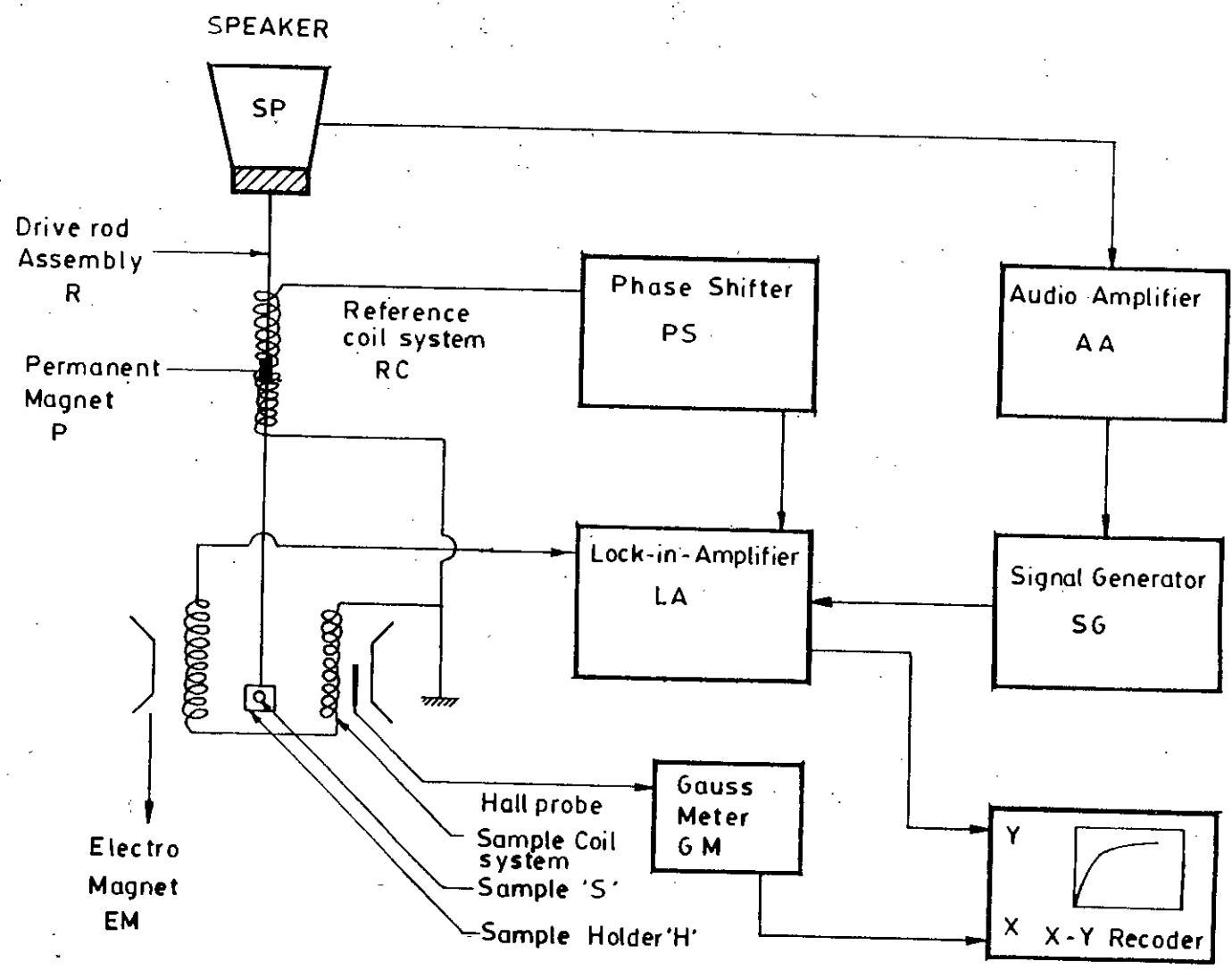


FIG. 3.9 SCHEMATIC DIAGRAM OF THE ELECTRONIC SYSTEM OF THE V.S.M.

This signal is termed as the reference signal and it is first fed to a unity gain phase-shifter unit *PS*. The phase shifter capable of continuously changing the phase from 0 to 360 degrees is used to bring the reference signal in phase with the sample signal. The reference signal is compared with the sample signal in a lock-in-amplifier. The output of the lock-in-amplifier is fed to the Y axis of the x-y recorder. The magnetic field is measured with hall probe which is fed to the input of the gauss meter. The output of the gauss meter is fed to the x input of the x-y recorder. The lock-in-amplifier is operated in the differential input mode and is used as a null detector. Since the sample *S* and the permanent magnet *P* are vibrated with the same drive rod assembly, the sample signal and the reference signal have a direct phase and amplitude relationship. As a result the ratio of the sample signal to the reference signal is proportional to the magnetic moment of the sample. The measurement is insensitive to small changes in the amplitude and frequency of vibration and the gain of the amplifier.

3.1.10. Description of Mechanical parts:

The various mechanical parts of the magnetometer are described in detailed in Figure-3.10. The base *B* of the V.S.M. is a circular brass plate of 8 mm thickness and 250 mm diameter. A brass tube *T* of 25 mm outer diameter and 0.25 mm thickness runs normally through the base such that the axis of the tube and the centre of the plate coincide. The base and the tube are joined together by soft solder. The tube extends 60 mm upward and 24 mm downward from the base. There is a vacuum part on the lower part of the tube 120 mm below the base. The lower end of the tube *T* is joined to a brass extension tube *L* by a threaded coupling and an *O*' ring seal. Another thin tube *K* made of german silver and of 8 mm inner diameter runs through the extension tube *L* from the coupling point to about 50

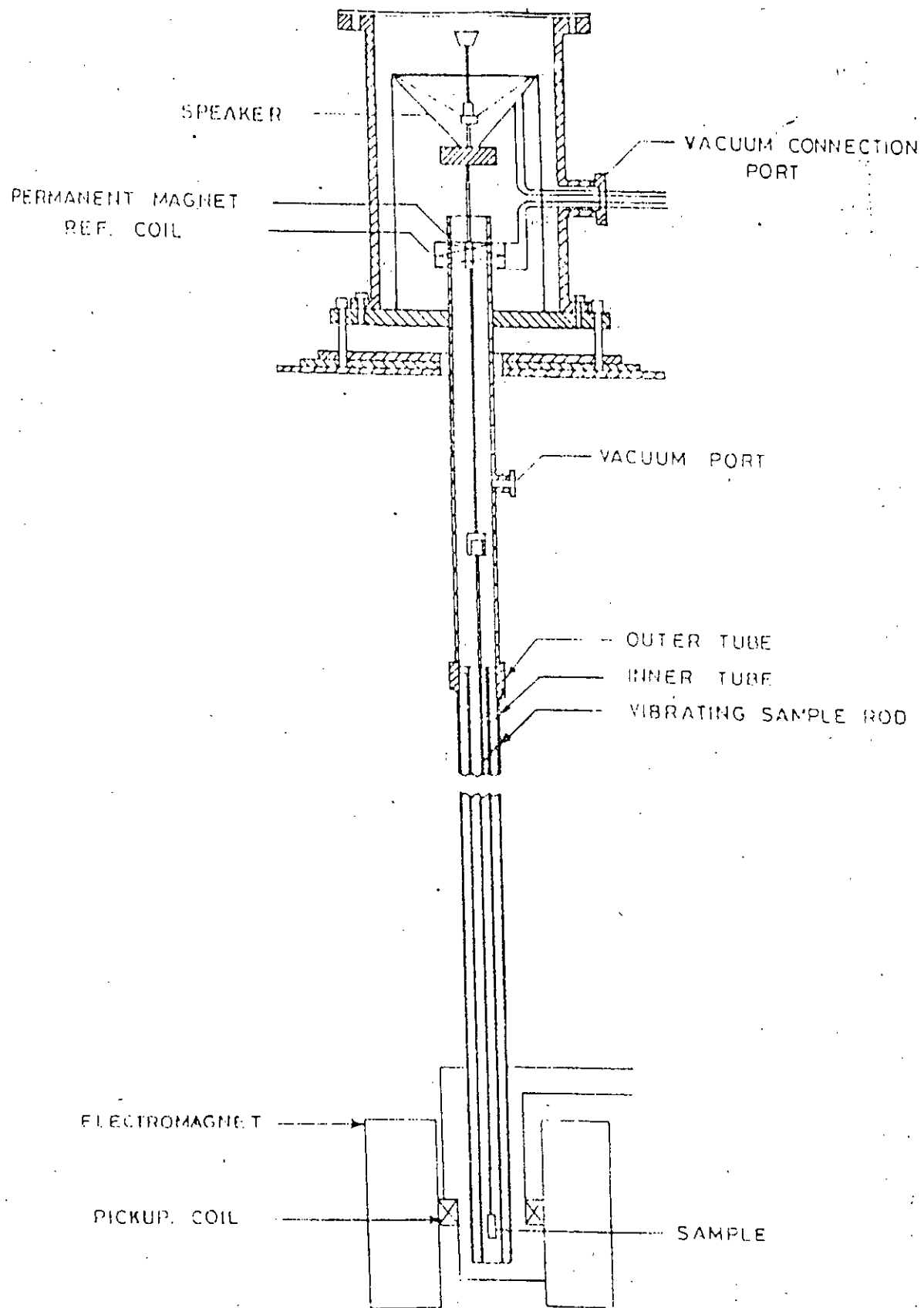


Fig. 3.10 Simplified form of vibrating sample magnetometer.

mm below the sample position. Above the base there is a hollow brass cylinder *M* of 180 mm length and 130 mm inner diameter and having 40 mm wide collars at its both ends. The lower collar seats on an *O'* ring seal which is situated in circular groove in the base plate. On the upper collar there seats an aluminium top *N* with an *O'* ring seal. The brass cylinder *M* has a side port *VP*. This is again a brass tube of 41 mm diameter and 43 mm length. The port has a collar at the end away from the cylinder. A perspex vacuum feed through it fitted at its end with *O'* ring seal. This port is connected to the cylinder by soft solder. Electrical connections from the audio amplifier to the speaker and from the reference coil system to the phase-shifter are taken via the perspex-through. By connecting the vacuum port of the tube *T* to a vacuum pump, the sample environment can be changed. The speaker *SP* is fitted 25 mm above the tube *T* with the help of a brass stand. The lower end of the stand are screwed to the base plate while the rim of the speaker is screwed on the top of the stand. The speaker has a circular hole of 10 mm diameter along the axis of it. An aluminium disc having female threads in it is fitted to the paper cone with araldite. The aluminium connector having male threads on it and attached to the drive rod assembly fits in the aluminium disc and thus the drive rod assembly is coupled to the speaker. The drive rod assembly consists of two detachable parts which are joined together by means of aluminium threaded connectors. Each part is a thin pyrex glass tubing of 4 mm diameter. The upper part has a small permanent magnet *P* situated 100 mm below the aluminium connector attached to it. At the lower end of the drive rod assembly a perspex sample holder having quite thin wall can be fitted tightly with the sample in it. A few perspex spacers are also attached to the drive rod throughout its length. The spacers guide the vibration of the sample only in its vertical direction and slopes sidewise vibration or motion. The total length of the drive rod assembly is 920mm.

3.1.11. Sample and reference coils:

Both the sample coil system and the reference coil system are each a double coil system. The reference coil system consists of two coils wound oppositely side by side on the two grooves of a former. The former is made of bakelite. Each coil is 4mm long, 2mm thick and its inner diameter is 25mm. The wire is superenamelled BICC copper wire of 0.02mm diameter. Total number of turns in each coil is 6000. Since the two coils are connected in series opposition the out put signal is only due to the vibrating permanent magnet P . Any noise induced in it due to background will be minimum. The coil system fits over the brass tube T about 25mm above the base. It is positioned by moving it up and down the tube T while vibrating the permanent magnet. The length of the coil is 6mm and its diameter is 4mm. The same superenamelled BICC wire of 0.02 mm diameter has been used in these coils. The number of turns of each coil is 6000 again. The signal due to the sample moment induced in the sample coils system is in principle, given by the relation

$$V_s = K_s W A \exp(Wit) I_s \quad (3.13)$$

Where K_s is a constant dependent on the coil geometry, W is the angular frequency of vibration, A is the amplitude of vibration. M_s is the magnetic moment of the sample. The e.m.f. induced in the reference coil is given by

$$V_r = K_r W A \exp(Wit) I_r \quad (3.14)$$

Taking the *r.m.s.* values of V_s and V_r it can be seen that the ratio of the two signal is independent of frequency and amplitude. The ratio is given by

$$V_{out} = \frac{(V_s)_{r.m.s.}}{(V_r)_{r.m.s.}} = \frac{K_s M_s}{K_r M_r}$$

$$I_s = KV_o \quad (3.15)$$

where K is a constant, since K_s , K_r and M_r are constant. Here V_{out} is actually the ratio transformer reading.

3.1.12. Sensitivity of V.S.M.:

The sensitivity of a V.S.M. is usually determined by the signal to noise ratio. The maximum sensitivity of the lock-in-amplifier is 10 micro volts r.m.s. So the differential method has been used to measure the sensitivity. It is found to be about 10^{-4} e.m.u. It may be mention here that the sensitivity of commercial v.s.m. made by PARC (Princeton Applied Research corporation U.S.A.) is about 5×10^{-5} e.m.u. With the sensitivity so far achieved, this v.s.m. can be used for investigation of ferro-magnetic, ferri-magnetic and strongly para-magnetic material at room temperature.

3.1.13 Advantage and Disadvantage of VSM:

This method is versatile and sensitive. It may be applied to both weakly and strong magnetic substances and it can detect a change in magnetic moment of 5×10^{-5} erg/oested which correspond to a change in mass susceptibility of 5×10^{-9} emu/gm for 1 gm. of sample in a field of 10,000 oested. The greatest advantage of this method is that any laboratory magnet can be used for this equipment. It is not generally suited to the determination of the magnetization curve or hysteresis loop of a magnetically soft material. The specimen has to be short and demagnetizing field is then such a large fraction of the applied field that the true field is uncertain. This problem can be removed by deterring saturation magnetization because knowledge of the true field at saturation is not necessary.

3.2. Effective Magnetic Field

Since our available field could not be increased beyond 9 K gauss which after correction for demagnetizing field reduce to an effective field of 2.5 K gauss, the saturation magnetization corresponding to infinite field are calculated for different alloys of Fe-Al alloys by extrapolating the experimental values to infinite field. This is done by plotting specific magnetization against reciprocal of the applied fields and is shown in Figure - 3.12.

3.3. Measurement of Magnetization

The magnetization measurement of iron-aluminium is chosen to find the magnetization process of the materials and also its saturation magnetization. This magnetic characteristics are important for determining the performance of this materials as it has been used for designing various devices and system. A commercial sample of iron-aluminium is chosen for magnetization measurement to look at the saturation magnetization and to investigate the possibility of its application in designing transducer.

The magnetization measurements of $\text{Fe}_{100-x}\text{Al}_x$ ($x = 2, 8, 10, 12$ and 14) are measured by means of a vibrating sample magnetometer. The magnetization σ as a function of magnetic field are measured in different applied fields with a maximum of 2.5 Kilo oersted.

The measurements are confined to room temperature only because of the nonavailability of high temperature oven and low temperature cryostat. The magnetization curves are shown in Figure- 3.11 and 3.13. It is seen that the magnetization is increasing slowly with the increase of the applied field tables 3.1-3.5. The specific magnetization values σ

are then plotted against $\frac{1}{H}$, which is found to be linear for higher value of H . The value of σ at $\frac{1}{H} = 0$ is taken as the value of magnetization at saturation. These curves are shown in Figure 3.12.

The concentration dependence of the saturation magnetization is shown graphically in Figure 3.13.

TABLE -3 1

VARIATION OF MAGNETIZATION WITH FIELD FOR $\text{Fe}_{98}\text{Al}_2$ AT ROOM TEMPERATURE

FIELD IN OERSTED	MAGNETIZATION emu/gm		FIELD IN OERSTED	MAGNETIZATION emu/gm
12.15	53.38		185.06	155.78
16.57	61.10		208.03	162.78
19.82	68.60		258.74	168.91
25.99	76.10		309.45	175.04
47.12	83.14		331.88	182.04
69.55	90.14		411.20	187.29
80.28	97.50		462.24	193.41
85.80	105.02		541.23	198.67
89.38	112.60		620.5	203.92
102.06	119.90		728.49	208.29
113.11	127.25		949.88	209.17
118.31	134.78		1171.59	210.04
140.74	141.78		1420.39	210.08
163.17	148.78			

TABLE-3.2

VARIATION OF MAGNETIZATION WITH FIELD FOR Fe₉₂Al₈ AT ROOM TEMPERATURE

FIELD IN OERSTED	MAGNETIZATION emu/gm	FIELD IN OERSTED	MAGNETIZATION emu/gm
18.12	63.42	398.75	155.24
74.68	69.61	403.75	163.08
82.81	77.35	468.12	170.94
91.25	85.08	432.81	178.15
99.37	92.82	569.68	181.77
107.81	100.55	698.75	185.64
115.93	108.29	755.62	191.82
212.81	113.19	957.18	193.37
350.31	116.79	1183.12	194.14
358.43	124.53	1420.63	194.54
385.00	131.68	1658.75	194.92
390.62	139.50	1904.06	195.07
393.75	147.40	2149.06	195.23

TABLE-3.3VARIATION OF MAGNETIZATION WITH FIELD FOR $\text{Fe}_{90}\text{Al}_{10}$ AT ROOM TEMPERATURE

FIELD IN OERSTED	MAGNETIZA- TION emu/gm		FIELD IN OERSTED	MAGNETIZA- TION emu/gm
21.80	31.77		322.39	143.80
40.26	39.29		366.41	150.00
45.78	47.23		384.56	158.02
51.00	55.18		403.02	165.54
69.46	62.70		421.17	173.07
87.61	70.23		542.47	177.25
106.07	77.75		612.35	183.10
111.29	85.70		733.64	187.28
116.82	93.64		906.36	189.79
160.83	100.33		1130.50	190.63
166.36	108.27		1367.87	191.04
184.82	115.79		1617.26	191.06
102.97	123.32		1866.64	191.08
208.50	131.62		2116.03	191.10
309.50	138.99		2367.04	191.10

TABLE-3.4VARIATION OF MAGNETIZATION WITH FIELD FOR $\text{Fe}_{88}\text{Al}_{12}$ AT ROOM TEMPERATURE

FIELD IN OERSTED	MAGNETIZA - TION IN emu/gm		FIELD IN OERSTED	MAGNETIZA - TION IN emu/gm
10.11	49.09		273.67	147.49
12.46	57.25		347.95	153.28
13.28	65.46		452.57	158.07
45.37	72.64		508.63	164.46
52.87	80.63		565.00	170.84
84.96	87.81		669.62	175.63
92.47	95.80		749.97	181.22
100.27	103.78		927.13	183.62
156.34	110.17		1128.57	185.22
164.14	118.15		1378.26	185.23
220.21	124.54		1627.96	185.24
228.01	132.52		1877.66	185.25
259.80	139.71		2127.85	185.26

TABLE-3.5

VARIATION OF MAGNETIZATION WITH FIELD FOR Fe₈₆Al₁₄ AT ROOM TEMPERATURE

Field in oersted	Magnetization in oersted	Field in Oers ted	Magnetiza tion in oersted	Field in Oersted	Magnetiza tion in Oersted
15.32	16.22	240.82	92.28	593.41	164.10
20.23	19.39	265.48	94.80	628.82	166.20
34.42	22.26	297.66	97.67	653.77	168.77
48.41	25.13	293.85	100.54	667.96	171.64
60.40	28.08	297.27	103.77	703.38	173.80
71.30	31.06	311.16	106.65	715.80	176.67
75.92	34.25	314.58	109.88	785.28	177.75
83.53	37.34	318.01	113.11	863.74	178.47
88.15	40.52	337.58	115.80	935.45	179.55
92.77	43.72	362.23	118.32	1029.96	179.55
104.26	46.68	384.79	120.91	1129.36	179.62
105	50	390.60	124.06	1221.06	179.65
111.11	53.14	388.24	127.48	1328.46	179.65
135.76	55.66	391.77	130.71	1428.16	179.66
139.18	58.89	427.48	132.86	1527.87	179.67
153.37	61.76	432.10	136.05	1627.56	179.68
167.56	64.63	434.03	139.33	1727.26	179.69
181.45	67.51	448.22	142.20	1826.99	179.70
184.47	70.74	492.40	145.07	1926.67	179.71
188.29	73.97	476.59	147.94	2026.37	179.72
202.48	76.84	490.48	150.82	2126.07	179.73
216.37	79.72	504.66	153.69	2226.07	179.73
219.79	82.95	529.62	156.20	2326.07	179.73
223.21	86.18	554.29	158.2	2426.07	179.73
258.93	88.33	568.95	161.59	2526.07	179.73

90098

TABLE-3.6

VARIATION OF SATURATION MAGNETIZATION OF $Fe_{100-x}Al_x$ WITH INVERSE FIELD AS A FUNCTION OF CONCENTRATION AT ROOM TEMPERATURE.

Concentration of Al in Fe	Saturation Magnetization emu/gm.	Field in oersted	$1/H_a \text{ Kg.}^{-1}$
2 at. %	210.04	1420.29	.704
8 at.%	195.30	1904.04	.525
10 at.%	191.10	2116.03	.4725
12 at.%	185.26	2377.35	.420
14 at.%	179.55	2526.07	.3958

TABLE -3.7:

COMPARISON OF MAGNETIZATION BETWEEN 2.5 K. OERSTED AND INFINITE MAGNETIC FIELD

Name of alloy	Magnetization at 2.5 K. oersted	Magnetization at infinite field
Fe ₉₈ Al ₂	210.04	213.5
Fe ₉₂ Al ₈	195.30	198.80
Fe ₉₀ Al ₁₀	191.04	194.25
Fe ₈₈ Al ₁₂	185.22	189
Fe ₈₆ Al ₁₄	179.55	182.5

TABLE-3.8

From the linear part of magnetization Versus field graph the calculated values of initial permeability for the different composition of Fe-Al alloy system are given in Table 3.8

Different composition of Fe-Al alloy	Field in oersted	Magnetization in emu/gm	Slope = Magnetization / Field in oersted
Fe ₉₈ Al ₂	30	47.5	1.58
Fe ₉₂ Al ₈	60	56.25	0.9375
Fe ₉₀ Al ₁₀	50	31.25	0.625
Fe ₈₈ Al ₁₂	150	60	0.40
Fe ₈₆ Al ₁₄	260	77	0.296

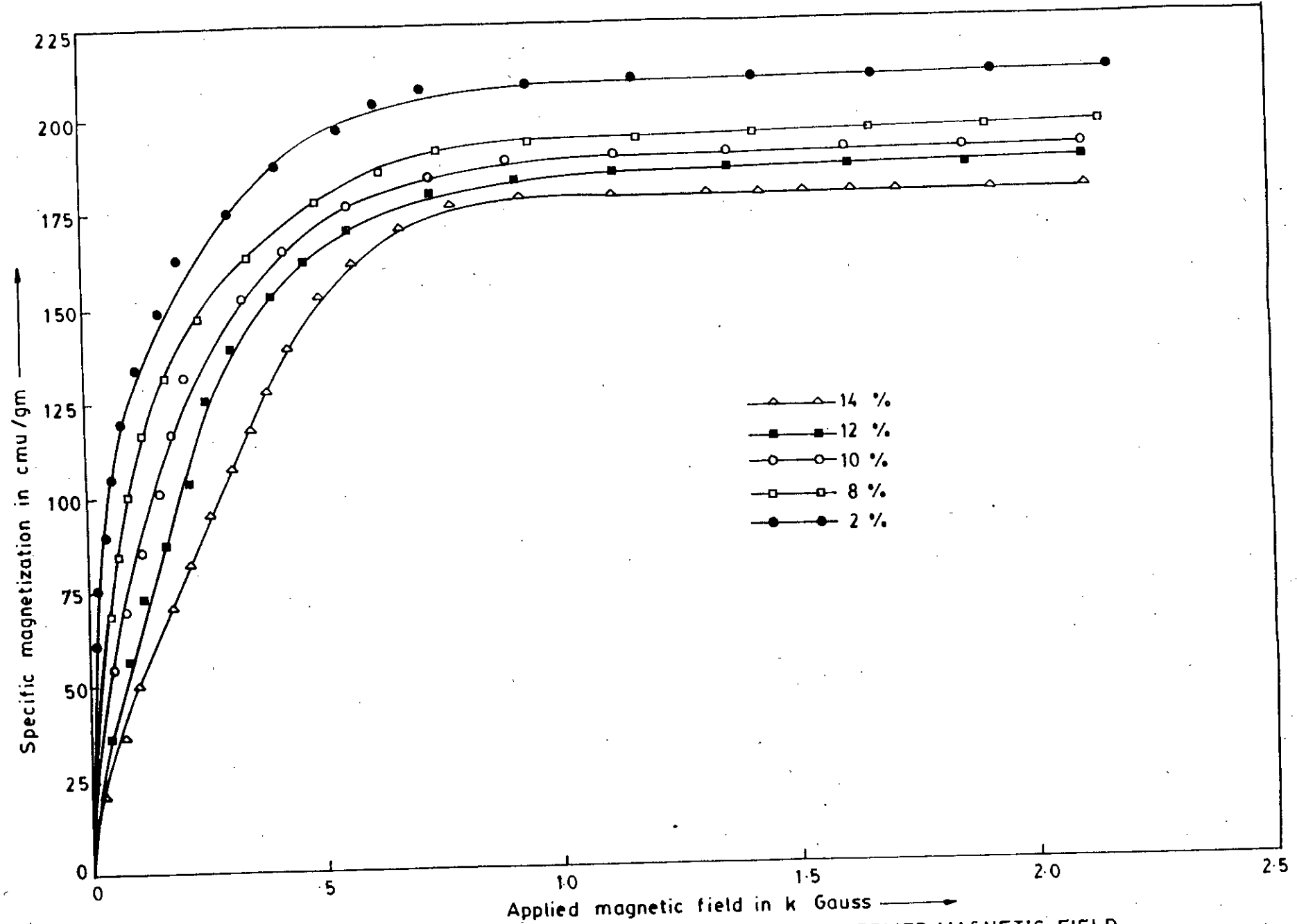


FIG. 3.11 VARIATION OF SPECIFIC MAGNETIZATION OF $Fe_{100-x}Al_x$ WITH APPLIED MAGNETIC FIELD.

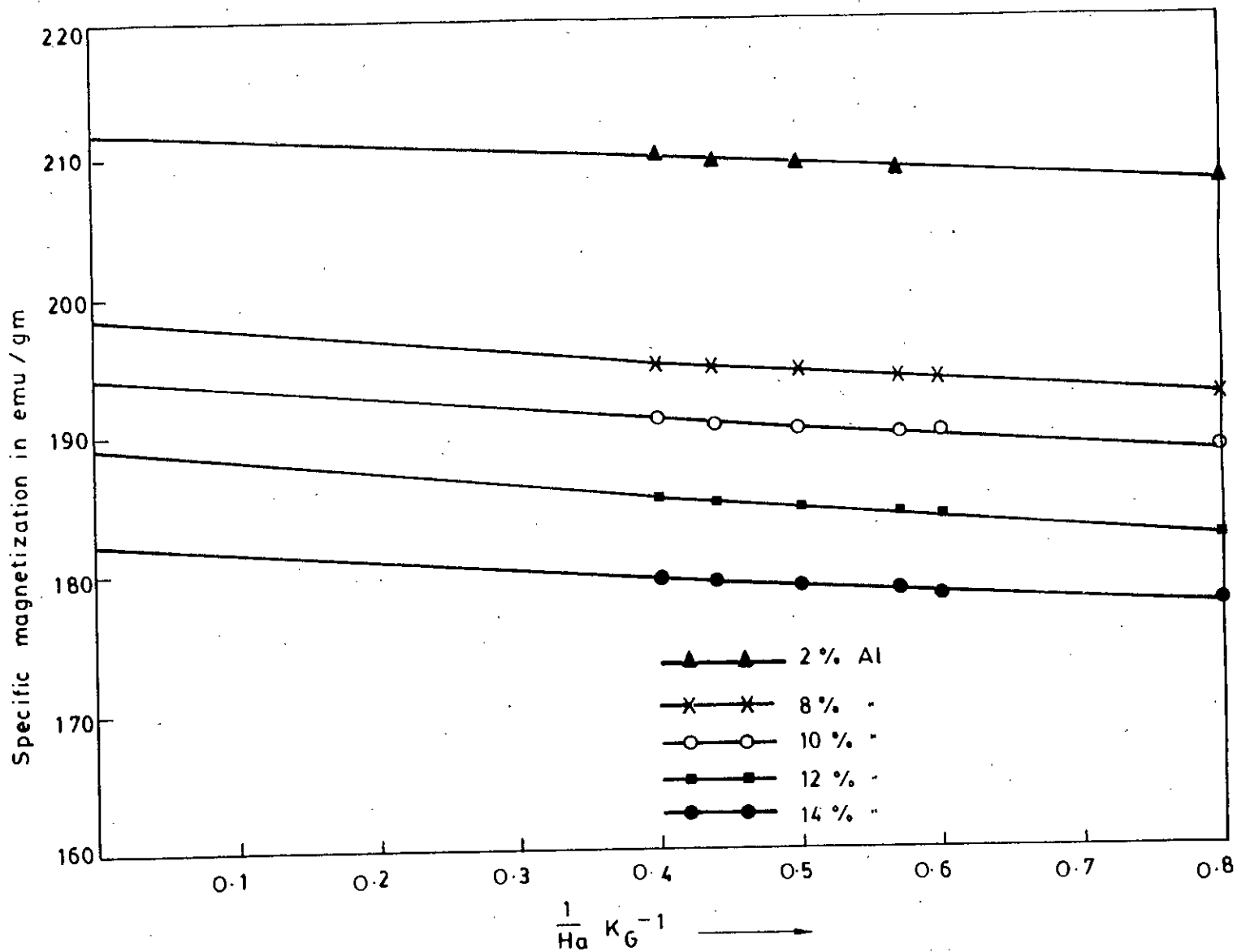


FIG. 3.12 PLOT OF THE SPECIFIC MAGNETIZATION OF $\text{Fe}_{100-x}\text{Al}_x$ AGAINST $\frac{1}{H_a}$
 [H_a = APPLIED MAGNETIC FIELD]

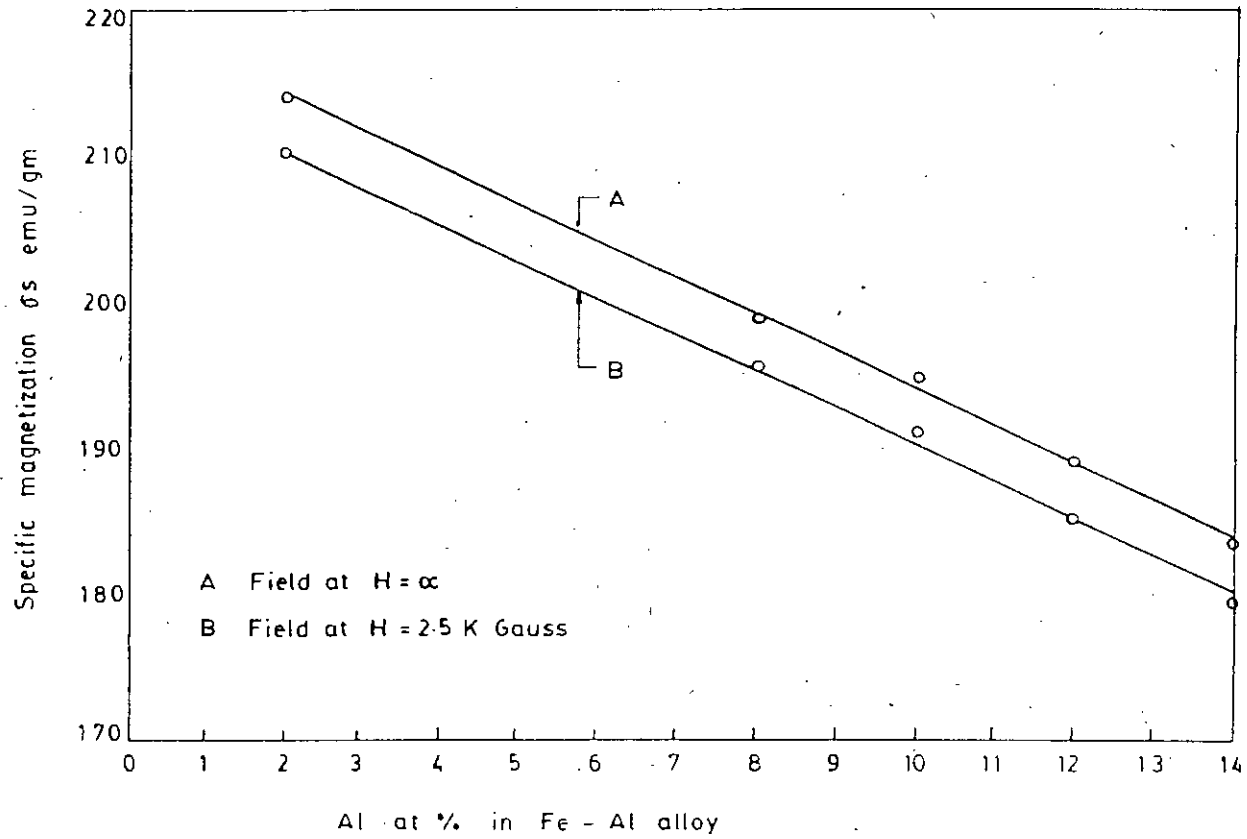


FIG 3.13 THE CONCENTRATION DEPENDENCE OF THE SATURATION MAGNETIZATION

3.4. Results and Discussion

Although the study of microscopic structure of magnetic materials has led to important advances, future improvements require further understanding of the fundamental processes of magnetization and a study of sub-microscopic and atomic influences. Aluminium is soluble in iron in the range of alloys up to the ordered alloy Fe_3Al . It also forms a super lattice $FeAl$ at 50 at.% of Aluminium. The ordered systems are b.c.c with the Al atom occupying alternate body centres in Fe_3Al and in $FeAl$, Al occupies all the body centre position. For the alloy up to 15 at. % of Al magnetization decreases with increasing Al content as if by simple substitution. Nathans, Pigatt and Shull^{3.5} have shown by neutron diffraction that Al atoms carry negligible moment. The Fe-I atoms carry a moment of $2.1\mu_B$, which is nearly the same as the usual value $2.2\mu_B$ of an iron atom, while the Fe-II carry a moment of $1.5\mu_B$. Arrot and Sato^{3.6} have shown that the most important commercial alloys are those with 12 to 16 atomic percent of Al in iron. Alloy containing up to 16 atomic% of aluminium have high resistivity and when correctly treated have high maximum permeabilities and low coercivities. The iron aluminium alloys up to 10 atomic percent of aluminium are characterized by ductility, good soft magnetic properties and increasing electrical resistivity with increasing aluminium content. Considerable work has been done on the alloys near 2% of Aluminium where fairly high degree of double orientation has been obtained. The purpose of this investigation is to study the alloys of aluminium content from 2% to 14% aluminium in iron in order to make use of the high magnetostrictive properties of these alloys. The body centred cubic phase of iron can be retained for additions of up to slightly more than one aluminium atom for every iron atom. The iron and aluminium atoms however do show strong tendencies toward ordering within this range of solid solution, the exact nature of the phase diagram is still under investigation.

Since the value of magneto-crystalline anisotropy decreases with increasing value of Aluminium it would normally be expected that the saturation field for iron-aluminium alloys should be lower for higher values of Aluminium. However we observed that the saturation value of the field increases with increasing percentage of aluminium. This is explained as due to increasing value of magnetostriction with the addition of aluminium. Since our specimens are likely to be strained, magnetostriction constrains the domain wall movements and hence the magnetization process of the alloys, with higher values of Aluminium thus requiring higher field for attaining saturation. The concentration dependance of the saturation magnetization is shown in Figure- 3.13.

Initial magnetization curves of iron aluminium for varying compositions are consistent with the assumption that the magnetization is controlled by domain wall pinning. The magnetization of iron aluminium alloys at room temperature has been visualised as the movement of domain. In our experiment the magnetization is found to be 210.04 emu/gm for 2 atomic percent of *Al* in iron, 195.30 emu/gm for 8 atomic percent of *Al* in iron, 191.04 emu/gm for 10 atomic percent of *Al* in iron, 185.22 emu/gm for 12 atomic percent of *Al* in iron and 179.55 emu/gm for 14 atomic percent of *Al* in iron respectively. The magnetic moments are assumed to be due to the iron atoms which are ferro-magnetically coupled to the nearest neighbours which are also iron atoms. For the aluminium iron alloys with low concentration of aluminium, the aluminium atoms acts as non magnetic substitute of magnetic iron atoms; thereby reducing the resulting magnetization in proportion to the atomic percentage of aluminium. From the results shown in the Figure 3.11 the reduction of magnetization is 13.99 for 14 atomic percent of aluminium. Since the measurements are done at room temperature, the agreement is in fact even better than expected. This is because only at absolute zero degree of temperature the saturation magnetization should follow the rule of proportional decrease of magnetization according to the rule of corresponding states. In our case the alloy

composition have different curie temperatures and the reduced temperatures are not used. Coupling of the angular momentum (L) and spin (S) also contribute small magnetic moments per atom. Our results have some approximations in these respect.

The actual mechanism of ferro-magnetic ordering is infact more complicated than simple dilution of magnetic iron atoms by non magnetic aluminium atoms. Besides the ferro-magnetic exchange interaction between the nearest neighbour iron atoms, there is also an antiferromagnetic exchange interaction by indirect super exchange between the iron atoms which are separated by an aluminium atom. This negative interaction becomes increasingly important when the probability of an aluminium atom to become the nearest neighbour of an iron atom increases due to increased percentage of aluminium.

In our choosen range of composition this effect can be neglected in the first approximation. However this aspect of complex exchange mechanism has to be kept in mind without which the sharper fall of magnetization with aluminium concentration at high values of aluminium in the iron-aluminium alloy system can not be understood.

Initial permeabilities of different alloys of iron-aluminium for different compositions as calculated from the linear part of the magnetization versus field curves are given in table-3.11

It is observed that the permeability decreases with increasing percentage of aluminium. The minimum is for 14 atomic percent of aluminium which is .296 emu/oersted.

Permeability is determined by magnetostriction and magneto-crystalline anisotropy, both of which decrease permeability with their increasing values. In the case of Fe-Al alloy

magnetocrystalline anisotropy decreases with increasing percentage of aluminium. It is therefore, expected that permeability should increase with increasing percentage of aluminium. This was also reported by Nachman and Buehler³⁻⁷. However, we observed an increase of permeability with increasing percentage of aluminium. This is explained as due to the contribution of increased magnetostriction with increasing percentage of aluminium. This becomes important when the materials are subjected to internal stresses. The specimens when prepared in a high vacuum and without internal stress, effect of magnetostriction can be avoided and anisotropy alone contributes to permeability. The difference between our results and those of other mentioned above can thus be explained.

Since our developed iron-aluminium alloy is intended to be used as magnetostrictive material rather than as a magnetically soft materials, this stress induced magnetic hardness is not much of an obstacle in the application of this alloy.

For power applications a magnetic material must be soft, with high induction value and high resistivity. Although silicon-iron is used as the most common soft magnetic material, iron aluminium also has the same properties as those of silicon iron. However, it has added advantage as also some disadvantages. The major differences that are found between low percent aluminium iron alloys and equivalent percent of silicon iron alloys are:

- i. aluminium iron is more powerful deoxidizer than silicon.
- ii. aluminium iron show improved ductility. It is thus possible to cold reduce aluminium, iron alloys containing up to 6% aluminium by as much as 90%.

Commercial production of aluminium iron alloys was limited in their early states of development because of the relative high cost of aluminium and because of the greater difficulty in preventing segregation of aluminium during melting process. However the

cost picture has equalized in recent year and with modern induction melting equipment the segregation problem has practically been eliminated. The work of sugihara^{3.8} and Helms^{3.9} illustrated that magnetic properties of isotropic aluminium iron alloys are comparable to those of equivalent silicon iron alloys.

Our measurements of magnetization and magnetostriction were carried out on the as prepared specimens. However, the effect of annealing has very important influence on magnetization process and magnetostriction because of the high value of magnetostriction of this alloy system. In order to use this alloy as a soft magnetic material to replace iron silicon alloy, the specimens should be stressfree. Further work on iron aluminium alloy system with higher range of composition and under relieved strains by appropriate heat treatments in vacuum can be very useful for better understanding of their magnetic characteristics. This will also require measurement at high and at very low temperatures.

The measured results unveil the fact that domain wall movements and magnetization is inhibited until the field reaches the critical field H_0 , the field required to free the domain walls from pinning centres. With this model it is predicted that $H_c = H_0$. The results of Figure-3.11 shows that our values of H_0 is affected by magnetostriction and stress.

CHAPTER-4

MEASUREMENT OF MAGNETOSTRICTION OF $Fe_{100-x}Al_x$ ALLOY, $Tb_{.27}Dy_{.73}Fe_2$ AND Ni:

4.1: Technique of Measurement of Magnetostriction:

The change in dimension of a magnetic material in an applied field which we call magnetostriction, is usually of the order of 10^{-3} to 10^{-6} . The measurement of such a small dimensional change can be conveniently measured using an electrical resistance strain gauges. The gauge is cemented on the specimen in a precisely determined direction along which the measurement is required to be made. The use of strain gauge is based on the assumption that any strain characteristic of the specimen on which the gauges is bonded, is transmitted faithfully to the electrically sensitive zone of the gauge and is observed as a resistance change.

The experimental set up consists of a strain sensing device that is strain gauge, a *d.c.* bridge, *d.c.* amplifier, x-y recorder and a rotatable electromagnet. A rotatable electromagnet is used to apply the magnetic field in the desired direction. The component elements are arranged in the wheatstone bridge fashion. Asgar^{4.1} measured magnetostriction of some ferromagnetic and antiferromagnetic metals using the same technique.

4.2. The Wheatstone Bridge Principle:

The use of wheatstone bridge is quite well known as a convenient method for measuring fractional change in resistance. A *d.c.* wheatstone bridge in slightly out of balance condition is used to measure the fractional change in resistance in the active gauge. The simple type of *d.c.* wheatstone bridge circuit is shown in figure-4.1.

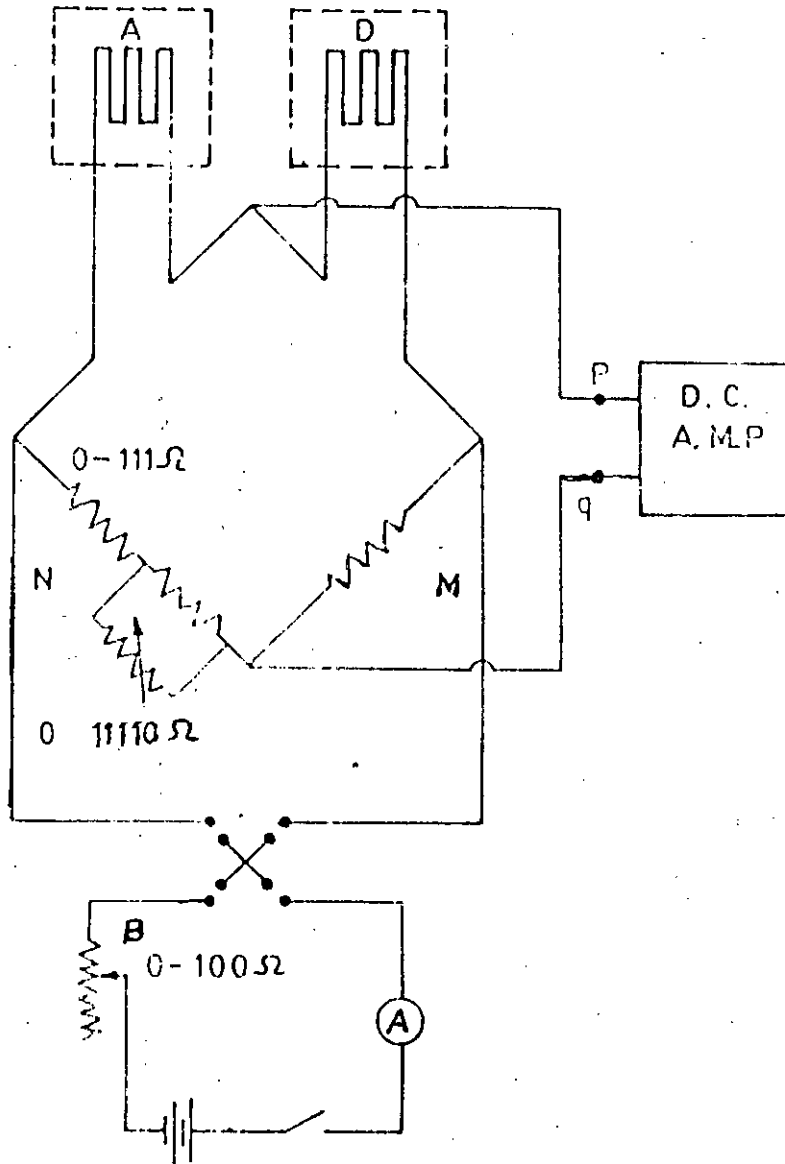


Fig. 4.1 D.C. Wheatstone Bridge circuit

When the resistance of the active gauge is changed from A to $A+dA$ a corresponding out of balance voltage is developed across the input of the d.c. amplifier. Then a deflection is observed in the Nanovoltmeter which is connected to the wheatstone bridge circuit. If the deflection of a nanovoltmeter is to be used as a measure of the strain, it is necessary to calibrate the Nanovoltmeter.

4.3. Straingauge Bonding

The idea of bonding the resistance type strain gauge directly to the material was conceived at California Institute of Technology in the application to a tensor impact test, Ruge at Massachuetts institute of Technology at about the same time conceived the idia of bonding the wire to a paper and bonding the paper with a common glue to the material where the strain is to be measured. This bonded wire type of electrical resistance strain gauge consists of a grid of fine alloy wire bonded to a paper base. In using this gauge, it is cemented to the surface of the specimen. It is necessary to have very fine scratches on the gauges and specimen surface. The specimen surface is naturally left with fine irregularities of six micron order which is the grain size of the grains of polishing paste used in specimen polishing.

Now some epoxy glue is applied to the gauge surface and the gauge area of the specimens. Then the gauge is placed on the specimen surface and the small pressure is applied for two days on the gauge and the system is allowed to dry at room temperature.

4.4. Strain gauge Technique

The strain gauge technique is used in magnetostriction measurement. This method was first developed by Goldman^{4.2}. The gauges can be used on a very small disk shaped specimen cut in a definite crystallographic plane and the gauge can be bonded in a precisely determined direction.

The strain gauge works on the principle that when a fine wire in the form of a grid or a thin foil and embedded in a paper or epoxy film, is bonded firmly on a specimen using a cement or some epoxy glue, it follows the strain of the specimen and shows a change in resistance proportional to the strain. Mathematically this effect can be expressed as

$$\frac{dR}{R} = G \cdot \frac{dl}{l}$$

Where dR/R is the fractional change in resistance, G is the gauge factor and dl/l is the strain along the gauge direction.

The magnetic strain in the crystal is determined from the change in resistance of the gauge fixed on the specimen in relation to the resistance of another dummy gauge bonded on a reference specimen using a resistance bridge in the out of balance condition.

4.5. Orientation of the gauge position relative to the Magnetic Field

The magnetization increase with an increase of the field and finally reaches the saturation magnetization which is normally denoted by I_s . Similarly the strain due to magnetostriction changes with increase of magnetic field intensity as shown in Figure-4.6, 4.12 & 4.14 and finally reaches the saturation value λ_s . The reason is that the crystal lattice inside each domain is spontaneously deformed in the direction of domain

magnetization and its strain axis rotates with a rotation of the domain magnetization, thus resulting in a deformation of the specimen as a whole.

When the magnetic field is applied the magnetic domain wall movement starts. In the initial state, if the magnetic field H makes an angle Ψ with the easy axis, the magnetization takes place by the displacement of 180° domain wall until the magnetization reaches the value $I_s \cos\Psi$, during this process no magnetostriction is observed. The entire magnetization takes place by the displacement of the walls, among which only 90° walls are effective in giving rise to the elongation. Thus the magnetostriction depends on the case of displacement of 90° walls relative to that of 180° walls. This gives rise to magnetostriction that is changing lattice dimension. This magnetostriction effect can be looked at as due to predominance of the strain axes in the direction of measurement. The variation of magnetostriction as a function of angular position is shown in Figure-4.7-4.11 & 4.13 respectively.

4.6. Bridge circuit sensitivity and calibration

The circuit used for measurement of the resistance change in the gauge is a *d.c.* wheatstone bridge circuit as shown in figure-4.1. It included a reversing switch S to ascertain to what extent, thermal e.m.f. in to the circuit are effecting the balance condition of the bridge. The nanovoltmeter used was a Keithley model 140 of high sensitivity and a period of 2.5 second. This low periodic time of the instrument enable quick recording of output of balance deflections, thus minimising errors due to drift and fluctuation from thermal e.m.f.'s in the circuit. The bridge sensitivity changed linearly with bridge current. Bridge current are restricted to a maximum of 25 mA to prevent over heating in the gauge circuit. In the figure 4.1 represent the active strain gauge in contact with the specimen and D represent the dummy gauge in the same enviroment as the active gauge. Any thermal fluctuations which

TABLE -4.1
VARIATION OF MAGNETIC FIELD WITH APPLIED ELECTRIC CURRENT
(CALIBRATION DATA OF THE ELECTRO-MAGNET)

FIELD CURRENT IN AMP.	FLUX METE METER R RREADING		AVERAGE DEFLECTION	MAGNETIC FIE IN GAUSS ^{LD}
	I(+)	I(-)		
.25	2	3	2.5	250
.50	4	4.50	4.25	425
.75	6	6	6.00	600
1.00	7	8	7.50	760
1.25	9.5	9.7	9.60	960
1.50	11	11.5	11.25	1125
1.75	13	13	13.00	1300
2.00	15	15	15.00	1500
2.25	17	17	17.00	1700
2.50	19	19	19.00	1900
2.75	21	21	21.00	2100
3.00	22	23	22.50	2250
3.25	24.5	25	24.75	2475
3.50	26	27	26.50	2650
3.75	28	29	28.50	2850
4.00	30.5	31	30.00	3075
4.25	32	33	32.50	3250
4.50	34	34.5	34.25	3425
4.75	36	36.5	36.25	3625
5.00	38	38	38.00	3800
5.25	39	40	39.50	3950
5.50	41	42	41.50	4150
5.75	43.5	44	43.75	4375
6.00	45	46	45.50	4550

occured in gauge A also occured in gauge D and since these are in opposing arms of the bridge, the net effect of the fluctuation should be zero. The D.C. bridge is calibrated by changing the variable resistance in N arm of Figure 4.1 and the corresponding Nanovoltmeter reading is obtained. Nanovoltmeter deflection Vs change in resistance is plotted in Figure 4.2 and the relation is found to be linear.

4.7 Gauge Circuit:

The gauge circuit is consist of an active gauge, a dummy gauge, a fixed resistance and a variable resistance which are set in the four arms of *d.c.* wheatstone bridge in slightly out of balance condition. When the resistance of the active gauge is changed from R to $R+\Delta R$, a corresponding out of balance voltage developed across the input of the *d.c.* amplifier. Then the deflection is observed in the nanovoltmeter which is connected to the wheatstone bridge curcuit input.

4.8 D.C. Amplifier:

Nanovoltmeter model-140^{4.3} is used for measuring the small out of balance *d.c.* voltage. It acted as a potentiometric amplifier and had a sensitivity of $0.1 \mu V$ for full scale deflection in the highest sensitivity range. A panel switch selector permitted the meter sensitivity to be altered. Any *a.c.* signal superimposed on the *d.c.* voltage to be measured is almost entirely attenuated, the filtering factor being inversely proportional to the frequency. We used an additional filter circuit to get rid of any *a.c.* components of very low frequency before the signal entered the recoder. The zero drift was less than $0.05 \mu v/\text{hour}$. When all sources of thermo e.m.f. are reduced by using low thermal

solders and protecting the metallic junctions from thermal fluctuations. The input resistance of the d.c. amplifier is about 1 megaohm in all ranges.

4.9 Sensitivity and Calibration of the D.C. Bridge:

The current flowing in *d.c.* bridge circuit is given in terms of the parameter of the *d.c.* bridge shown in figure-4.1 is

$$I_G = \frac{E}{(B+D+A+\frac{BD}{M})(Z+N+A+\frac{ZN}{M})} \times \left(\frac{\Delta A}{1+K\Delta A} \right) \quad (4.1)$$

Thus

$$K = \frac{M(D+Z)+(B+N)(M+D+Z)}{M(B+D+A+\frac{BD}{M})(Z+N+A+\frac{ZN}{M})} \quad (4.2)$$

Equation-4.1 is an exact algebraic solution for I_G , where the circuit on the right hand side of points PQ has been treated as a current measuring device of input resistance Z . Since the bridge is only slightly unbalanced $K\Delta A \ll 1$ and the factor $1+K\Delta A$ can be replaced by unity. Also, since the input resistance of the measuring unit is of the order of one megaohm, we can put $Z \rightarrow \infty$ in equation-4.1 and obtain the expression for the maximum voltage sensitivity corresponding to $B=0$, close to the balance condition of the bridge

$$X \left(\frac{\Delta I_G}{\Delta A} \right)_0 = \frac{ED}{(D+A)^2} \quad (4.3)$$

In our bridge D represents the resistance of the dummy gauge and A that of the active gauge. Both have the same value of 120 ohm in the unstrained condition. Thus the fractional change in resistance can be written as

$$\left(\frac{\Delta A}{A} \right) = \frac{4Z\Delta I_G}{E} \quad (4.4)$$

Thus the out of balance voltage $Z\Delta I/g$ measured, maintains a linear relationship with $\Delta A/A$, giving a constant sensitivity. The deviation from linear relationship will only occur if the condition $1+K\Delta A=1$ does not hold. It can be shown that the fractional error involved for this assumption is at most $\Delta A/A$. In our measurement $\Delta R/R$ is never exceeded 10^{-3} which corresponds to a fractional error of 0.1%.

The bridge is calibrated by changing the resistance parallel to the 10 ohm resistance in the arms N of the bridge. The minimum voltage that could be measured without noise and drift is of the order of 10^{-6} corresponding to 1mm deflection in the nanovoltmeter. The gauge factor of the strain gauge is 2.09 and the voltage supplied to the bridge is two volts. Thus the maximum strain sensitivity is of the order of 2.5×10^{-6} from equation-4.4. The sensitivity of the bridge could be increased further either by increasing the current in the circuit or by using higher gain in the amplifier. The upper usable limit is determined by the maximum allowable joule heating in the gauges and the signal to noise ratio. For minimizing the noise, all connection are made with co-axial cables, so that all parts are well screened.

4.10. The choice of dummy Material:

It is essential to make the gauging circuit invariant in respect to active gauge. That is why the dummy material require an identical and similar behaviour of the active gauge for justifying the use of a compensating gauge for all strain measurements. The nearest approach to this condition can be achieved by using two identical gauges with identical strain and kept in the same thermal conditions. we used fused silica glass as dummy materials for its negligible thermal expansion co-efficients. The other gauge is connected to the material sample for which we desired to measure the magnetostriction.

4.11 The Specimen Holder:

The specimen and the dummy must be placed in an identical thermal condition for accurate measurement. Any difference in the thermal environment of the active and dummy gauge effect the results drastically. To maintain an identical thermal environment for the gauges, a cylindrical shaped specimen holder is made as shown in Figure-4.3 Initially a copper rod of diameter 16 mm is taken in which two identical grooves of thickness 7 mm and width 10 mm are cut and partition by a thin section of width of 2 mm. This arrangement made it possible to keep the active and dummy specimen as close as possible. A specimen and the dummy are fixed on the opposite face of a thin partition which is in between the two cavity. Two identical strain gauge one on the face of the active specimen other on the dummy specimen are glued. Electrical connection from the gauges are taken

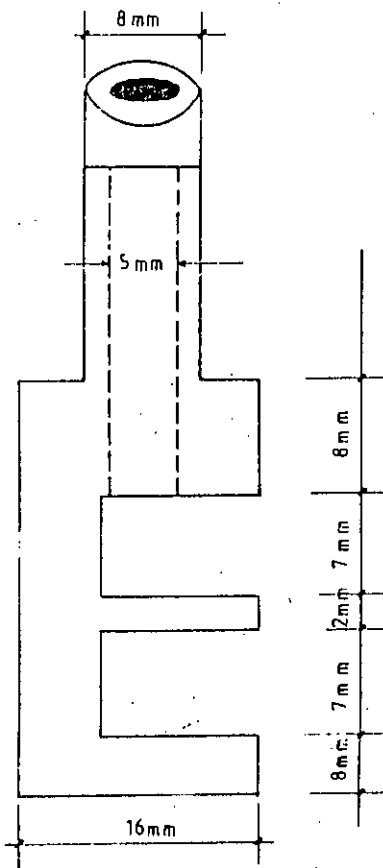


Fig. 4.2: Specimen Holder

out through the hole of 2 mm diameter made in the centre of the specimen holder. A quartz glass tube of 8 mm diameter and 100 cm in length is taken. One end of this glass tube glued with a copper strip. The specimen holder is then attached to this slip with screw. Electrical connection is taken out through the glass tube. A copper hollow tube of 16 mm internal diameter is used as a jacket to keep the active and the dummy at the same temperature and to isolate them from thermal fluctuations. The arrangement is found quite satisfactory for our experiment.

4.12 Specimen Mounting

Special care must be taken before to mounting a ferromagnetic crystal to minimise two opposing factors. The crystal must not be mechanically constrained by the specimen holder so that the spontaneous distortion of the crystal due to temperature or magnetic field can faithfully be transmitted to the strain gauge, especially, when the crystal is elastically soft but highly magnetic. The mechanical constraint may even cause distortion of the symmetry of the crystal. From this consideration, therefore the mounting has to be flexible. On the other hand, to avoid any rotation of the specimen due to the torque produced by the magnetic anisotropy, the sample must be hold sufficiently rigid. The best compromise is made by using a thin cork spacer between the specimen and the base of the specimen holder. The specimen is glued to the cork by durofix and the cork in turn to the specimen holder. The mosaic pattern of the cork spacer allows the specimen to expand or contract quite freely but constrains it from rotation due to body forces. Comparison of thermal expansion of a copper specimen when fixed to a cork spacer and when free showed that the constraint due to the above mentioned arrangement does not affect the results.

4.13 The Calibration of Electro Magnet

An electro-magnet type Varian is used for the production of magnetic field. When the maximum current of 6 ampere *d.c.* is used with conical pole tips and a gap of 35 mm the field produced at the centre of the pole pieces is 4.5 K Gauss. The magnet could be rotated about a vertical axis through the centre of the pole gaps and could be locked in any position. The angular position of the magnet could be read in degree from the scale attached to the magnet and the calibrated circular scale fixed at the base. The field versus current curve for the magnet, for the pole gap used, is calibrated using Norma Electronic Flux meter. The obtained data is listed in table 4.1 and field versus current curve is shown in Figure-4.4. A very small hysteresis effect is observed for increasing and decreasing currents. Using control knob of the *d.c.* source, the current could be increased or decreased contineously to within 50 mA.

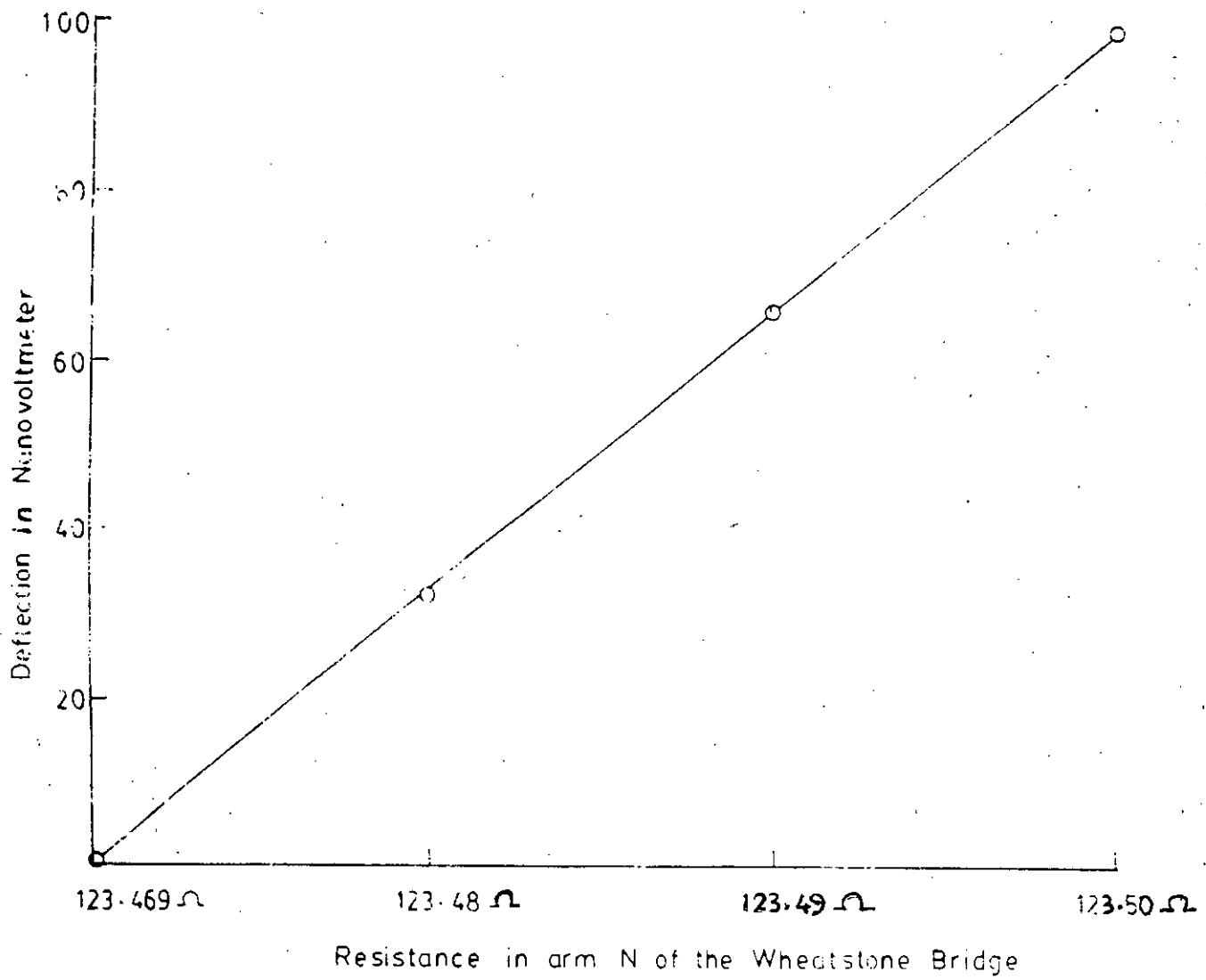


Fig. 4.3 Deflection against change in resistance

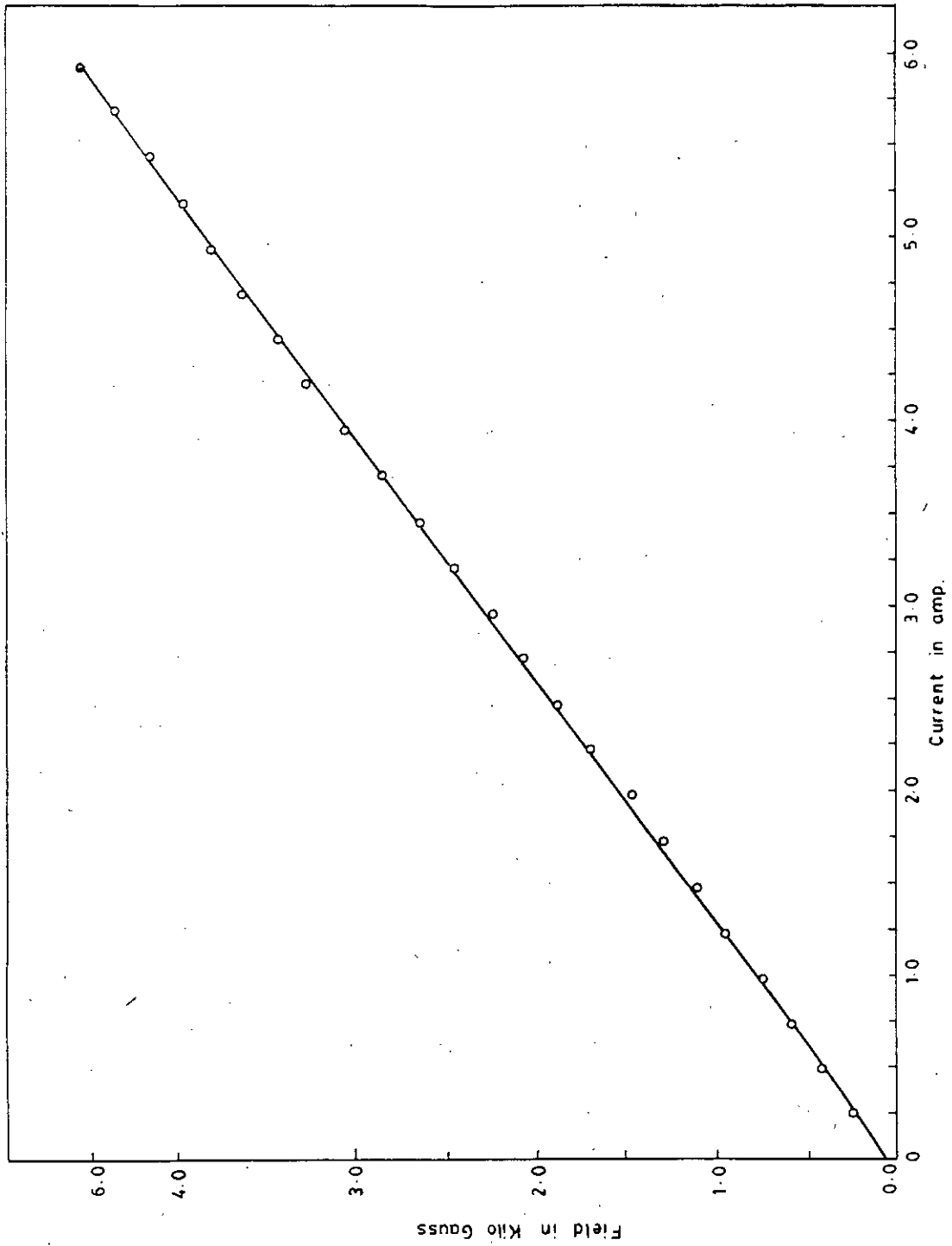


FIG. 4.4 CALIBRATION CURVE FOR THE ELECTROMAGNET (FIELD VS. CURRENT)

4.14 Magneto Mechanical Coupling

The magneto mechanical coupling factor K is the most important single parameter in determining the efficiency of conversion magnetic energy in to mechanical energy using magnetostrictive transducers. If we neglect loss and radiation, then for a magneto-mechanical vibrator K is defined in such a way that K^2 denotes the fraction of the magnetic energy which can be converted to elastic energy per cycle. K^2 also denotes the fraction of the stored elastic energy which can be converted to magnetic energy.

For a magneto mechanically driven system we can write.

$$(1 - K^2)E_{elas.} = K^2 E_{mag} \quad (4.6)$$

Now representing components of strain by t , magnetic induction by B , stress by T and magnetic field by H , we can write

$$t = S^H T + D H \quad (4.7)$$

where S^H is compliance at constant field and D denotes coupling

Again

$$B = D T + \mu^T H \quad (4.8)$$

where μ^T denotes permeability at constant strain.

Defining the permeability of constant strain μ^t and the compliance at constant induction

S^B , it follows that

$$\mu^t = \left(1 - \frac{D^2}{S^H \mu^T}\right) \mu^T \quad (4.9)$$

and

$$S^H = \left(1 - \frac{D^2}{S^H \mu^T}\right) S^H \quad (4.10)$$

writing equation (4.5) in term of moduli $C = 1/S$, we get

$$C^H = \left(1 - \frac{D^2}{S^H \mu^T}\right) C^B \quad (4.11)$$

The maximum fraction of magnetic energy which can be transformed is

$$\frac{\frac{1}{2}\mu^T H^2 - \frac{1}{2}\mu^I H^2}{\frac{1}{2}\mu^T H^2} = \frac{\mu^T - \mu^I}{\mu^T} \quad (4.12)$$

Similarly the maximum fraction of elastic energy which can be transformed is

$$\frac{\frac{1}{2}C^B \frac{1}{2}C^H l^2}{\frac{1}{2}C^B l^2} = \frac{C^B - l^H}{C^B} = \frac{D^2}{s^H \mu^T} = K^2 \quad (4.13)$$

From equation (4.4) we find that the permeability is reduced from its intrinsic value μ^T whenever energy is transferred to the elastic system. Likewise the intrinsic i.e. uncoupled elastic stiffness C^B is reduced to a lower value C^B , where energy is transferred from elastic to magnetic system. From equation (4.12) the magnetomechanical coupling K can be obtained by measuring the complex impedance of a coil containing the magnetostrictive material.

4.15 Construction of a Solenoid

A solenoid has been designed and developed for measuring the coupling factors. A glass rod of diameter 10 cm and length 31 cm is taken. The wire wound on this glass rod is a superenamelled wire of 18 S.W.G. It has 4.1 Ohm resistance per 1000 ft. having a current carrying capacity 2.6 A. After the winding of 7500 turns, the outer diameter of the glass rod became 40 cm. This was used for generating a varying magnetic field and the corresponding dynamic magnetostrictive strain was looked for using an oscilloscope. However, the noise background was relatively high, specially for small size of the specimens. The computation therefore, could not be performed quantitatively

4.16 Measurement of Magnetostriction

The magnetostriction of Nickel, $Fe_{100-x}Al_x$ ($x=2, 8, 10, 12$ and 14), and $Tb_{.27}Dy_{.73}Fe_2$ are measured by strain gauge technique as a function of field. The magnetostriction for different magnetic field is measured with a maximum field of 4550 gauss. The measurements are confined to room temperature. The variation of magnetostriction for these specimen as a function of magnetic field direction is presented in Figure 4.5, 4.7, 4.8, 4.9, 4.11 and 4.13. These values of the magnetostriction are calculated by using the relation,

$$\lambda = \frac{2}{3G} \times \frac{dR}{R} \quad (4.5)$$

Where sensitivity per Nanovoltmeter deflection $dR/R = 2.5 \times 10^{-6}$ and G is the gauge factor which is 2.09 in our experiment.

By determining the difference in deflection in the Nanovoltmeter for magnetic field along the length of the strain gauge cemented on the specimen and in the direction perpendicular to the length of the strain gauge enable one to calculate λ . The values of magnetostriction of Ni , $Fe_{98}Al_2$, $Fe_{92}Al_8$, $Fe_{90}Al_{10}$, $Fe_{88}Al_{12}$, $Fe_{86}Al_{14}$ and $Tb_{.27}Dy_{.73}Fe_2$ are listed in table-(3), (5), (7), (9), (11), (13) and (15) respectively. The variation of magnetostriction with applied magnetic field for these specimen is shown in Figure 4.6, 4.12 and 4.14. The variation of magnetostriction as a function of specific magnetization is shown in Figure 4.15.

TABLE -4.2

VARIATION OF MAGNETOSTRICTION WITH MAGNETIC FIELD FOR NICKEL
 SENSITIVITY PER DEFLECTION $\Delta R/R=2.5 \times 10^{-6}$
 GAUGE FACTOR $G= 2.09$

FIELD IN GAUSS	425	800	1175	1550	1875	2250	2650	3050	3400	3800	4125	4550
CUR-RENT	.5	1	1.5	2	2.5	3	3.5	4	4.5	5	5.5	6
0	0	0	0	0	0	0	0	0	0	0	0	0
10	+2	+6	+10	+12	+12	+12	+12	+12	+12	+12	+12	+12
20	+5	+8	+13	+16	+16	+16	+16	+16	+16	+16	+16	+16
30	+6	+10		+18	+18	+18	+18	+18	+18	+18	+18	+18
40	+5	+9	+14	+17	+17	+17	+17	+17	+17	+17	+17	+17
50	+3	+7	+12	+15	+15	+15	+15	+15	+15	+15	+15	+15
60	+2	+5	+8	+11	+11	+11	+11	+11	+11	+11	+11	+11
70	+1	+3	+4	+5	+5	+5	+5	+5	+5	+5	+5	+5
80	0	0	0	0	0	0	0	0	0	0	0	0
90	-1	-3	-7	-10	-10	-10	-10	-10	-10	-10	-10	-10
100	-3	-7	-12	-15	-15	-15	-15	-15	-15	-15	-15	-15
110	-5	-10	-17	-20	-20	-20	-20	-20	-20	-20	-20	-20
120	-7	-13	-20	-23	-23	-23	-23	-23	-23	-23	-23	-23
130	-9	-15	-22	-26	-26	-26	-26	-26	-26	-26	-26	-26
140	-10	-16	-23	-28	-28	-28	-28	-28	-28	-28	-28	-28
150	-9	-14	-21	-24	-24	-24	-24	-24	-24	-24	-24	-24
160	-7	-11	-17	-20	-20	-20	-20	-20	-20	-20	-20	-20
170	-3	-5	-8	-12	-12	-12	-12	-12	-12	-12	-12	-12
180	0	0	0	0	0	0	0	0	0	0	0	0

TABLE-4.3

VARIATION OF MAGNETOSTRICTION WITH MAGNETIC FIELD FOR
 NICKEL SENSITIVITY PER DEFLECTION $\Delta R/R=2.5 \times 10^{-6}$

BRIDGE CURRENT-25 mA

GAUGE FACTOR $G=2.09$

FIELD CURRENT IN AMP.	MAGNETIC FIELD IN GAUSS	DEFLECTION OF NANO VOLTMETER	$\Delta R/R \times \text{NANO}$ VOLTMETER DEFLECTION	MAGNETOSTRIC TION $=2/3G \times$ R/R
0	0	0	0	0
0.5	425	16	40×10^{-6}	12.76×10^{-6}
1	800	26	65×10^{-6}	20.73×10^{-6}
1.5	1175	38	95×10^{-6}	30.30×10^{-6}
2	1550	46	115×10^{-6}	36.68×10^{-6}
2.5	1875	46	115×10^{-6}	36.68×10^{-6}
3	2250	46	115×10^{-6}	36.68×10^{-6}
3.5	2650	46	115×10^{-6}	36.68×10^{-6}
4	3050	46	115×10^{-6}	36.68×10^{-6}
4.5	3400	46	115×10^{-6}	36.68×10^{-6}
5	3800	46	115×10^{-6}	36.68×10^{-6}
5.5	4125	46	115×10^{-6}	36.68×10^{-6}
6	4550	46	115×10^{-6}	36.68×10^{-6}

TABLE - 4.4

VARIATION OF MAGNETOSTRICTION WITH MAGNETIC FIELD FOR Fe₉₈Al₂
AT ROOM TEMPERATURE

SENSITIVITY PER DEFLECTION $\Delta R/R = 2.5 \times 10^{-6}$

GAUGE FACTOR G= 2.09

BRIDGE CURRENT 25 mA

FIELD IN GAUSS	425	800	1175	1550	1875	2250	2650	3050	3400	3800	4125	4550
CURREN AMP.	0.5	1	1.5	2	2.5	3	3.5	4	4.5	5	5.5	6
0	0	0	0	0	0	0	0	0	0	0	0	0
10	+0.25	+1.5	+1.5	+2.5	+2.5	+2.5	+2.5	+2.5	+2.5	+2.5	+2.5	+2.5
20	+0.5	+1.5	+3	+4.5	+4.5	+4.5	+4.5	+4.5	+4.5	+4.5	+4.5	+4.5
30	+1	+2.5	+4	+5.75	+5.75	+5.75	+5.75	+5.75	+5.75	+5.75	+5.75	+5.75
40	+1.5	+3.5	+5	+7.0	+7.0	+7.0	+7.0	+7.0	+7.0	+7.0	+7.0	+7.0
50	+1.25	+3	+4.75	+6.5	+6.5	+6.5	+6.5	+6.5	+6.5	+6.5	+6.5	+6.5
60	+1	+2.5	+4	+5.50	+5.50	+5.50	+5.50	+5.50	+5.50	+5.50	+5.50	+5.50
70	+0.5	+1.8	+3	+4.5	+4.5	+4.5	+4.5	+4.5	+4.5	+4.5	+4.5	+4.5
80	+0.25	+1	+1.5	+3	+3	+3	+3	+3	+3	+3	+3	+3
90	0	0	0	0	0	0	0	0	0	0	0	0
100	-0.25	-0.75	-1	-1.5	-1.5	-1.5	-1.5	-1.5	-1.5	-1.5	-1.5	-1.5
110	-0.50	-1.25	-2	-3.5	-3.5	-3.5	-3.5	-3.5	-3.5	-3.5	-3.5	-3.5
120	-0.75	-2	-3	-5	-5	-5	-5	-5	-5	-5	-5	-5
130	-1.0	-2.5	-4	-6	-6	-6	-6	-6	-6	-6	-6	-6
140	-0.75	-3	-4.5	-6.5	-6.5	-6.5	-6.5	-6.5	-6.5	-6.5	-6.5	-6.5
150	-0.65	-2.5	-4	-6	-6	-6	-6	-6	-6	-6	-6	-6
160	-0.50	-1.9	-3	-5	-5	-5	-5	-5	-5	-5	-5	-5
170	-0.25	-1	-1.5	-3	-3	-3	-3	-3	-3	-3	-3	-3
180	0	0	0	0	0	0	0	0	0	0	0	0

TABLE-4.5

VARIATION OF MAGNETOSTRICTION WITH MAGNETIC FIELD FOR $\text{Fe}_{98}\text{Al}_2$
AT ROOM TEMPERATURE

SENSITIVITY PER DEFLECTION $\Delta R/R=2.5 \times 10^{-6}$

BRIDGE CURRENT 25 mA

GAUGE FACTOR $G=2.09$

FIELD CURRENT IN AMP.	MAGNETIC FIELD IN GAUSS	DEFLECTION OF NANO VOLTMETER	$\Delta R/R \times \text{NANO}$ VOLTMETER DEFLECTION	MAGNETOSTRICTION $=2/3G \times \Delta R/R$
0	0	0	0	0
0.5	425	2.25	5.63×10^{-6}	1.80×10^{-6}
1	800	6.5	16.25×10^{-6}	5.18×10^{-6}
1.5	1175	9.5	23.75×10^{-6}	7.58×10^{-6}
2	1550	13.5	33.75×10^{-6}	10.77×10^{-6}
2.5	1875	13.5	33.75×10^{-6}	10.77×10^{-6}
3	2250	13.5	33.75×10^{-6}	10.77×10^{-6}
3.5	2650	13.5	33.75×10^{-6}	10.77×10^{-6}
4	3050	13.5	33.75×10^{-6}	10.77×10^{-6}
4.5	3400	13.5	33.75×10^{-6}	10.77×10^{-6}
5	3800	13.5	33.75×10^{-6}	10.77×10^{-6}
5.5	4125	13.5	33.75×10^{-6}	10.77×10^{-6}
6	4550	13.5	33.75×10^{-6}	10.77×10^{-6}

TABLE-4.6

VARIATION OF MAGNETOSTRICTION WITH MAGNETIC FIELD FOR Fe₉₂Al₈
AT ROOM TEMPERATURE

SENSITIVITY PER DEFLECTION $\Delta R/R = 2.5 \times 10^{-6}$

GAUGE FACTOR $G = 2.09$

BRIDGE CURRENT 25 mA

FIELD IN GAUSS	425	800	1175	1550	1875	2250	2650	3050	3400	3800	4125	4550
CURRENT IN AMP.	0.5	1	1.5	2	2.5	3	3.5	4	4.5	5	5.5	6
0	0	0	0	0	0	0	0	0	0	0	0	0
10	+0.25	+0.5	+1	+2	+3	+4	+4	+4	+4	+4	+4	+4
20	+0.50	+2	+3	+4.5	+6	+8	+8	+8	+8	+8	+8	+8
30	+1	+3	+5	+7	+9	+12	+12	+12	+12	+12	+12	+12
40	+2	+4	+7	+9	+11	+14	+14	+14	+14	+14	+14	+14
50	+1	+3.9	+6.5	+8.75	+10.5	+13	+13	+13	+13	+13	+13	+13
60	+0.5	+3.75	+5	+7	+9	+12	+12	+12	+12	+12	+12	+12
70	+0.25	+2	+3	+5	+6.5	+8	+8	+8	+8	+8	+8	+8
80	0	+1	+1.5	+3	+4	+5	+5	+5	+5	+5	+5	+5
90	0	0	0	0	0	0	0	0	0	0	0	0
100	0	-.5	-1	-1.5	-2	-3	-3	-3	-3	-3	-3	-3
110	-0.25	-1	-2	-4	-5	-6	-6	-6	-6	-6	-6	-6
120	-0.5	-2	-3	-5	-6	-9	-9	-9	-9	-9	-9	-9
130	-1.75	-3	-4.5	-6	-7	-11	-11	-11	-11	-11	-11	-11
140	-2	-3.5	-5	-7	-8	-12	-12	-12	-12	-12	-12	-12
150	-1.25	-3	-4.5	-6	-7.75	-11	-11	-11	-11	-11	-11	-11
160	-0.5	-2	-3	-4	-6.5	-9	-9	-9	-9	-9	-9	-9
170	0	-1	-2	-3	-3.5	-5	-5	-5	-5	-5	-5	-5
180	0	0	0	0	0	0	0	0	0	0	0	0

TABLE-4.7

VARIATION OF MAGNETOSTRICTION WITH MAGNETIC FIELD FOR Fe₉₂Al₈

SENSITIVITY PER DEFLECTION $\Delta R/R=2.5 \times 10^{-6}$

BRIDGE CURRENT 25 mA.

GAUGE FACTOR $G=2.09$

FIELD CURRENT IN AMP.	MAGNETIC FIELD IN GAUSS	DEFLECTION OF NANO VOLTMETER	$\Delta R/R \times \text{NANO}$ VOLTMETER DEFLECTION	MAGNETOSTRICTION $=2/3G \times \Delta R/R$
0	0	0	0	0
0.5	425	4	10×10^{-6}	3.19×10^{-6}
1	800	7.5	18×10^{-6}	5.98×10^{-6}
1.5	1175	12	30×10^{-6}	9.57×10^{-6}
2	1550	16	40×10^{-6}	12.76×10^{-6}
2.5	1875	19	47.5×10^{-6}	15.15×10^{-6}
3	2250	26	65×10^{-6}	20.73×10^{-6}
3.5	2650	26	65×10^{-6}	20.73×10^{-6}
4	3050	26	65×10^{-6}	20.73×10^{-6}
4.5	3400	26	65×10^{-6}	20.73×10^{-6}
5	3800	26	65×10^{-6}	20.73×10^{-6}
5.5	4125	26	65×10^{-6}	20.73×10^{-6}
6	4550	26	65×10^{-6}	20.73×10^{-6}

TABLE-4.8

VARIATION OF MAGNETOSTRICTION WITH MAGNETIC FIELD FOR
 $\text{Fe}_{90}\text{Al}_{10}$ AT ROOM TEMPERATURE

SENSITIVITY PER DEFLECTION $\Delta R/R = 2.5 \times 10^{-6}$

GAUGE FACTOR $G = 2.09$

BRIDGE CURRENT 25 mA

FIELD IN GAUSS	425	800	1175	1550	1875	2250	2650	3050	3400	3800	4150	4550
CURRENT IN AMP.	.5	1	1.5	2	2.5	3	3.5	4	4.5	5	5.5	6
0	0	0	0	0	0	0	0	0	0	0	0	0
10	+0.5	+1.5	+2.5	+4	+7	+10	+10	+10	+10	+10	+10	+10
20	+1	+2	+6.5	+9	+12	+16	+16	+16	+16	+16	+16	+16
30	+3	+6	+10	+14	+17	+20	+20	+20	+20	+20	+20	+20
40	+4	+9	+13.5	+17	+21	+24	+24	+24	+24	+24	+24	+24
50	+3.5	+8.5	+13	+16.7	+20.5	+23.9	+23.9	+23.9	+23.9	+23.9	+23.9	+23.9
60	+3	+7	+10	+14	+17	+21	+21	+21	+21	+21	+21	+21
70	+2	+5	+7	+9	+12	+16	+16	+16	+16	+16	+16	+16
80	+1	+3	+4	+5	+7	+11	+11	+11	+11	+11	+11	+11
90	0	0	0	0	0	0	0	0	0	0	0	0
100	-0.5	-1	-1.5	-2	-3	-5	-5	-5	-5	-5	-5	-5
110	-1	-2	-3.5	-5	-6	-9	-9	-9	-9	-9	-9	-9
120	-1.9	-3	-5	-7	-9	-12	-12	-12	-12	-12	-12	-12
130	-2	-4	-6.5	-9	-11	-14	-14	-14	-14	-14	-14	-14
140	-2.25	-4.5	-7	-8.75	-10.5	-13.9	-13.9	-13.9	-13.9	-13.9	-13.9	-13.9
150	-2	-4	-6.5	-7.5	-9	-12	-12	-12	-12	-12	-12	-12
160	-1	-1.5	-3	-4.5	-6	-9	-9	-9	-9	-9	-9	-9
170	-0.5	-1	-2	-2.5	-3	-5	-5	-5	-5	-5	-5	-5
180	0	0	0	0	0	0	0	0	0	0	0	0

TABLE - 4.9

VARIATION OF MAGNETOSTRICTION WITH MAGNETIC FIELD FOR
 $\text{Fe}_{90}\text{Al}_{10}$

SENSITIVITY PER DEFLECTION $\Delta R/R = 2.5 \times 10^{-6}$

BRIDGE CURRENT 25 mA.

GAUGE FACTOR $G = 2.09$

FIELD CURRENT IN AMP.	MAGNETIC FIELD IN GAUSS	DEFLECTION OF NANO VOLT METER	$\Delta R/R \times \text{NANO}$ VOLT METER DEFLECTION	MAGNETOSTRICTION $= 2/3G \times \Delta R/R$
0	0	0	0	0
0.5	425	7	17.5×10^{-6}	5.58×10^{-6}
1	800	13	32.5×10^{-6}	10.37×10^{-6}
1.5	1175	20	50×10^{-6}	15.95×10^{-6}
2	1550	26	65×10^{-6}	20.73×10^{-6}
2.5	1875	32	80×10^{-6}	25.52×10^{-6}
3	2250	37.9	94.75×10^{-6}	30.22×10^{-6}
3.5	2650	37.9	94.75×10^{-6}	30.22×10^{-6}
4	3050	37.9	94.75×10^{-6}	30.22×10^{-6}
4.5	3400	37.9	94.75×10^{-6}	30.22×10^{-6}
5	3800	37.9	94.75×10^{-6}	30.22×10^{-6}
5.5	4125	37.9	94.75×10^{-6}	30.22×10^{-6}
6	4550	37.9	94.75×10^{-6}	30.22×10^{-6}

TABLE - 4.10

VARIATION OF MAGNETOSTRICTION WITH MAGNETIC FIELD FOR Fe₈₈Al₁₂ AT ROOM TEMPERATURE
 SENSITIVITY PER DEFLECTION $\Delta R/R = 2.5 \times 10^{-6}$
 GAUGE FACTOR $G = 2.09$

BRIDGE CURRENT 25 mA FIELD IN GAUSS	425	800	1175	1550	1875	2250	2650	3050	3400	3800	4125	4550
CURRENT IN AMP.	0.5	1	1.5	2	2.5	3	3.5	4	4.5	5	5.5	6
0	0	0	0	0	0	0	0	0	0	0	0	0
10	+0.5	+1	+3	+4	+8	+12	+12	+12	+12	+12	+12	+12
20	+2.5	+5	+7	+10	+14	+20	+20	+20	+20	+20	+20	+20
30	+5	+8	+11	+16	+20	+26	+26	+26	+26	+26	+26	+26
40	+7	+11	+16	+21	+25	+30	+30	+30	+30	+30	+30	+30
50	+6	+10	+15	+20	+24.5	+29	+29	+29	+29	+29	+29	+29
60	+4	+8	+13	+16	+21	+26	+26	+26	+26	+26	+26	+26
70	+3	+5	+9	+11	+16	+20	+20	+20	+20	+20	+20	+20
80	+1	+2	+4	+5	+8	+12	+12	+12	+12	+12	+12	+12
90	0	0	0	0	0	0	0	0	0	0	0	0
100	-0.5	-1	-2.5	-4	-6	-8	-8	-8	-8	-8	-8	-8
110	-2	-3	-5	-7	-10	-12	-12	-12	-12	-12	-12	-12
120	-2.5	-5	-8	-11	-14	-18	-18	-18	-18	-18	-18	-18
130	-3	-7	-11	-15	-18	-22	-22	-22	-22	-22	-22	-22
140	-2.9	-6	-10	-14.5	-17	-21	-21	-21	-21	-21	-21	-21
150	-2	-5	-8	-12	-12	-16	-16	-19	-19	-19	-19	-19
160	-1.9	-3	-6	-8	-12	-14	-14	-14	-14	-14	-14	-14
170	-0.5	-1	-3	-4	-7	-9	-9	-9	-9	-9	-9	-9
180	0	0	0	0	0	0	0	0	0	0	0	0

TABLE-4.11

VARIATION OF MAGNETOSTRICTION WITH MAGNETIC FIED FOR
 $\text{Fe}_{88}\text{Al}_{12}$ SENSITIVITY PER DEFLECTION $\Delta R/R=2.5 \times 10^{-6}$

GAUGE FACTOR $G=2.09$

BRIDGE CURRENT 25 mA

FIELD CURRENT IN AMP.	MAGNETIC FIELD IN GAUSS	DEFLECTION OF NANO VOLTMETER	$\Delta R/R \times \text{NANO}$ VOLTMETER DEFLECTION	MAGNETOSTRICTION $=2/3G \times \Delta R/R$
0	0	0	0	0
0.5	425	10	25×10^{-6}	7.98×10^{-6}
1	800	18	45×10^{-6}	14.36×10^{-6}
1.5	1175	27	67.5×10^{-6}	21.53×10^{-6}
2	1550	36	90×10^{-6}	28.71×10^{-6}
2.5	1875	43	107.5×10^{-6}	34.29×10^{-6}
3	2250	52	130×10^{-6}	41.47×10^{-6}
3.5	2650	52	130×10^{-6}	41.47×10^{-6}
4	3050	52	130×10^{-6}	41.47×10^{-6}
4.5	3400	52	130×10^{-6}	41.47×10^{-6}
5	3800	52	130×10^{-6}	41.47×10^{-6}
5.5	4125	52	130×10^{-6}	41.47×10^{-6}
6	4550	52	130×10^{-6}	41.47×10^{-6}

TABLE-4.12

VARIATION OF MAGNETOSTRICTION WITH FIELD FOR Fe₈₆Al₁₄ AT ROOM TEMPERATURE

SENSITIVITY PER DEFLECTION $\Delta R/R = 2.5 \times 10^{-6}$

GAUGE FACTOR $G = 2.09$

BRIDGE CURRENT 25 mA

FIELD IN GAUSS	425	800	1175	1550	1875	2250	2650	3050	3400	3800	4125	4550
CURRENT IN AMP.	0.5	1	1.5	2	2.5	3	3.5	4	4.5	5	5.5	6
0	0	0	0	0	0	0	0	0	0	0	0	0
10	+0.5	+1	+2	+3	+4	+6	+6	+6	+6	+6	+6	+6
20	+2	+3	+4	+6	+8	+12	+12	+12	+12	+12	+12	+12
30	+2.25	+5	+7	+10	+12	+18	+18	+18	+18	+18	+18	+18
40	+3	+6.25	+10	+14	+18	+22	+22	+22	+22	+22	+22	+22
50	+4	+7	+12	+16	+20	+24	+24	+24	+24	+24	+24	+24
60	+3	+5.9	+10	+14	+18	+22	+22	+22	+22	+22	+22	+22
70	+2.25	+4	+7	+11	+13	+16	+16	+16	+16	+16	+16	+16
80	+1	+2	+4	+5	+7	+8	+8	+8	+8	+8	+8	+8
90	0	0	0	0	0	0	0	0	0	0	0	0
100	-0.5	-1	-1.5	-2	-3	-4	-4	-4	-4	-4	-4	-4
110	-1	-2	-3.5	-5	-7	-10	-10	-10	-10	-10	-10	-10
120	-2	-3	-5	-8	-11	-14	-14	-14	-14	-14	-14	-14
130	-3	-4	-6	-10	-14	-18	-18	-18	-18	-18	-18	-18
140	-2.75	-3.75	-5.5	-9	-13	-17.9	-17.9	-17.9	-17.9	-17.9	-17.9	-17.9
150	-2.25	-3.5	-5	-11	-16	-16	-16	-16	-16	-16	-16	-16
160	-1.5	-2.5	-3	-5	-8	-12	-12	-12	-12	-12	-12	-12
170	-0.5	-1	-1.75	-3	-4	-8	-8	-8	-8	-8	-8	-8
180	0	0	0	0	0	0	0	0	0	0	0	0

TABLE-4.13

VARIATION OF MAGNETOSTRICTION WITH MAGNETIC FIELD FOR

Fe₈₆Al₁₄SENSITIVITY PER DEFLECTION $\Delta R/R=2.5 \times 10^{-6}$

BRIDGE CURRENT 25 mA

GAUGE FACTOR $G=2.09$

FIELD CURRENT IN AMP.	MAGNETIC FIELD IN GAUSS	DEFLECTION OF NANO VOLTMETER	$\Delta R/R \times \text{NANO}$ VOLTMETER DEFLECTION	MAGNETOSTRICTION $=2/3G \times \Delta R/R$
0	0	0	0	0
0.5	425	6	17×10^{-6}	4.79×10^{-6}
1	800	13	32.5×10^{-6}	10.37×10^{-6}
1.5	1175	20	50×10^{-6}	15.95×10^{-6}
2	1550	26	65×10^{-6}	20.74×10^{-6}
2.5	1875	34	85×10^{-6}	27.16×10^{-6}
3	2250	42	105×10^{-6}	33.49×10^{-6}
3.5	2650	42	105×10^{-6}	33.49×10^{-6}
4	3050	42	105×10^{-6}	33.49×10^{-6}
4.5	3400	42	105×10^{-6}	33.49×10^{-6}
5	3800	42	105×10^{-6}	33.49×10^{-6}
5.5	4125	42	105×10^{-6}	33.49×10^{-6}
6	4550	42	105×10^{-6}	33.49×10^{-6}

TABLE-4.14

VARIATION OF MAGNETOSTRICTION WITH MAGNETIC FIELD FOR
 $Tb_{.27}Dy_{.73}Fe_2$ AT ROOM TEMPERATURE

SENSITIVITY PER DEFLECTION $\Delta R/R = 2.5 \times 10^{-6}$

GAUGE FACTOR $G = 2.09$

BRIDGE CURRENT 25 mA

FIELD IN GAUSS	424	800	1175	1550	1875	2250	2650	3050	3400	3800	4125	4550
CURRENT IN AMP.	.5	1	1.5	2	2.5	3	3.5	4	4.5	5	5.5	6
0	0	0	0	0	0	0	0	0	0	0	0	0
10	+30	+100	+250	+300	+400	+700	+1200	+2100	+2100	+2100	+2100	+2100
20	+100	+250	+500	+700	+1200	+1500	+2300	+2900	+2900	+2900	+2900	+2900
30	+175	+500	+1000	+1300	+1900	+2200	+2800	+3200	+3200	+3200	+3200	+3200
40	+200	+200	+600	+1300	+1800	+2400	+2750	+3000	+3300	+3300	+3300	+3300
50	+175	+500	+1200	+1700	+2300	+2700	+2980	+3200	+3200	+3200	+3200	+3200
60	+100	+400	+950	+1300	+1900	+2200	+2800	+3000	+3000	+3000	+3000	+3000
70	+75	+300	+700	+900	+1100	+1500	+2200	+2800	+2800	+2800	+2800	+2800
80	+20	+175	+300	+400	+500	+600	+1000	+2000	+2000	+2000	+2000	+2000
90	0	0	0	0	0	0	0	0	0	0	0	0
100	-20	-100	-175	-200	-300	-500	-800	-1400	-1400	-1400	1400	-1400
110	-50	-200	-300	-500	-700	-1100	-1500	-2200	-2200	-2200	2200	-2200
120	-100	-300	-500	-700	-1100	-1500	-2000	-2600	-2600	-2600	2600	-2600
130	-150	-375	-700	-1000	-1500	-1900	-2300	-2700	-2700	-2700	2700	-2700
140	-175	-400	-900	-1300	-1800	-2000	-2500	-2800	-2800	-2800	2800	-2800
150	-100	-300	-700	-900	-1300	-1700	-2200	-2700	-2700	-2700	2700	-2700
160	-75	-200	-400	-600	-800	-1100	-1600	-2400	-2400	-2400	2400	-2400
170	-50	-100	-175	-300	-375	-500	-800	-1800	-1800	-1800	1800	-1800
180	0	0	0	0	0	0	0	0	0	0	0	0

TABLE-4.15

VARIATION OF MAGNETOSTRICTION WITH MAGNETIC FIELD FOR
 $Tb_{.27}Dy_{.73}Fe_2$

SENSITIVITY PER DEFLECTION $\Delta R/R=2.5 \times 10^{-6}$

GAUGE FACTOR $G = 2.09$

BRIDGE CURRENT 25 mA

FIELD CURRENT IN AMP.	MAGNETIC FIELD IN GAUSS	DEFLECTION OF NANO VOLTMETER	$\Delta R/R \times \text{NANO}$ VOLTMETER DEFLECTION	MAGNETOSTRICTION $= 2/30 \times \Delta R/R$
0	0	0	0	0
0.5	425	375	$.937 \times 10^{-3}$	0.299×10^{-3}
1	800	1000	2.5×10^{-3}	0.798×10^{-3}
1.5	1175	2200	5.5×10^{-3}	1.75×10^{-3}
2	1550	3100	7.75×10^{-3}	2.47×10^{-3}
2.5	1875	4200	10.5×10^{-3}	3.35×10^{-3}
3	2250	4750	11.8×10^{-3}	3.78×10^{-3}
3.5	2650	5500	13.75×10^{-3}	4.39×10^{-3}
4	3050	6100	15.25×10^{-3}	4.86×10^{-3}
4.5	3400	6100	15.25×10^{-3}	4.86×10^{-3}
5	3800	6100	15.25×10^{-3}	4.86×10^{-3}
5.5	4125	6100	15.25×10^{-3}	4.86×10^{-3}
6	4550	6100	15.25×10^{-3}	4.86×10^{-3}

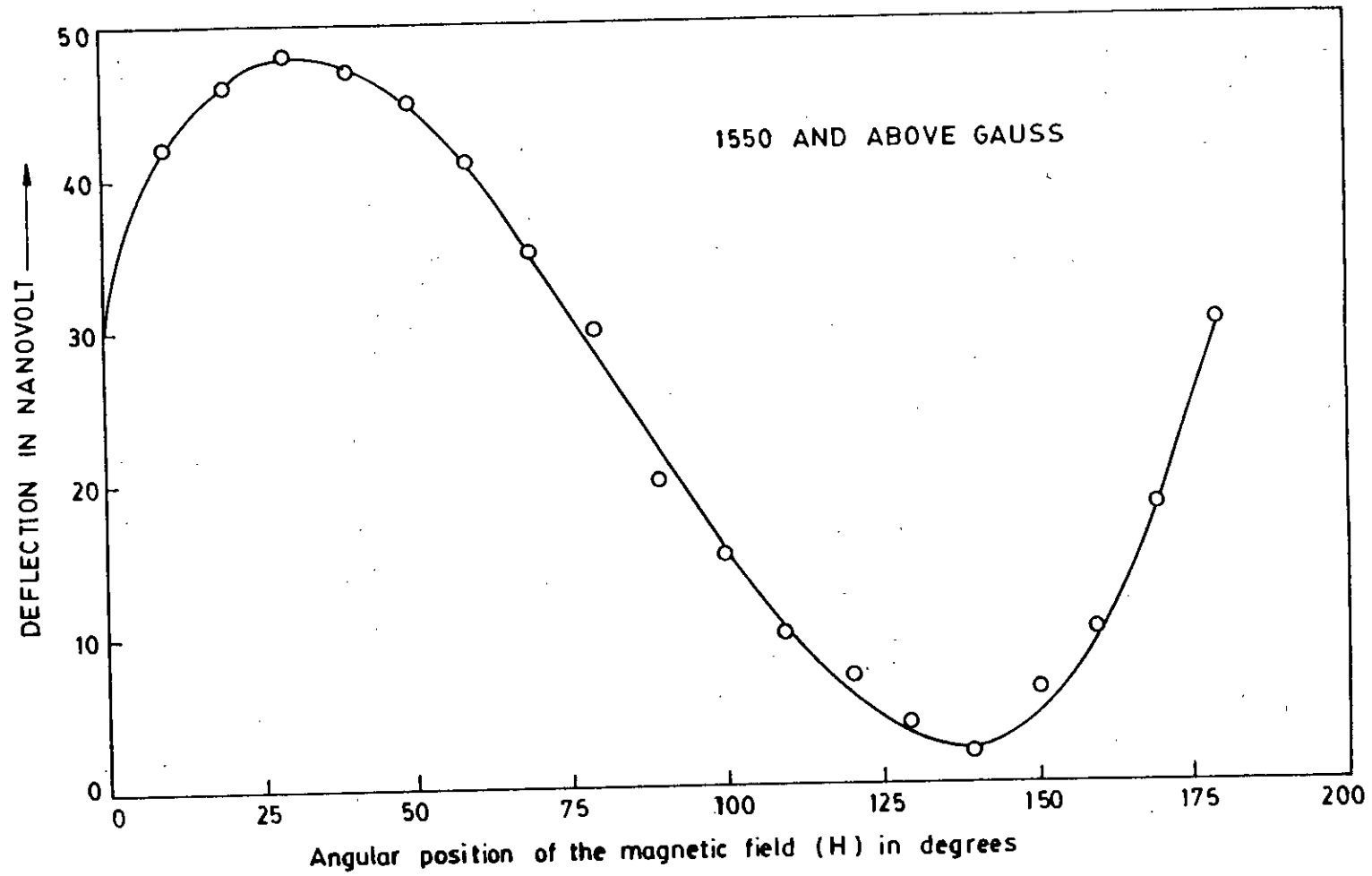


FIG. 4.5 VARIATION OF THE MAGNETOSTRICTION (PROPORTIONAL TO THE DEFLECTION IN NANOVOLTMETER) AGAINST THE DIRECTION OF THE APPLIED MAGNETIC FIELD FOR NICKEL

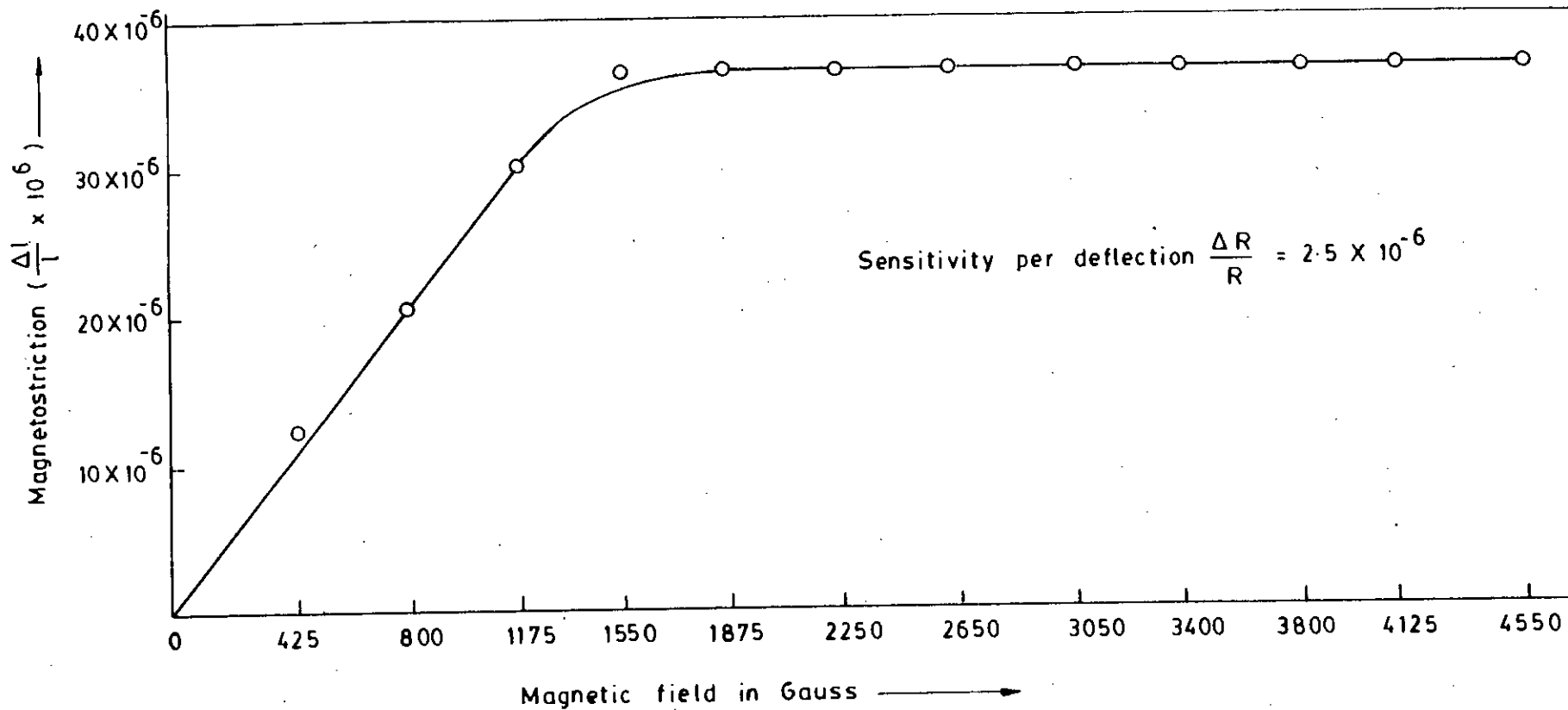


FIG. 4.6 VARIATION OF THE MAGNETOSTRICTION WITH APPLIED MAGNETIC FIELD FOR NICKEL AT ROOM TEMPERATURE.

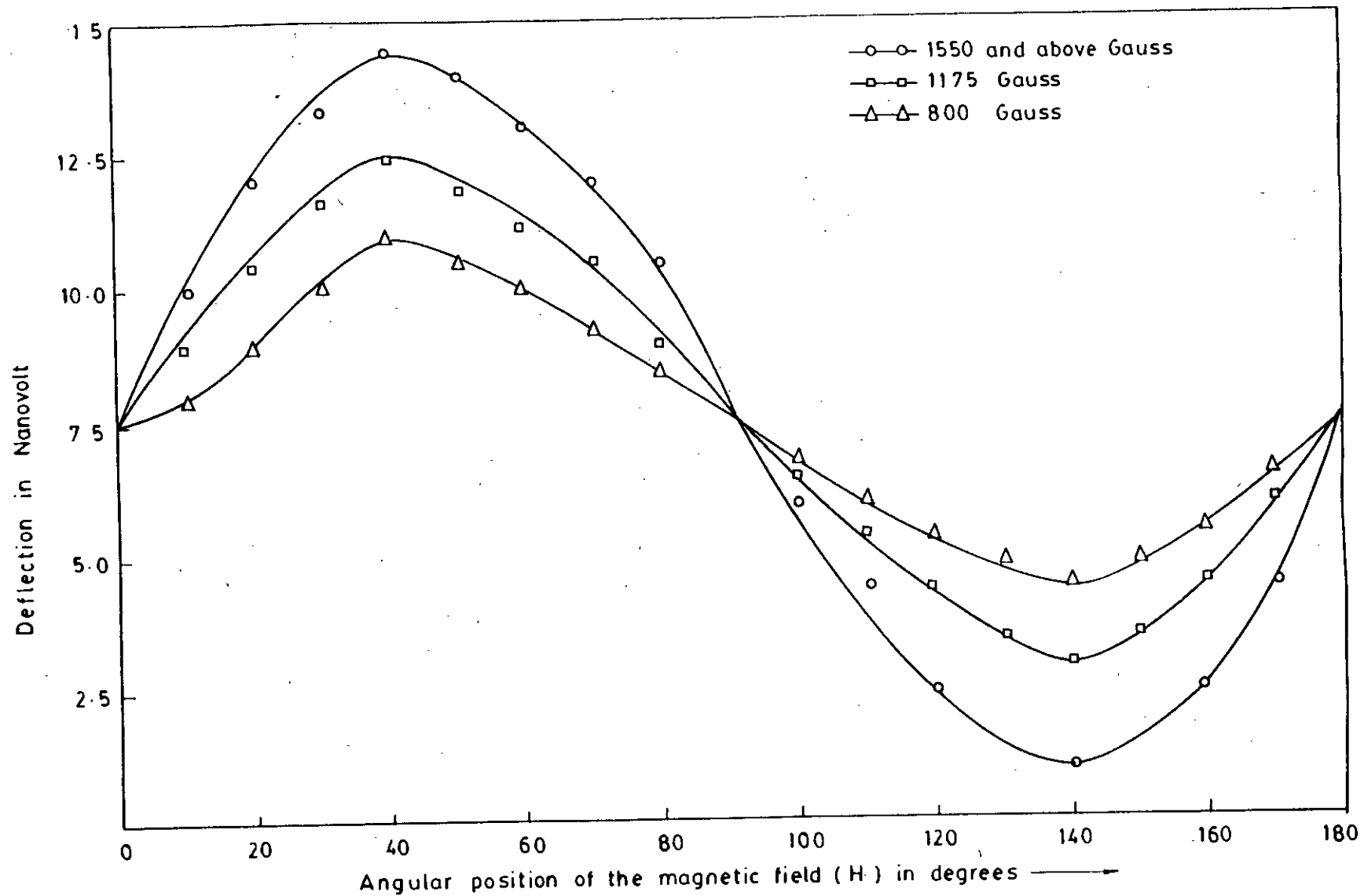


FIG. 4.7 VARIATION OF THE MAGNETOSTRICTION (PROPORTIONAL TO THE DEFLECTION IN NANOVOLTMETER) AGAINST THE DIRECTION OF THE APPLIED MAGNETIC FIELD FOR $\text{Fe}_{98}\text{Al}_2$

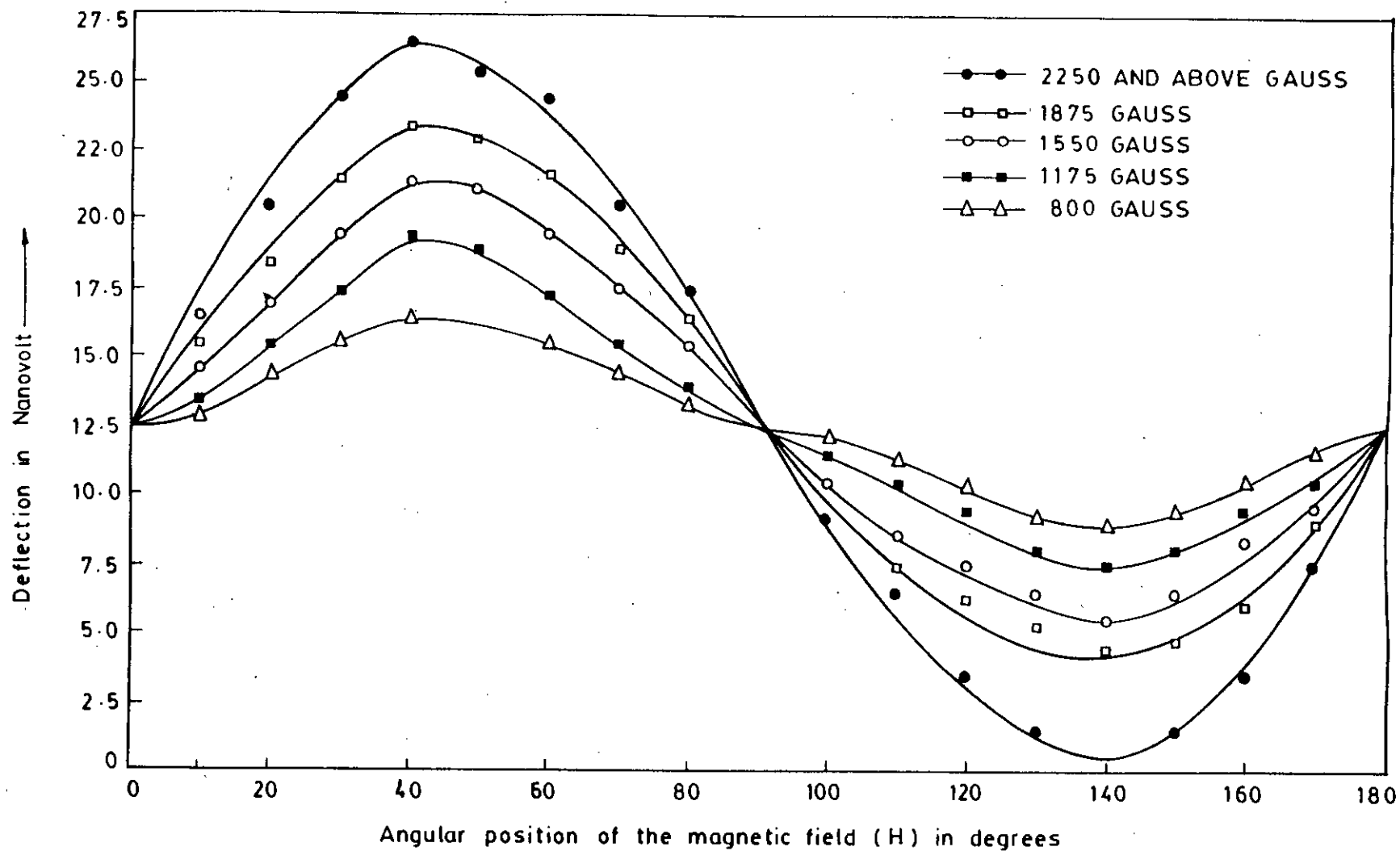


FIG. 4.8 VARIATION OF THE MAGNETOSTRICTION (PROPORTIONAL TO THE DEFLECTION IN NANOVOLTMETER) AGAINST THE DIRECTION OF THE APPLIED MAGNETIC FIELD FOR $\text{Fe}_{92}\text{Al}_8$

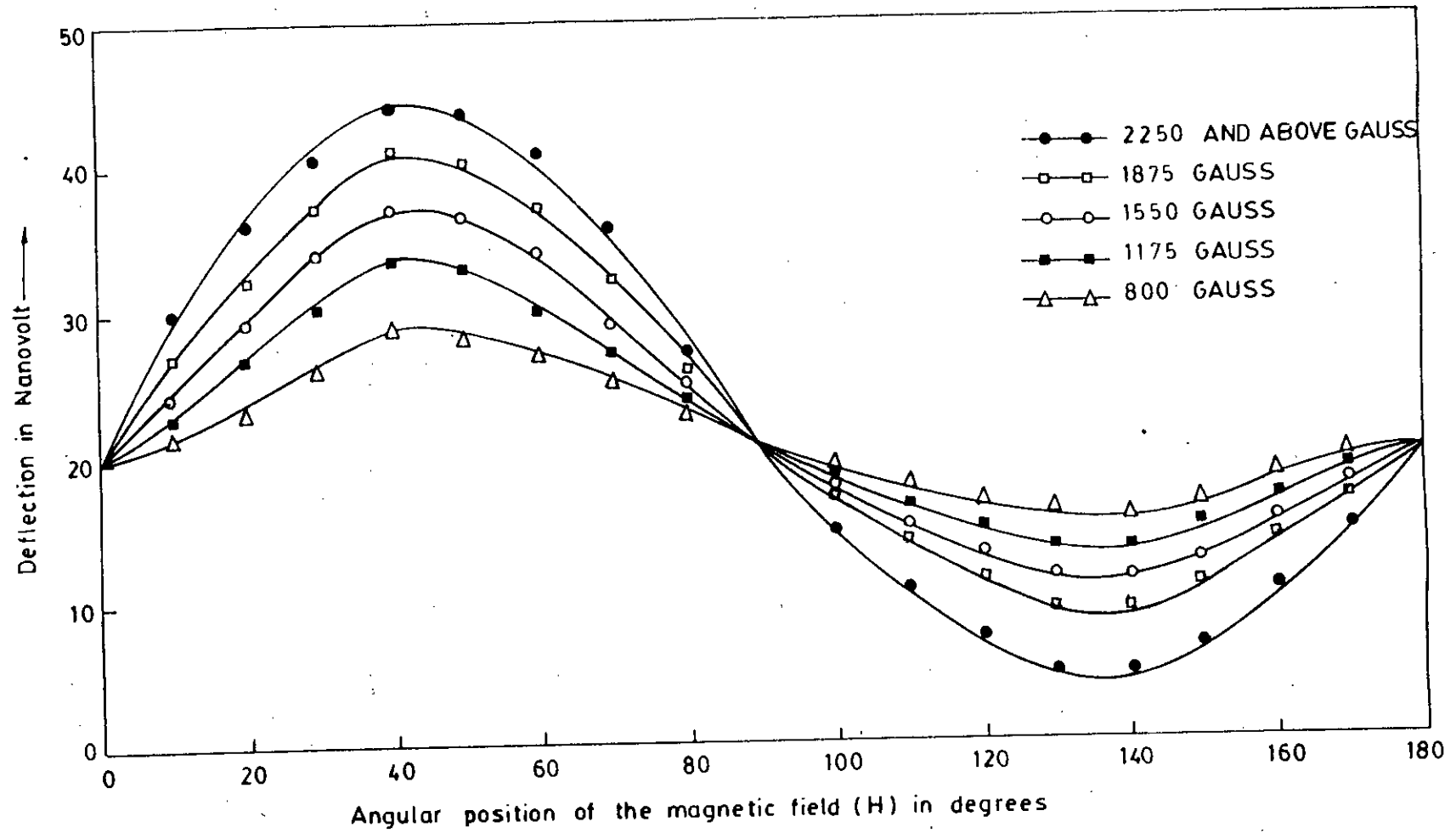


FIG. 4.9 VARIATION OF THE MAGNETOSTRICTION (PROPORTIONAL TO THE DEFLECTION IN NANOVOLTMETER) AGAINST THE DIRECTION OF THE APPLIED MAGNETIC FIELD FOR $\text{Fe}_{90}\text{Al}_{10}$.

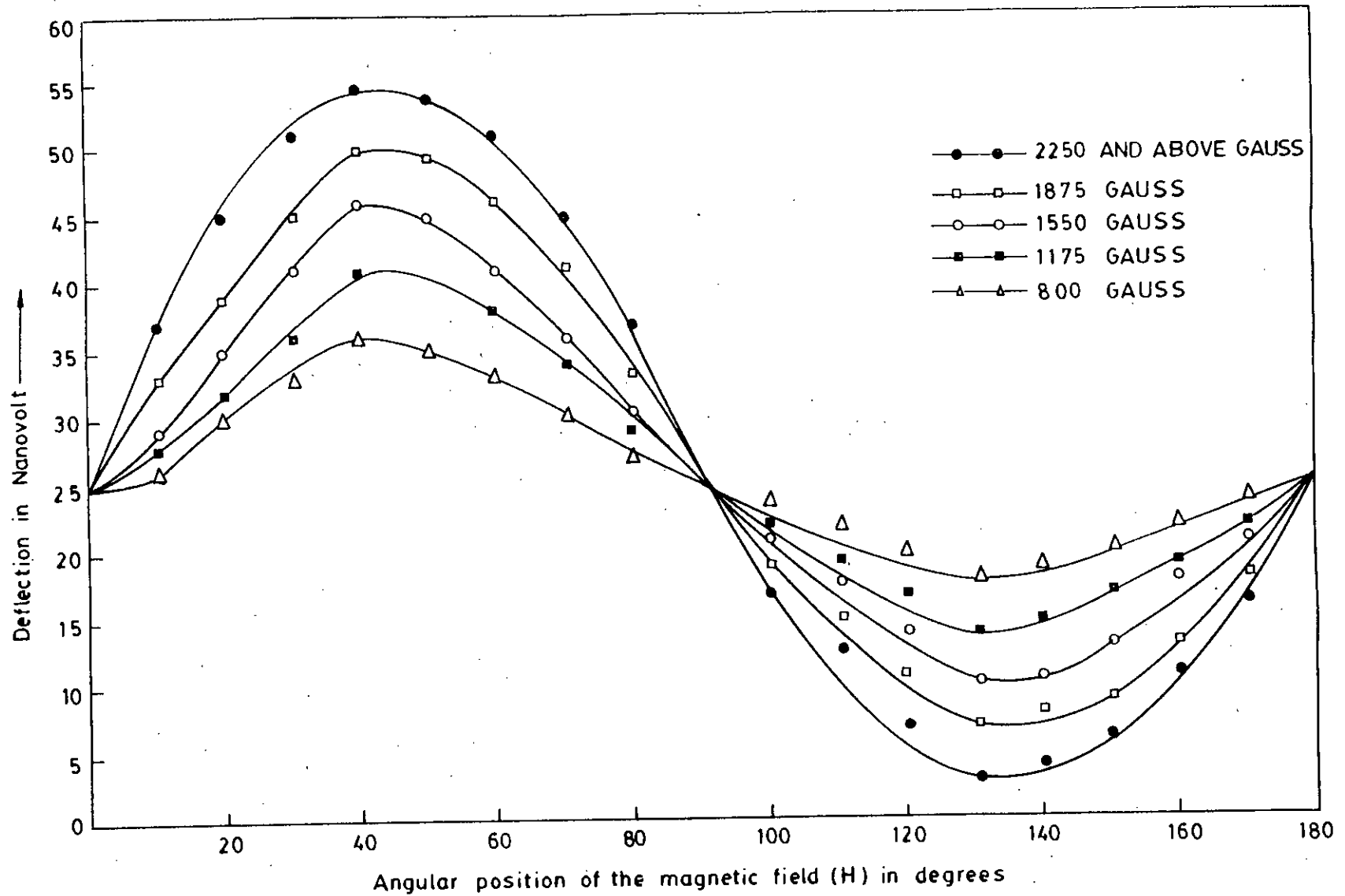


FIG. 4.10 VARIATION OF THE MAGNETOSTRICTION (PROPORTIONAL TO THE DEFLECTION IN NANOVOLTMETER) AGAINST THE DIRECTION OF THE APPLIED MAGNETIC FIELD FOR $\text{Fe}_{88}\text{Al}_{12}$

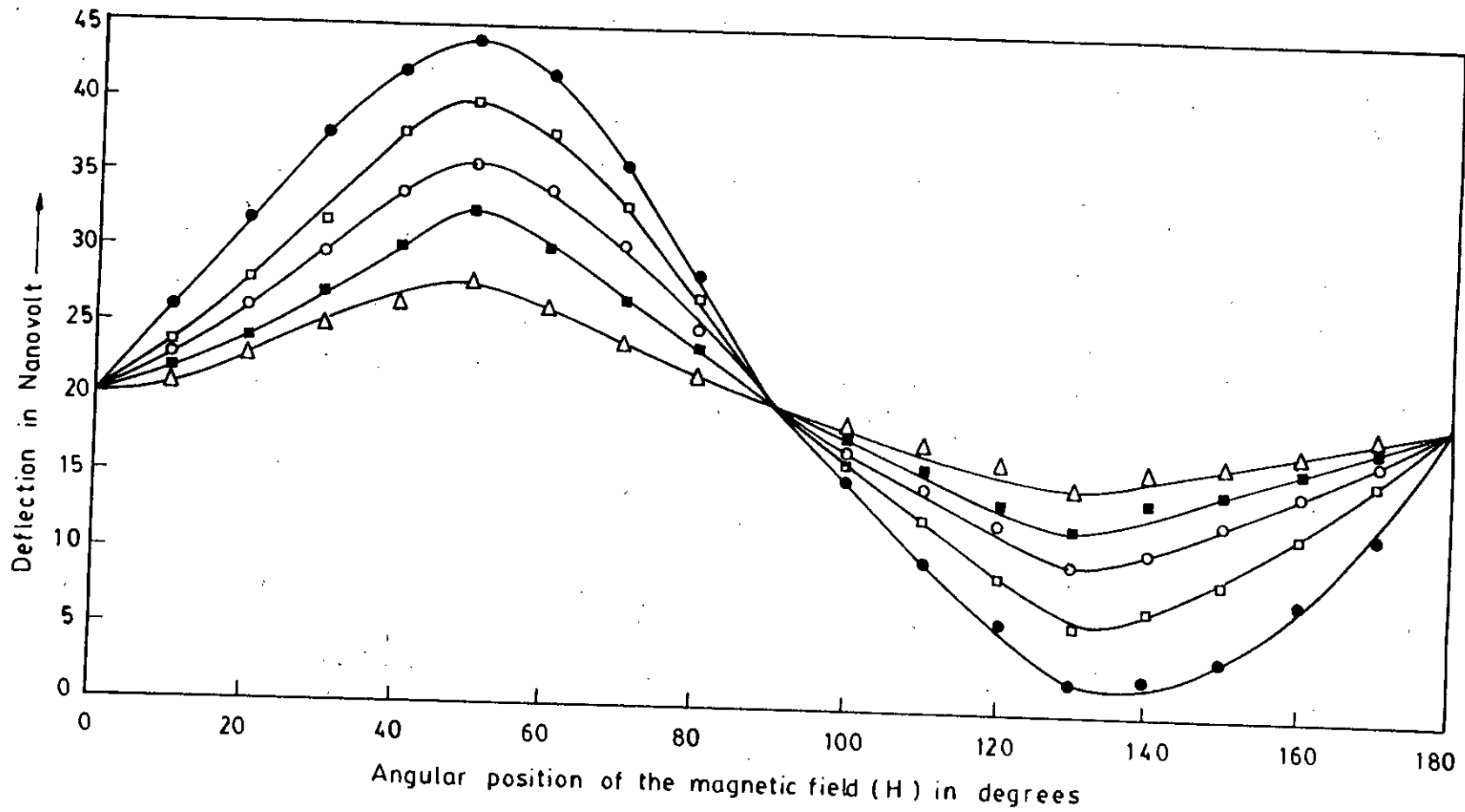


FIG. 4.11 VARIATION OF THE MAGNETOSTRICTION (PROPORTIONAL TO THE DEFLECTION IN NANOVOLTMETER) AGAINST THE DIRECTION OF THE APPLIED MAGNETIC FIELD FOR $Fe_{86}Al_{14}$.

III

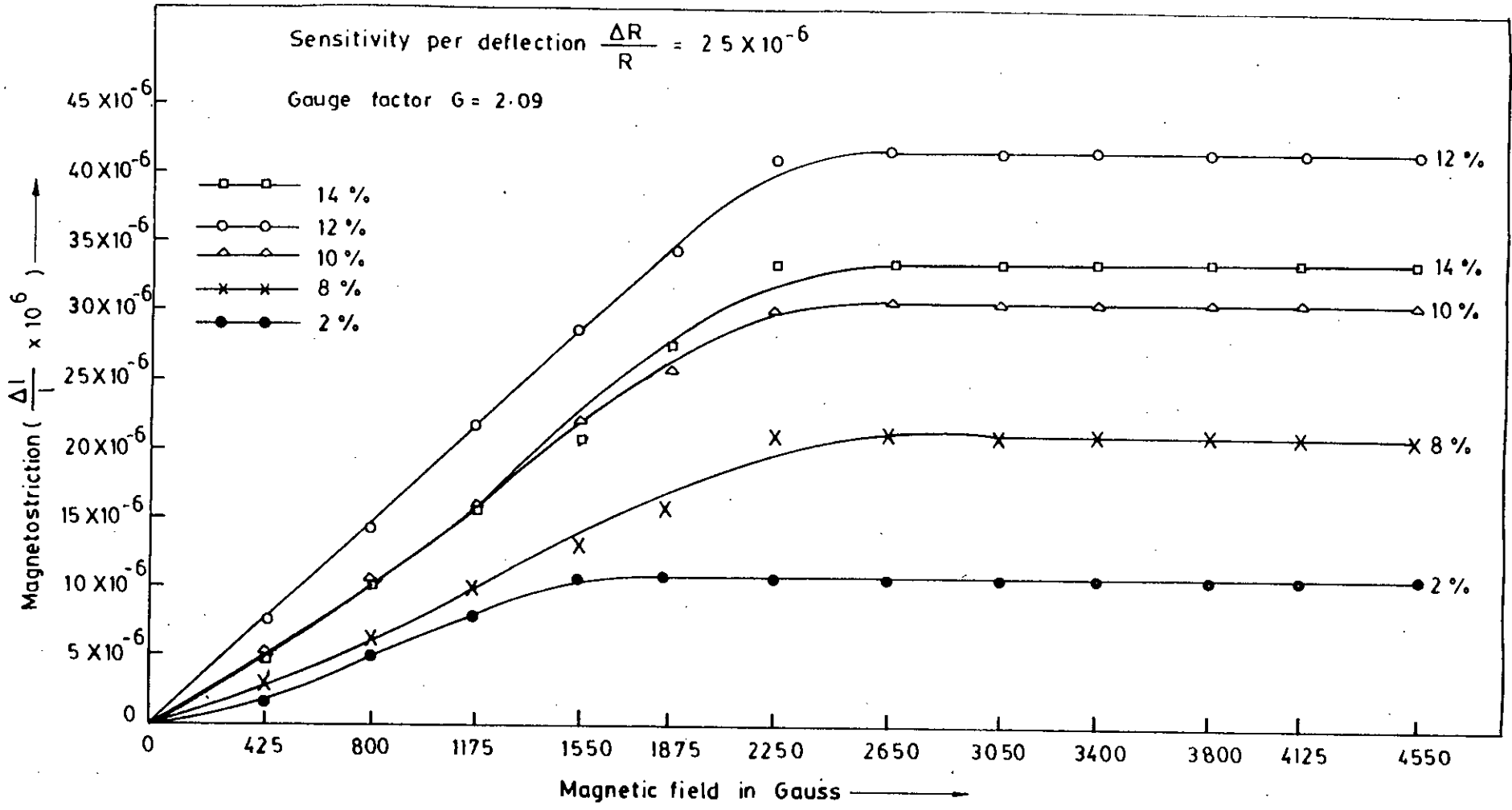


FIG. 4.12 VARIATION OF THE MAGNETOSTRICTION WITH APPLIED MAGNETIC FIELD FOR $Fe_{100-x}Al_x$ AT ROOM TEMPERATURE

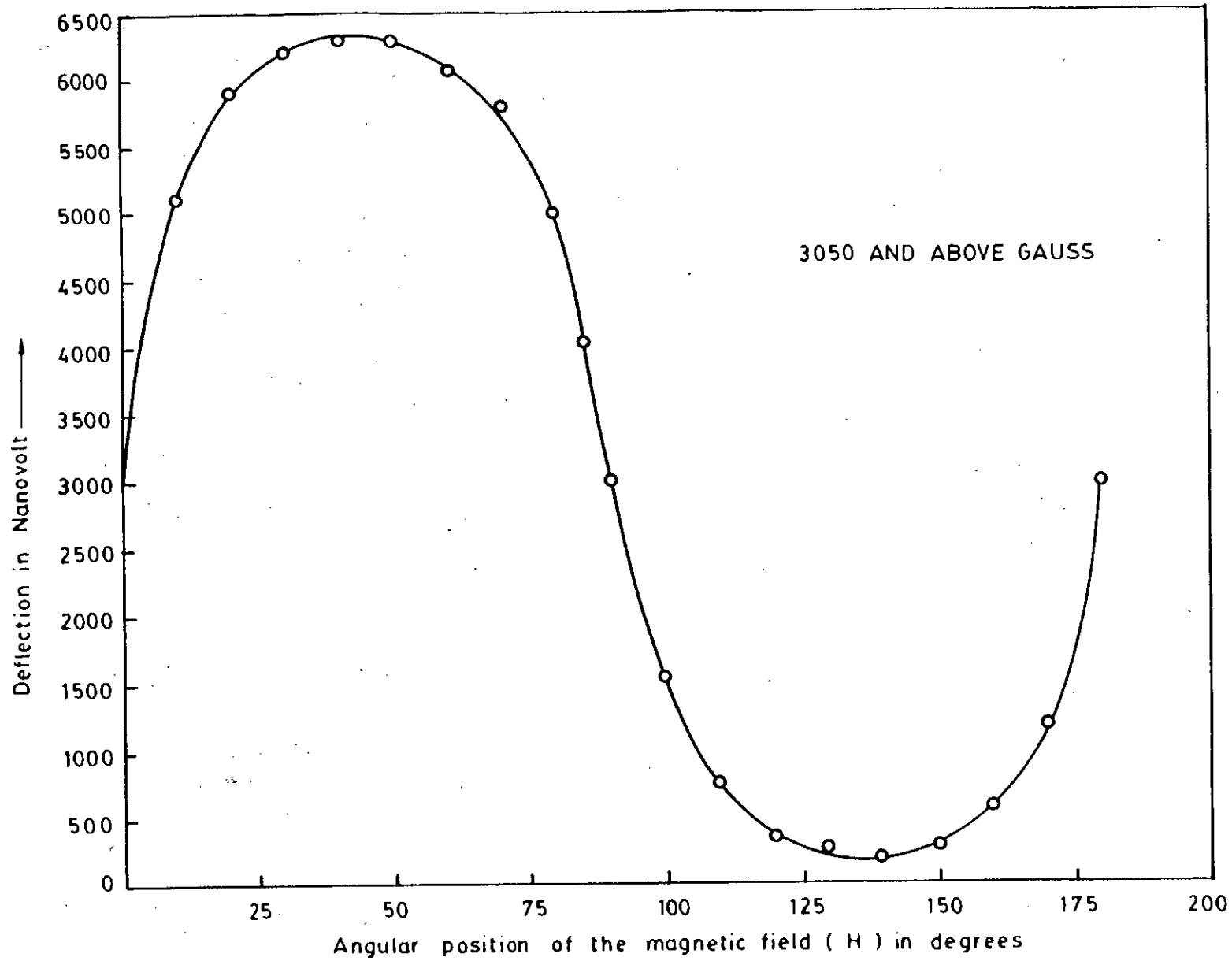


FIG. 4.13 VARIATION OF THE MAGNETOSTRICTION (PROPORTIONAL TO THE DEFLECTION IN NANOVOLTMETER) AGAINST THE DIRECTION OF THE APPLIED MAGNETIC FIELD FOR $Tb_{27}Dy_{73}Fe_2$.

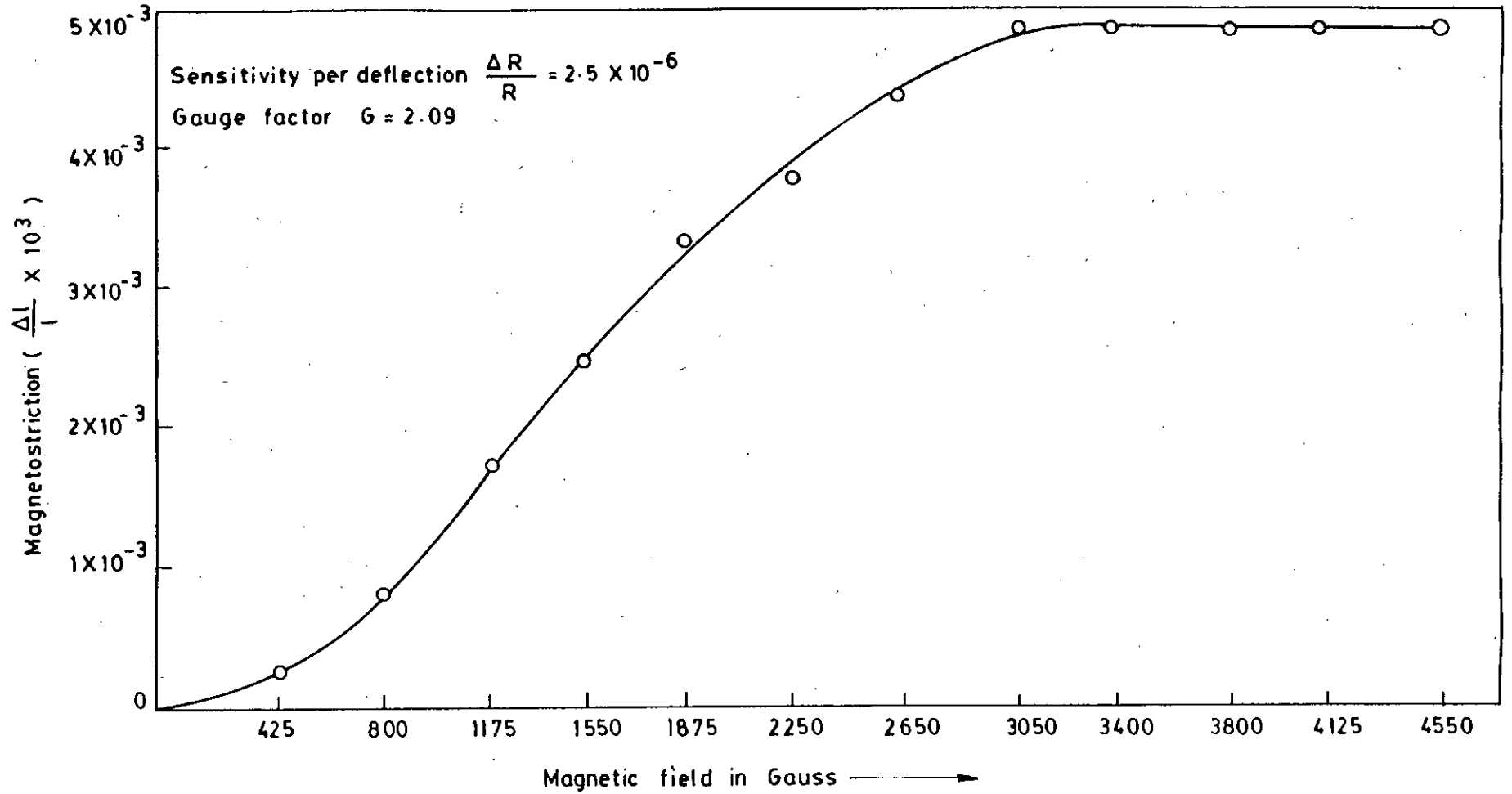


FIG. 4.14 VARIATION OF THE MAGNETOSTRICTION WITH APPLIED MAGNETIC FIELD FOR $Tb_{27} Dy_{73} Fe_2$ AT ROOM TEMPERATURE

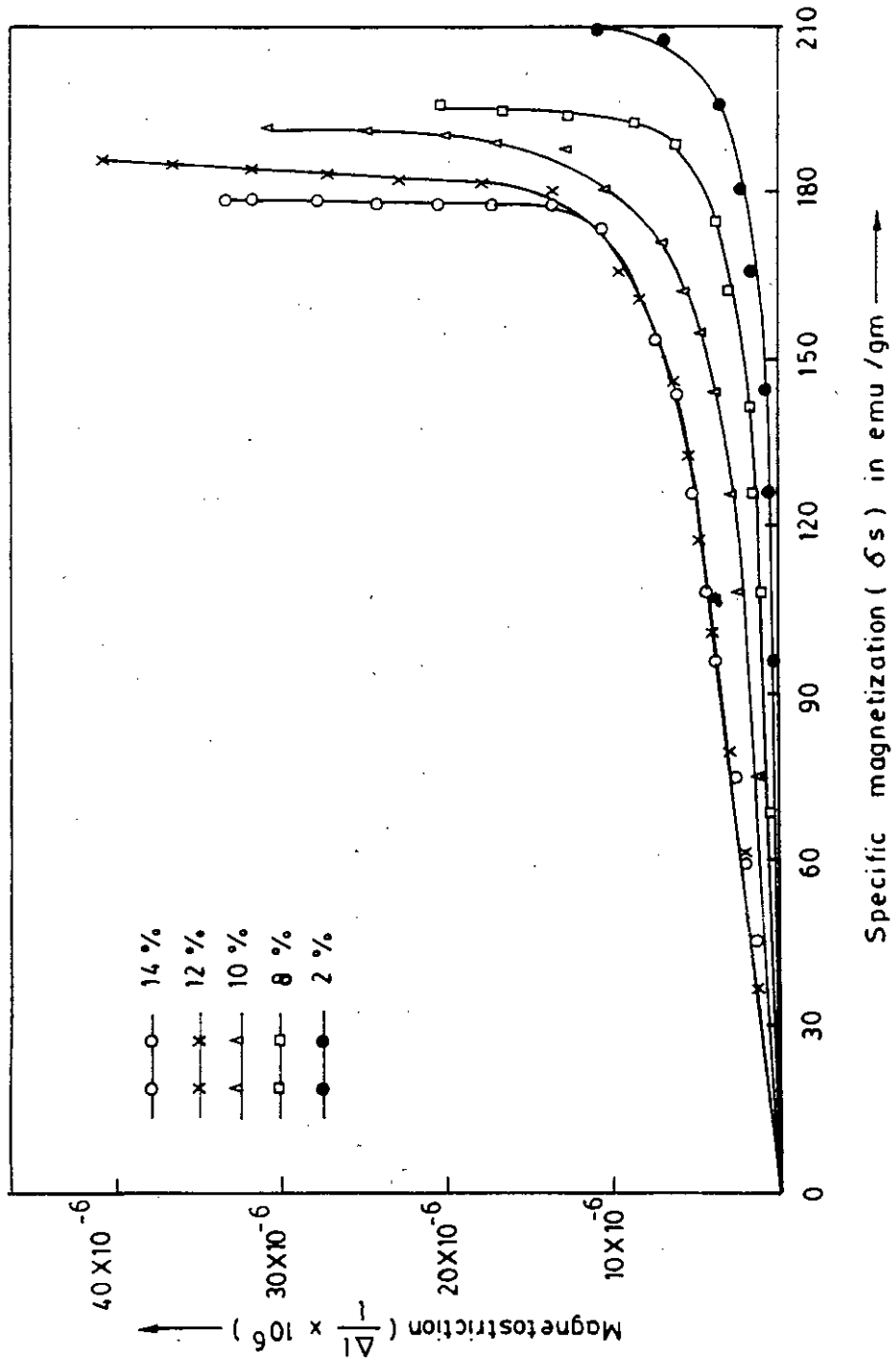


FIG. 4.15 MAGNETOSTRICTION AS A FUNCTION OF SPECIFIC MAGNETIZATION (δ_s)

4.17 Results and Discussion

Magnetostriction as a function of field and saturation magnetostriction λ_s for different compositions of iron aluminium i.e. $Fe_{100-x}Al_x$ (where $x = 2, 8, 10, 12, \text{ and } 14$) and $Tb_{.27}Dy_{.73}Fe_2$ alloys and also of nickel as standard material are measured. The measurements are done by strain gauge technique at room temperature and under varying fields which have the maximum value of 4.5 K. Gauss. The magnetostriction of polycrystalline nickel is measured for comparison and calibration of our measuring system.

The magnetostriction of $Ni, Fe_{100-x}Al_x$ and $Tb_{.27}Dy_{.73}Fe_2$ as measured under varying fields are shown in Figures 4.6, 4.12 and 4.14 respectively. The variation of magnetostriction as a function of specific magnetization is shown in Figure -4.15.

4.17.1. Nickel

The variation of magnetostriction of Nickel with field for different angular position has been measured at room temperature and is given in table-4.2 and the variation of magnetostriction with the angular position of the magnetic field is shown in Figure-4.5.

The saturation field for magnetostriction in Nickel is observed to be 1550 oersted at room temperature. This value of the magnetic field needed for the saturation magnetostriction in Ni determines the operating field for using Nickel as a magnetostrictive transducer. This experiment was done to check our measurement system and for standardizing the instrumental set up.

Nickel has *f.c.c.* structure over the whole temperature range with a curie point of 358°C (631 K). The spontaneous magnetization $\sigma_{00} = 57.5$ emu/gm corresponds to a magneton number of $0.606 \mu_B$ per atom spins $0.606 (2/g) = 0.55$ i.e in the *3d* band 5 spins up, 4.45 spin down and 0.55 conduction electron to give the total of *g* electrons, where $g = 2.185$. The magnetostriction is thus associated with 0.55 electron holes in the *d* band and contributes to the elongation of the specimen under the influence of the applied magnetic field. Above the curie point the susceptibility follows a curie-weiss law up to 900°C with $c = 0.00548$ per gm (0.322 per gm atom) $Q_p = 377^\circ\text{C}$ at higher $c = 0.00685$ per gm (0.402 per gm atom) with $Q_p = 265^\circ\text{C}$.

The variation of magnetostriction with magnetic field at room temperature arises due to spin orbit interaction. Each individual spin possesses a temperature independent anisotropy energy and thermal variations of macroscopic anisotropy energy arise from an average over the directions of spins. The magnitude of magnetostriction which is predicted in this model is guided by the ratio of the anisotropy energy to the molecular field. The larger part of anisotropic magnetostriction is not due to the spin contribution to magnetostriction but to the orbital one. In the approach to saturation in polycrystalline materials there is always a stress dependent term $c = 2c_{44}/(c_{11} - c_{12})$ which give rise to non vanishing contribution to magnetostriction.

Tatsumoto, Okamoto, Iwata and Kadana^{4.4} calculated the value of magnetostriction of Nickel at 0°K and 20°K. These are given as $\lambda_{100} = -55 \times 10^{-6}$ and $\lambda_{111} = -28 \times 10^{-6}$ at 0 k and $\lambda_{100} = -56 \times 10^{-6}$ and $\lambda_{111} = -23 \times 10^{-6}$ at 20°K and the saturation magnetostriction $\lambda_s = -36 \times 10^{-6}$. Fletcher calculated the same parameters at 0° k and his values are $\lambda_{100} = -46.7 \times 10^{-6}$ and $\lambda_{111} = -11.1 \times 10^{-6}$ Asgar^{4.5} calculated the value of magnetostriction of single crystal of Nickel and the results are $\lambda_{100} = -66.5 \times 10^{-6}$ and $\lambda_{111} = -35 \times 10^{-6}$. In

our experiment the result obtained for saturation magnetostriction of polycrystalline Nickel is $\lambda_s = 36.68 \times 10^{-6}$.

4.17.2 *Fe*_{100-x}*Al*_x Alloys

After we obtained results for Nickel with our experimental set-up which showed a good agreement with established values, we measured the magnetostriction of *Fe*_{100-x}*Al*_x alloy system. The obtained values are given in tables-4.2-4.15. The results are shown in Figure-4.5 and 4.14 respectively. The magnetostriction as a function of the specific magnetization is shown in Figure-4.15.

The field dependence of magnetization and magnetostriction for Fe-Al alloy of different compositions shown in Figure 3.11 and 4.12 indicate the saturation fields for different compositions.

Saturation magnetization of different alloys are plotted in Figure- 3.11. The magnetostriction value increases with increasing amount of aluminium and become maximum at 12 atomic percent of Al. This maximum value λ_s is 41.47×10^{-6} which is more than four times the magnetostriction of pure Fe and of the same order of magnitude as the magnetostriction of Nickel but of opposite sign. Iron-Aluminium is thus a good material for making magnetostrictive transducer and can replace Nickel for its lower cost.

Increasing value of magnetostriction of Iron-Aluminium alloy with the addition of aluminium is explained as due to increased spin orbit interaction. The decrease of magnetostriction above 12 atomic percent of Al is explained as due to decreasing value of magnetic moment.

From the magnetization versus field and magnetostriction versus field measurements, we have plotted magnetostriction against magnetization for different composition and is shown in Figure-4.15. This result is very important in providing information regarding the magnetization process due to domain wall movements.

It is observed that, initially the magnetostriction increases with magnetization rather slowly for all the compositions. This is explained as due to 180° domain wall motions in the initial stage with little 90° domain wall movements or rotations. Since 180° domain wall motions do not involve the rotation of strain axes, initial magnetization process takes place without increasing magnetostriction significantly. For magnetization above the 170 emu/gm, the rotational process of 90° domains becomes sharp. This magnetization value correspond to magnetic field of 260 oersted.

For iron aluminium alloys, $3d$ orbital moment is quenched and the magnetic anisotropy and ordinary magnetostriction arise from spin orbit coupling essentially as a perturbation effect. Due to the small spin orbit coupling and for low anisotropic localized nature of $3d$ electronic charge distribution, the $Fe_{100-x}Al_x$ alloys show high magnetostrictive strain which are found in our experiment for 2 atomic percent of Al in iron and is 10.77×10^{-6} . This value is found to increase with the increasing aluminium content up to 12 atomic percent. The maximum value is 41.47×10^{-6} . For further increase of aluminium to 14 atomic percent, the value slightly falls to 33.49×10^{-6} . Therefore it is evident that for alloys above 12 atomic percent of Al, the magnetostriction decreases with increasing Al content due to decreasing value of the corresponding magnetization.

Although the magnetostriction for 8 and 10 atomic percent of Al in iron rises to 20.73×10^{-6} and, 30.22×10^{-6} respectively, the alloys show a high resistivity and is suitable for induction purposes provided the strains can be kept low. It is observed in

our experiment that for $Fe_{100-x}Al_x$ alloy system, the magnetostrictive strain is produced when the direction of magnetization is changed and it is usually of the order of 10^{-6} . This means that the amount of reorientation of electron cloud is dependent on the content of aluminium and changes the value of magnetostriction. For $Fe_{100-x}Al_x$ alloys crystal field and exchange interaction have been considered as the main contributors to the free energy in order to explain the magnetostrictive behaviour.

4.17.3 $Tb_{.27}Dy_{.73}Fe_2$ Alloy

The exceptional magneto-elastic properties of rare earth iron $Tb_{.27}Dy_{.73}Fe_2$ compound offer a great potential for a variety of applications. Different techniques for the characterisation of their magnetostriction and magneto-elastic performance have been developed which provide consistent data. Magnetic properties of rare earth element $Tb_{.27}Dy_{.73}Fe_2$ arises mainly due to the unfilled $4f$ shell which widely differ in important respects from the magnetic transition metals, whose magnetization originates from the $3d$ electrons. The $4f$ electrons tend to be localized deep inside the atom and is thus well shielded from direct interactions with $4f$ electrons on other atomic sites. It also has very much stronger spin orbit coupling than the transition metal elements. Magnetostriction for the alloys is found to occur due to these properties where total angular momentum $J=L+S$ is usually a good quantum number. The interaction between the $4f$ magnetic electrons and the environment out-side the atom is mostly indirect and takes place via the various conduction electrons. Although the $4f$ coupling with lattice is indirect, it is not generally weak. As a general rule the $3d$ wave function are much more extended than the $4f$ electron wave functions and can exhibit direct overlap between wave functions on neighboring sites. The large spin orbit coupling and highly anisotropic localized nature of the $4f$ electronic charge distribution for non-s-state rare

earth elements, therefore, routinely result in large magnetic anisotropies as well as large magnetostrictive strain at saturation.

The variation of magnetostriction as a function of field is measured and the result is listed in Table-4.14. The variation of magnetostriction as a function of angular position is shown in Figure-4.13 and the variation of magnetostriction as a function of field is shown in Figure-4.14.

In our experiment the variation of magnetostriction with field is found to be 4.86×10^{-3} for $Tb_{.27}Dy_{.73}Fe_2$ at room temperature. Rare earth $Tb_{.27}Dy_{.73}Fe_2$ alloy is an exceptional alloy as it is ferro-magnetic at a temperature above the room temperature and its orbital moments are not quenched i.e. the spin orbit coupling is strong. Moreover, the electron cloud about each nucleus is decidedly non spherical as a result when applied field rotates the spin, the orbit rotates too and considerable distortion results. The rare earth iron laves phase compound $Tb_{.27}Dy_{.73}Fe_2$ displays a spin-reorientation at room temperature. The behaviour of the elastic moduli at room temperature suggest a first order phase change and it increases significantly with applied magnetic field. Savage and Abbundi^{4.6}, Legvold, Alstad and Rhyne^{4.7}, Greenough and Schulze^{4.8} investigated the properties of magnetostrictive rare earth iron compounds. Data for K_{33} is largely dependent upon the geometry of the sample and the magnitude of the coupling coefficient. Tb has a helical spin structure similar to that in Dy , however, the antiferromagnetic interaction is much weaker in Tb and a very small applied field will remove the helical state and produce ferromagnetic ordering along the field direction. This change in dimension is presumed to arise in the magnetostriction process as a result of domain rotation in which the magnetic moment must cross the hard magnetic direction giving rise to the strains observed at a field above technical saturation at room temperature.

4.18 Conclusion

For power applications a magnetic materials must be soft with high induction value and resistivity. Although silicon iron is used as the most common soft magnetic material, iron aluminium also have the same properties in many ways. It has the added advantage and also some disadvantages. The major differences found between low percentage aluminium iron alloys and equivalent percentage of silicon iron alloys are

- i. Aluminium iron is more powerful de-oxidizer than silicon.
- ii Aluminium iron improves ductility. It is thus possible to cold roll aluminium iron

alloys containing upto 6% aluminium by as much as 90%.

Commercial production of aluminium iron alloys can be limited in their early states of development because of the relatively high cost of aluminium versus silicon and because of the greater difficulty in preventing segregation of aluminium during melting process. However, the cost picture has equalized in recent years and with modern induction melting equipment the segregation problem has practically been eliminated. The work of Sugihara^{4.9} and Helms^{4.10} illustrated that magnetic properties of isotropic aluminium iron alloys are comparable to those of equivalent silicon iron alloys.

Our measurements of magnetization and magnetostriction were carried out on the as prepared specimens. However, the effect of annealing has very important influence on magnetization process and magnetostriction because of the high value of magnetostriction of those alloy system. In order to use this materials as a soft magnetic materials to replace iron silicon alloy, the specimens should be stress free. Further work on iron aluminium alloy system with higher range of composition and under relieved strains by appropriate heat treatments in vacuum can be very useful for better understanding of the magnetic characteristics of these materials. This will also require measurements at high and at very low temperatures.

References:

Chapter -1

- 1.1 J.E. Goldman, Phys. Rev.72 529 (1947)
- 1.2 Asgar M.A. Ph.D thesis. University of Southampton, England, 1970.
- 1.3 S.S. Sikder M.Phil. thesis 1988.
- 1.4 Callen,E and H.B. Callen (1963) Phys. Rev. 129 578.
- 1.5 R.M. Bozorth and J.G. Walker Phys. Rev. 88 1209
- 1.6 Beninger G.N. and Pavlovic A.S.(1967) J. Appl. Phys. 38 1325-1326.
- 1.7 Lee E.W (1955) Rept. Progr. Phys.18 184-229
- 1.8 Asgar M.A. Ph.D thesis. University of Southampton,England (1970)
- 1.9 Clark A.E. and H.Belson (1972) Phys. Rev. B₅ 3642.
- 1.10 Fallot M. (1936) Ann. Phys. (Paris) 6 305-381.
- 1.11 Arrot, A and Sato H.(1959)Phys. Rev.114 (1420-1426) Rev. Mod. Phys. 21541
- 1.12 Kittel.C (1949) Rev. Mod. Phys. 21541
- 1.13 Clark A.E. and H.Belson (1972) IEEE Trans. MAG.8 477
- 1.14 Abbundi,R. A.E. Clark and N.C. Koon (1979) J. Appl. Phys.50 1671

Chapter - 2

- 2.1 Bozorth, R.M. Ferro-magnetism,Princeton,New Jersey,D Van Nostrand co.
- 2.2 Bates L.F. Modern Magnetism (3rd ed.) London cambridge University press 1951
- 2.3 Kneller, E, Ferro-magnetism, Berlin Gottingen, Heidelberg,Springer 1962
- 2.4 Chikazumi, S. Physics of magnetism, Newyork, John wiley & sons 1963
- 2.5 Morish, A.H. The physical principles of magnetism Newyork John wiley & sons 1965
- 2.6 Shtrikman, S and D, Treves, micro-magnetics in magnetism. A treatise on modern theory and materials G.T. Rado and H. Suhl editors vol-3 Newyork, Academic press 1963 .
- 2.7 Brown Jr. W.F. Micro-magnetics,Newyork,John wiley & sons (inter science) 1963

- 2.8 Akulov, N.S. Z. Phys. 57, 249
- 2.9 Akulov, N.S. Z. Phys. 69, 78
- 2.10 Slater, J.C. J. Appl. Phys. 8 (1937) 385
- 2.11 Pauling, L. Phys. Rev. 54 (1938) 899
- 2.12 Weiss, P. J. Phys. Radium, 6, 661
- 2.13 Heisenber, W, Physik. Z. 49 (1928) 1080
- 2.14 E.C. Stoner, Phil. mag 17 15 1080 1933
- 2.15 J.C. Slater, Phys. Rev. 49 537, 981 1936
- 2.16 H. Krutter Phys. Rev. 48 664 (1935)
- 2.17 G.F. Koster, Phys. Rev. 98 901 1955
- 2.18 Zener, C, Phys. Rev. 81 (1951) 446, 82 (1951) 403, 83(1951) 299, 85 (1951) 324
- 2.19 Gans, R, Ann. Phys. Lpz(v), 15, 28 (1932)
- 2.20 Weiss, P, J. Phys. Radium, 9, 373 (1932)
- 2.21 Akulov, N.S. Z. Phys. 69, 822 (1931)
- 2.22 Becker, R and Doring, W. Ferromagnetismus, Berlin Springer(1939)
- 2.23 Holstein, T, and Primakoff, H, Phys. Rev. 58 1098 (1940)
- 2.24 Weiss, P, and Forrer, R. Ann. Phys. Paris(X) 12 279, 316.(1929)
- 2.25 Czerlinski, E, Ann. Phys. Lpz(v) 13, 80 1932.
- 2.26 Polley, H. Ann. Phys. Lpz(v) 36, 625 (1939)
- 2.27 Brown, W.F. Phys. Rev. 60 139 (1941)
- 2.28 Neel, L. J. Phys. Radium (VIII), 9, 184 (1948)
- 2.29 Holstein, T. and Primakoff, H. Phys. Rev. 59 388 (1941)
- 2.30 Akulov N.S. (1928) Z. Phys. 52 389.
- 2.31 Becker, R. and W.D. Doring (1939) Ferromagnetismus (Springer, Berlin)
- 2.32 Mahajani G.S. (1929) Phil. Trans. A, 228, 63.
- 2.33 T.Hirone, Sci. Rep. Tohoku University, 26, 117 (1937).
- 2.34 Fallot, M. (1936) Ann. Phys. (Paris) 6, 305-387.
- 2.25 Stoner, E.C. (1935) Phil. Mag. 19, 565.
- 2.36 Neel, L. (1944) J. Phys. Radium, 5 241
- 2.37 Vanveleck (1945) Rev. Mod. Phys. 17, 27.
- 2.38 Brown W.F. (1941) Phys. Rev. 60, 139.
- 2.39 Kittel, C. (1949) Rev. Mod. Phys. 21 541.
- 2.40 Lee E.W. (1955) Rept. Progr. Phys. 18, 184-229.
- 2.41 W. J. Carr., Jr. Ferromagnetism, Handbuch der Physik Springer Verlag P. 274 (1966)
- 2.42 J. Kanamuri. Magnetism (Academic Press Inc. New York 1963) 1st edn. vol. 1, chapter-4
- 2.43 Birss R.R. (1959) Advance Phys. 8 252-291.
- 2.44 Asgar, M.A. (1985) Proceeding of the conference on Phys. and energy, Dhaka. 153-167.
- 2.45 Joule, J.P. (1847) Phil. Mag. 30, 76, 225.

- 2.46 Masumoto, H. and G. Otomo (1950) *Sci. Rep. RITU A₂* 413.
- 2.47 Gersdorf, R. (1960) *Physica* 26 553-574.
- 2.48 Lee E.W. (1953) *Proc. Phys. Soc. A* 66, 623.
- 2.49 Toupin, R. (1956) *J. Rational mechanics and analysis*-5 850-915.
- 2.50 Brown Jr. W.F. (1965) *J. Appl. Phys.* 36 994-1000.
- 2.51 Tiersten H.F. (1964) *J. Math. and Phys.* 5 1-21.
- 2.52 Corner, W.D. and Hutchinson, F. (1958) *Proc. Phys. Soc.* 72 1049-1052
- 2.53 Hall R.C. (1959) *J. Appl. Phys.* 30 816-819.
- 2.54 Birss R.R. (1959) *Adv. Phys.* 8 252-291.
- 2.55 Borodkina M. M., Z. N. Bulycheva and Ya.P. Sellinski (1960) *Phys. Met. et al logr*, 9, 61.
- 2.56 Bulycheva Z.N., M.M. Borodkina and V.L. Sandomirskaya (1965) *Phys. Met. Metalogr.* 19 147.
- 2.57 Legvold, S.J. Alstad and J. Rhyne (1963) *Phys. Rev. Lett.* 10 509.
- 2.58 Clark, A.E.R. Bozorth and B. Desavage (1963) *Phys. Lett.* 5 100.
- 2.59 Rhyne, J. and S. Legvold (1965) *Phys. Rev.* 138A 507.
- 2.60 Tatsumoto, E. Okamoto, T. Iwata, N and Kadena, Y (1965) *J. Phys. Soc. Japan* 20 1541-1542.
- 2.61 Aubert, G. (1968) *J. Appl. Phys.* 39 504-510.
- 2.62 Asgar M.A. (1970) Ph.D. thesis University of Southampton.
- 2.63 Klinker, H. M. Rosen, M.P. Dariel and U. Atzmony (1974) *Phys. Rev. B*-10 2968.
- 2.64 Clark A.E. (1974) *American Institute Of Phys. Conf. Proc.* NO 18
- 2.65 Beeker, R. *1932) *Phys Z.* 33 905
- 2.66 Lee. E. W. and Asgar. M. A. *Phys. Rev. Letters* 22 (1969) 1936
- 2.67 H.T. Savage, A.E. Clark and J.M. Powers *IEEE Transaction on Magnetics Vol. Mag. II No-5*
- 2.68 Asgar. M.A. *Proceeding of the Intl. conf. on Phys. and energy for dev., Dhaka 26-19 January 1985 Page-153*
- 2.69 N.C. Koon, C.M. Williams and B.N. Dass *Naval Research Lab., Washington DC 20375-5000USA*
- 2.70 R.D. Greenough, A.G.J. Jenner, M.P. Schulze and A.J. Wilkinson, *J. of Mag. and Mane. Material. Vol; 101 (1991) 75-80*
- 2.71 Folks, C.D. Milham and R. Street *Research Centre for Advanced Mineral and Materials Processing. The University of Western Australia Nedlands WA 6009, Australia*
- 2.72 Callen, E and H.B. Callen 1965
- 2.73 Asgar M.A. Ph.D thesis, University of Southampton 1970
- 2.74 Van Vleck (1947) *Ann. Inst. Poincare*, 10, 57
- 2.75 W.P. Mason and J.A. Lewis, *Phys. Rev.* 94 1939 (1959)

Chapter- 3

- 3.1 Foner. S. Rev. Sci. Instr. 27 (1956) 548
- 3.2 Foner. S. Bull. Am. Phys. Soc. Ser 11.2 (1957) 128
- 3.3 Foner. S. Rev. Sci. Instr. 30 (1959) 548
- 3.4 Mazid, M.A. Chowdhury. M.A. and S. Akther, Design and Construction of a Foner type Vibrating sample magnetometer, Magnetic material division, AEC. Dhaka, June 1986.
- 3.5 Nathan, R, Pigott M. T. and Shull C.G. (1958), J. Phys. Chem. Solids 6, 38-42
- 3.6 Arrot. A and Sato, H (1959), Phys. Rev. 114-1420-1426.
- 3.7 J.F. Nachman and W.J. Buehler, Naval Ord. Report 4130 (1955)
- 3.8 M. Sugihara J. Phys. Soc. Japan. 15, 1456 (1960)
- 3.9 Helms Jr. H. unpublished Cited by Adams 1962.

Chapter - 4

- 4.1 Asgar. M.A. PhD Thesis, Univ. of Southampton (1970)
- 4.2 Goldman J.E., Phys. Rev. 72 (1947) 529
- 4.3 Instruction manual, Keithley Instrument Model 1140, Precision Nanovolt D.C. Amplifier. Keithley Instrument Inc. 28775, Aurora Road, Eleveland and Ohio.
- 4.4 Tatsumoto, E. Okamoto. T Iwata, N and Kadena, Y. (1965), J. Phys. Soc. Japan 20, 1541-1542
- 4.5 Asgar. M.A. PhD Thesis, University of Southampton 1970.
- 4.6 H.T. Savage and R. Abbundi, Transactions on Mangetics, vol. MAG-14 No. 5, September 1978.
- 4.7 S. Legvold, J. Alstad and J. Rhyne, Physical Review Letters, vol. 10, No 12, 15th June, 1963.
- 4.8 R.D. Greenough and M. Schulze, IEEE Transactions on magnetics vol. 26 No. 5 September 1990.
- 4.9 M. Sugihara, J. Phys. Soc., Japan, 15, 1456 (1960).
- 4.10 Helms Jr., unpublished cited by Adams, 1962.

